NASA Contractor Report 174747

Multi-Mesh Gear Dynamics Program Evaluation and Enhancements

Linda Smith Boyd and James Pike

Hamilton Standard
Division of United Technologies Corporation
Windsor Locks, Connecticut

June 1985

Prepared for
Lewis Research Center
Under Contract NAS 3-23928

National Aeronautics and
Space Administration

TABLE OF CONTENTS

Nomenclature for Multi-mesh Gear Dynamics Program Evaluation and Enhancements

Symbol	Description
	Variable Friction --Variables
L/W	Load per Unit Face Width
V_T	Total Velocity
V_S	Sliding Velocity
u_o	Absolute Viscosity of Oil
μ	Coefficient of Friction
ρ	Specific Gravity of the Oil
z_K	Kinematic Viscosity
T_f	Flash Temperature
T_λ°	Inlet Temperature
	Runout --Variables
$\triangle_{rs}$	Equivalent Tooth Spacing Error
$\triangle_r$	Input Displacement Error due to runout
n	Current Tooth Number
N	Total Number of Pinion Teeth
ϕ_o	Pressure Angle
	Flexible/Ring Carrier --Equation Variables
$m_s = I_s$	Sun Rotational Inertia
$m_{r_\lambda} = I_{r_\lambda}$, $m_{p_\lambda} = I_{p_\lambda}$	Ring, Planet, and Carrier Rotational Inertias
$m_{c_\lambda} = I_{c_\lambda}$	
d_{sp_λ}, d_{rp_λ}	Tooth Pair Damping
k_{c_λ}, k_{r_λ}	Ring or Carrier Segment Stiffness
k_{sp_λ}, k_{rp_λ}	Tooth Pair Stiffness
$Y_s = \Theta_s$	Sun Tooth Displacement along line of action
$Y_{p_\lambda} = \Theta_{p_\lambda}$	Planet Tooth Displacement along line of action
$Y_{c_\lambda} = \Theta_{c_\lambda}$	Carrier Tooth Displacement along line of action
$Y_{r_\lambda} = \Theta_{r_\lambda}$	Ring Tooth Displacement along line of action
T_{in}	Torque Input
R_{bs}, R_{br}	Involute Base Radii
R_{p_λ}, R_{bc}	
T_{out_c}, T_{out_r}	Output Torque
n	Total Number of Planets
X_s, X_{p_λ}	Deflections (After transformation to first order
X_{r_λ}, X_{c_λ}	differential equations)
e_{sp_λ}, e_{rp_λ}	Tooth Spacing Error
p_{sp_λ}, p_{rp_λ}	Profile Modifications
ϕ_{sp_λ}, ϕ_{rp_λ}	Tooth-pair Contact Identity Function

Single Mesh --Equation Variables

Y_{sp} , Y_{rp}	Relative Displacement along line of action
L_o	Static Tooth Load
$\bar{X}_{sp}, \beta_{sp}, \bar{X}_{rp}, \beta_{rp}$	Involute Profile Modification
η_{sp} , η_{rp}	Tooth Pair Stiffness
L_{sp} , L_{rp}	Tooth-Pair Meshing Loads

- -

Subscripted Notation for Equation Variables

r	Ring
s	Sun
c	Carrier
p	Planet
b	Base
sp	Combination of Sun and Planet
rp	Combination of Ring and Planet
i	Mesh number
j	Tooth Pair Number

I. INTRODUCTION AND SUMMARY

A. Background

A multiple mesh gear dynamics computer program has been continually developed and modified during the last three years under NASA funding; see Reference 1. The original single mesh program was expanded to include epicyclic gear systems with internal, buttress, or helical tooth forms. This NASA contract includes the following modifications: variable contact friction, planet cage and ring gear rim flexibility options, user friendly options, dynamic side bands, speed survey option, and combining the single mesh and multiple mesh options into one general program. In addition to the program modifications, the program was evaluated by comparing calculated values to published test data and to test data taken on Hamilton Standard turboprop reduction gearbox.

B. Analysis Approach

The basic assumptions of References 1 and 2 for the theoretical derivations apply in addition to the following assumptions for the flexible planet carrier and ring gear rim development and the sun-planet(s) or ring-planet(s) options:

1. The flexible ring gear rim and carrier flexibility option is assumed to be only along the lines-of-action of the respective gear meshes.

2. The static output torque is assumed to be divided evenly among either the planet carrier segments or the ring gear rim segments, depending on the type of planetary system.

3. Any radial component of motion is assumed to be secondary to the tooth-pair motion along the line-of-action.

4. The damping of carrier and ring rim segments is assumed to be insignificant relative to the tooth-pair meshing damping.

5. For the non-planetary options, the input torque and speed are assumed to be at the sun gear for the sun-planet(s) option and at the planet(s) for the ring-planet(s) option.

6. For the non-planetary options the planet carrier is assumed rigid and fixed or grounded.

C. Summary

The first program modification incorporates a more accurate, variable contact coefficient of friction model. This utilizes the method of Kelley and results in lower flash temperatures, provided the constant coefficient of friction previously assumed was .05 to .06.

The next modification adds flexibility to the planet carrier and ring gear rim by introducing azimuthal (along the line-of-action) degrees-of-freedom between each planet for each carrier and ring rim section. This results in more than doubling the number of first-order equations to be solved numerically, i.e. (6n + 2) equations, where n is the number of planets. The effect of this modification on the dynamic results has not been resolved. The check cases run to check the analytical model and computer code resulted in numerical instabilities. Cases that had been successfully run without the added degrees-of-freedom were difficult to obtain converged solutions for with reasonable carrier flexibilities. The analytical approach and system equations were successfully checked by obtaining average system natural frequencies from the eigenvalue solution and comparing against known results. The problem most likely is associated with the code used for the numerical solution of the system equations.

Another program modification makes the program more user friendly. Changes were made to allow for varying levels of input. The basic level requires only the basic geometric and operational data (rpm, torque) with the other values being defaulted. At the higher levels more and more of the detailed information is required. This type of input should be helpful to the gear designer where at the early design phase the basic level (level 1) is all that is required. Whereas at the final design phase all three levels will be required. In addition, the output was refined for better understanding of the results.

The dynamic side band option modification allows the user to investigate the effect of run-out error on the input pinion (sun) for a single mesh of two external gears. A sinusoidal error distribution is applied after the tooth error solution is obtained, to simulate runout error. The solution is obtained for each tooth mesh and the maximum summary tables are output. The loads are saved and can be used for a Fourier analysis to obtain a frequency spectrum for sideband evaluations.

Another program modification was the addition of a speed survey option thereby allowing the user to investigate tooth pair loads for a range of input speeds. The maximum load is located and the corresponding speed is used for the remaining stress calculations.

The final modification was to incorporate the option for a single mesh into the multiple mesh program for both spur and helical gears. Both sun-planet(s) and ring planet(s) options were added for either spur or helical gears. The spur gear cases were compared to the closed form solutions from the single mesh program with the results giving excellent correlation. Thus, the validity of the multiple mesh program's numerical solution was also verified. The combination of the two programs makes a more complete package of the analyses.

The first test case used for the program evaluation was a Stoeckicht 2K-H planetary gear system with three planets and spur gear teeth. Strain gauge data was available through published articles (JSME) for three different static load cases; References 6, 7 and 9. The dynamic loads predicted by the theory were within the reported range of + 2 x standard deviation (i.e., 95%) of the experimental data. The theoretical loads were near the high side of the experimental load range for the highest static load, near the middle of the range for the middle load, and near the lower experimental limit for the lowest load case. In each case, the theory underestimates the loads at high speeds but this is most likely due to the sun gear's reported effective mass being too large, causing the peak resonance to theoretically occur at a lower speed. Various combinations of tooth errors were applied to the two lower load cases resulting in good correlation between the experimental load range and theoretical load range.

In addition to the non-synchronous system, a similar planetary with synchronous meshing was also tested with high static load. The theory correlated well with the experimental range. However, the test results indicated that a non-tooth meshing natural frequency existed in the operating range which influenced the dynamic tooth loads. The analytical model is for tooth meshing responses only and, therefore, could not predict this mode.

The second system used for program evaluation was a three planet planetary used in the PT-6 series of aircraft engines. The strain gauge data available was for a very limited speed range. The theory predicted stresses considerably higher than the reported experimental stresses, more so for the higher load case. The lower load cases had better correlation with generally conservative theoretical predictions. Various effective masses were tried to examine the effect on the peak responses. The result of decreasing the masses was to shift the speeds at which resonance occurred to higher speeds. The effect resulted in better correlation between the test and the theoretical data. However, a basic problem exists when comparing analytical to experimental stresses of gear teeth for dynamic response. Strain gauge size and location can influence the results significantly. Frequently the gauges are used as the load transducers by calibration from a known static load. The PT-6 data, though, was reported as stress only.

The last system compared was a Hamilton Standard first-stage turboprop reduction gearbox. Limited gear tooth strain gauge data was available for four levels of loading. For the lowest load case, the theory yielded low estimates of the stresses, especially at higher speeds, while for the higher load cases the theory predicted conservative stress levels. The strain gauge data had to be used directly because a static load calibration had not been done. Therefore, the same problems exist for this data as with the PT-6 data. A speed survey was done comparing loads with and without profile modifications. The speed survey illustrated the effect of a fixed center input pinion versus a floating pinion. The analytical model assumes a fixed

center and with the non-synchronous meshing resulted in an unequal load share between the planets (idlers) for portions of the operating range. The actual test setup had a floating pinion which resulted in nearly equal load share Therefore, the analytical capability of a floating sun should be given consideration for future development.

In general, the correlation between the test data and the program was good. The program predicted the general location of the natural tooth meshing frequencies, which in itself is a major accomplishment because of the nonlinear meshing action of the teeth, i.e. the non-synchronous meshing, the nonlinear tooth-pair stiffness, and the variable contact ratio. The program also indicated that non-synchronous meshing in planetary systems indeed does minimize the dynamic response of the system because of the varying time at which the respective meshes come into contact. In fact, the program showed that with non-synchronous meshing and contact ratios greater than 1.0 the dynamic tooth load/static single tooth load factor could be designed to be always less than 1.0 because at any instant in time the input torque would be divided by more than the number of planets. In fact, the average number of teeth in contact is the contact ratio times the number of planets.

II. PROGRAM MODIFICATIONS

A. Variable Contact Friction

Prior to this contract, the multiple mesh program required a constant coefficient of friction to be inputted. Modifications have been made to the program to internally calculate the coefficient of friction as a variable throughout the mesh. The required input now is the type of oil used.

The coefficient of friction is a function of the Benedict-Kelley parameter[3]:

$$X = log_{10}\left[\frac{u_o V_S V_T^2}{L/W}\right] \tag{1}$$

where L/W is the load per unit face width, V_T is the sum velocity, V_S is the sliding velocity, and U_0 is the absolute viscosity of the oil.

The empirical equation of the line representing the data points presented by Benedict & Kelley[3] and shown in Figure 1 is:

$$\mu = -.0130556\,X + .1093 \tag{2}$$

where μ is the coefficient of friction.

The absolute viscosity, U_0, used for the above expression must be input to the program via an oil type. The other variables are already available in the program. The absolute viscosity is given by:

$$u_o = \rho\, Z_K \tag{3}$$

where ρ is the specific gravity of the oil and Z_K is the kinematic viscosity, plotted in Figures 2 and 3 vs. oil inlet temperature.

The input parameter has been changed from a constant coefficient of friction to an oil type code. A code of 1 is for MIL-L-23699 oil, a code of 2 is for MIL-L-7808 oil, and a code of 0 will default to MIL-L-23699 oil. There are also codes 3 and 4 which are available for two other oil types that can be added later.

The coefficient of friction influences the flash temperature, T_f, by the equation:

$$T_f = T_i + m\mu \tag{4}$$

where T_i is the inlet temperature and M is a function of several parameters which can be found in Reference 1.

A comparison case was executed using a single sun-planet mesh. The calculated coefficients of friction are less than the .05 assumed for the original case, thus the new flash temperatures are lower and should be more realistic. Figure 4 shows the flash temperatures before and after the friction coefficient modifications.

The modified program also calculates an average coefficient of friction throughout the mesh for each sun-planet and ring-planet mesh.

B. Flexible Planet Carrier and Ring Gear Rim

The previously developed dynamic load equations for planetary gear systems assumed rigid planet carriers and ring gear rims. The only flexibilities modeled in the planetary dynamic model were the tooth-pair flexibilities. Presently designed aircraft type planetary gear systems generally have flexible planet carriers and ring gear rims because of weight requirements. It was felt that the gear tooth dynamics would be influenced by these flexibilities. Therefore, the dynamic load equations and program were expanded to include the planet carrier and ring gear rim flexibilities.

The equations defining the planetary model are based on relative tooth-pair motions acting along the respective meshing lines-of-action. For the effect of the planet carrier and ring gear rim flexibilities on the gear tooth dynamics, the motions of the planet carrier and ring gear rim were considered only along the meshing lines-of-action. In other words, azimuthal motions of the carrier and ring rim were used and any radial component of motion was assumed to be secondary to the tooth-pair meshing flexibility.

Figure 5a is a schematic of the dynamic model. Azimuthal springs are introduced between each planet to represent the carrier and ring rim flexibilities. Each azimuthal carrier and ring rim segment also has a respective inertia.

Damping of the segments is assumed to be insignificant relative to the tooth meshing damping. Tooth meshing damping has been found to be approximately 5-10% of critical and ordinary structural damping is less than 2% of critical.

Using the model of Figure 5 the equilibrium equations can be written. For the sun gear

$$m_s \ddot{y}_s + \sum_{i=1}^{n} d_{sp_i} (\dot{y}_s - \dot{y}_{p_i} - \dot{y}_{c_i}) + \sum_{i=1}^{n} k_{sp_i} (y_s - y_{p_i} - y_{c_i}) = \frac{T_{in_s}}{R_{b_s}} \quad (5)$$

For the planet gears

$$m_{p_i}\ddot{Y}_{p_i} - d_{sp_i}(\dot{Y}_s - \dot{Y}_{p_i} - \dot{Y}_{c_i}) - d_{rp_i}(\dot{Y}_{p_i} - \dot{Y}_{c_i} - \dot{Y}_{r_i})$$

$$-k_{sp_i}(Y_s - Y_{p_i} - Y_{c_i}) + k_{rp_i}(Y_{p_i} - Y_{c_i} - Y_{r_i}) = 0. \qquad (6)$$

For the planet carrier segments

$$m_{c_i}\ddot{Y}_{c_i} - d_{sp_i}(\dot{Y}_s - \dot{Y}_{p_i} - \dot{Y}_{c_i}) - d_{rp_i}(\dot{Y}_{p_i} - \dot{Y}_{c_i} - \dot{Y}_{r_i})$$

$$-k_{sp_i}(Y_s - Y_{p_i} - Y_{c_i}) - k_{rp_i}(Y_{p_i} - Y_{c_i} - Y_{r_i})$$

$$+k_{c_i}(Y_{c_i} - Y_{c_{i+1}}) + k_{c_{i-1}}(-Y_{c_{i-1}} + Y_{c_i}) = -\frac{T_{OUT_c}}{n R_{b_c}}. \qquad (7)$$

For the ring gear segments

$$m_{r_i}\ddot{Y}_{r_i} - d_{rp_i}(\dot{Y}_{p_i} - \dot{Y}_{c_i} - \dot{Y}_{r_i}) - k_{rp_i}(Y_{p_i} - Y_{c_i} - Y_{r_i})$$

$$+k_{r_{i-1}}(-Y_{r_{i-1}} + Y_{r_i}) + k_{r_i}(Y_{r_i} - Y_{r_{i+1}}) = -\frac{T_{OUT_r}}{n R_{b_r}}. \qquad (8)$$

The rotation is that used in References 1 and 2 and defined in Figure 5. The second order differential equations are solved numerically because of the large number of equations, (3n + 1), where n is the number of planet gears. The routine used requires that the differential equations be transformed to first order differential equations. This is done by the following transformation.

Let $X_{s_0} = Y_s$, $X_{p_{i0}} = Y_{p_i}$, $X_{c_{i0}} = Y_{c_i}$, $X_{r_{i0}} = Y_{r_i}$

$X_{s_1} = \dot{Y}_s$, $X_{p_{i1}} = \dot{Y}_{p_i}$, $X_{c_{i1}} = \dot{Y}_{c_i}$, $X_{r_{i1}} = \dot{Y}_{r_i}$

$\dot{X}_{s_1} = \ddot{Y}_s$, $\dot{X}_{p_{i1}} = \ddot{Y}_{p_i}$, $\dot{X}_{c_{i1}} = \ddot{Y}_{c_i}$, $\dot{X}_{r_{i1}} = \ddot{Y}_{r_i}$ (9)

Substituting (9) into (5) through (8) gives

$$\dot{X}_{s_1} + \frac{1}{m_s}\sum_{i=1}^{n} d_{sp_i}(X_{s_1} - X_{p_{i1}} - X_{c_{i1}}) + \frac{1}{m_s}\sum_{i=1}^{n} k_{sp_i}(X_{s_0} - X_{p_{i0}} - X_{c_{i0}})$$

$$= \frac{T_{IN}}{m_s R_{b_s}} \qquad (10)$$

$$\dot{X}_{p_{i1}} - \frac{1}{m_{p_i}} d_{sp_i}(X_s - X_{p_{i1}} - X_{c_{i1}}) - \frac{1}{m_{p_i}} d_{rp_i}(X_{p_i} - X_{c_{i1}} - X_{r_{i1}})$$

$$-\frac{1}{m_{p_i}} k_{sp_i}(X_{s_0} - X_{p_{i0}} - X_{c_{i0}}) + \frac{1}{m_{p_i}} k_{rp_i}(X_{p_{i0}} - X_{c_{i0}} - X_{r_{i0}}) = 0. \qquad (11)$$

$$\dot{X}_{c_i1} - \frac{1}{m_{c_i}} d_{sp_i}\left(X_{s_1} - X_{p_{i1}} - X_{c_{i1}}\right) - \frac{1}{m_{c_i}} d_{rp_i}\left(X_{p_{i1}} - X_{c_{i1}} - X_{r_{i1}}\right)$$
$$- \frac{1}{I_{c_i}} k_{sp_i}\left(X_{s_0} - X_{p_{i0}} - X_{c_{i0}}\right) - \frac{1}{I_{c_i}} k_{rp_i}\left(X_{p_{i0}} - X_{c_{i0}} - X_{r_{i0}}\right)$$
$$+ \frac{k_{c_i}}{I_{c_i}}\left(X_{c_{i0}} - X_{c_{i+1_0}}\right) + \frac{k_{c_{i-1}}}{I_{c_{i-1}}}\left(-X_{c_{i-1_0}} + X_{c_{i0}}\right) = -\frac{T_{out_c}}{I_{c_i} n R_{b_c}} \quad (12)$$

$$\dot{X}_{r_{i1}} - \frac{1}{I_{r_i}} d_{rp_i}\left(X_{p_{i1}} - X_{c_{i1}} - X_{r_{i1}}\right) - \frac{1}{I_{r_i}} k_{rp_i}\left(X_{p_{i0}} - X_{c_{i0}} - X_{r_{i0}}\right)$$
$$+ \frac{1}{I_{r_{i-1}}} k_{r_{i-1}}\left(-X_{r_{i-1_0}} + X_{r_{i0}}\right) + \frac{1}{I_{r_i}} k_{r_i}\left(X_{r_{i0}} - X_{r_{i+1_0}}\right) = -\frac{T_{out_r}}{I_{r_i} n R_{b_r}} \quad (13)$$

$$\dot{X}_{s_0} = X_{s_1} \quad (14)$$

$$\dot{X}_{p_{i0}} = X_{p_{i1}} \quad (15)$$

$$\dot{X}_{c_{i0}} = X_{c_{i1}} \quad (16)$$

and

$$\dot{X}_{r_{i0}} = X_{r_{i1}} \quad (17)$$

for a total of (6n+2) first order differential equations. The output torque is assumed to be divided evenly among either the planet carrier segments or the ring gear rim segments depending on which type of planetary is being modeled.

The tooth-pair load terms of equations (10) through (13)

are

$$k_{sp_i}\left(X_{s_0} - X_{p_{i0}} - X_{c_{i0}}\right) \quad (18)$$

and

$$k_{rp_i}\left(X_{p_{i0}} - X_{c_{i0}} - X_{r_{i0}}\right) \quad (19)$$

Tooth spacing error, profile modification terms, and a tooth-pair contact identity function must be added to the tooth-pair load terms as shown

$$k_{sp_i}\left(x_{s_o} - x_{p_{io}} - x_{c_{io}} - e_{sp_i} - \rho_{sp_i}\right)\phi_{sp_i} \tag{20}$$

and

$$k_{rp_i}\left(x_{p_{io}} - x_{c_{io}} - x_{r_{io}} - e_{rp_i} - \rho_{rp_i}\right)\phi_{rp_i} \tag{21}$$

The tooth-pair contact identity functions ϕ_{sp_i} and ϕ_{rp_i} are either 1 or 0 depending on whether the individual tooth-pairs are in contact or not. Contact is determined by the value in the parentheses of (20) and (21). If the value is positive, the tooth-pair is in contact. If the value is negative, the tooth pair is not in contact.

When a planetary system is being modeled, the ring gear is grounded and the x_{r_i} terms vanish. When a star system is being modeled the planet carrier is grounded and the x_{c_i} terms vanish.

The above development results in more than doubling the required number of equations. The previous solution, Reference 1, used the relative tooth-pair displacements as the generalized coordinates, whereas this development uses the absolute tooth-pair displacements as the generalized coordinates. The absolute displacements must be used because of the additional degrees-of-freedom needed for the planet carrier and (or) ring gear rim segments.

C. User Friendly Options

Some "user friendly" options have been incorporated into the program. The user can choose to run at any of three levels. The first level requires minimal input such as diametral pitch, pressure angle, number of teeth, face widths, torque, speed range, equivalent masses, type of system, number of planets, and contact ratio if it is greater than 2. The remaining variables default (see user manual for values) allowing the user to obtain approximate results with minimum input. The next level requires the input of level 1 plus damping, flash temperature data, iteration data, and planet phasing constants. Other optional variables that may be input at level 2 include: profile modification data, face width crowning, Hertz stress for compliance calculation, plane stress or plane strain trigger, active face widths, convective compliance matrix (helical gears), geometric data, geometric tolerances, helix errors, tooth pair spacing errors, and initial boundary conditions. These level 2 optional variables will default to zero, or the values indicated in the user guide if not specified. Level 3 includes all of the above, as well as profile modification shape factors, compliance

constants, and 3-dimensional factors. In addition to the choice of levels, the documentation has been expanded to ease the user's task of setting up the input data for any level. The program output has also been modified for clarity. For further input details and default values, refer to the user manual.

D. Dynamic Side Bands

Dynamic sidebands are observed in frequency spectra where they usually occur in plus or minus integer multiples of the primary gear mesh frequency. This phenomenon is often associated with inherent manufacturing errors, such as gear runout.

For the sideband option, runout errors are simulated by applying a sinusoidal error distribution on the input pinion. The user inputs the displacement deviation in center location of the sun. This is then used to generate a tooth spacing error array using the following equation.

$$\Delta_{r_s} = \Delta_r \sin\left(2\pi\left(\frac{n}{N}\right)\right) \sin\phi_o \qquad (22)$$

where Δ_{r_s} is the spacing error
Δ_r is the input displacement error
n is the current tooth number
N is the total number of teeth on the pinion
and ϕ_o is the pressure angle

The error array internally generated is printed after the no-error solution and is followed by error passes illustrating the various tooth pair meshes with corresponding summary tables of maximum values output.

In order to obtain sideband information, the load data must be used in conjunction with a Fourier analysis in order to look at the results in the frequency domain. The program outputs all of the loads and corresponding times, in a WRITE (7,5029) format so the data can be analyzed separately.

An example case was executed with a displacement error of .001 inch. The maximum normal load varied from 3045. lbs. to 5723. lbs., while the no-error maximum load was 4387. lbs. The load data was used in conjunction with a Fourier analysis program, the results of which are illustrated in Figures 6a and 6b.

E. Speed Survey Option

The program has been modified to include the option of surveying a range of input speeds. The user inputs the initial and final speeds of the range desired, and the number of intervals into which the range is to be divided. The program steps through the speed range determining the maximum tooth load for each speed, where step size = (final -initial speed)/number of intervals.

The difference between consecutive loads is calculated. A change in sign from positive to negative indicates a peak has been passed. The speed step size is then divided by five, and the prior two intervals are reanalyzed to find the peak value. The program then continues through the range checking for other peaks. At the end of the range, the speed corresponding to the overall maximum load is retained and used for the remaining calculations. Examples can be seen in Figure 23 and Figure 30.

The user should note that a peak could be missed if the number of intervals specified is too small; however, CPU time will increase proportionally with increased number of intervals. A missed peak is likely to occur for cases with low damping, which would lead to narrow sharp peaks. One indication of a missed peak would be if the loads for the smaller step size continually decrease through the interval. If this occurs, the user should re-run the program with different intervals. One should also note that the boundary conditions are iterated for each RPM; thus, if the number of boundary condition iterations is large, a smaller range should be used with user specified boundary conditions to avoid using excessive CPU time

There are also two messages that may appear in the printout. If the load monotonically decreases in the first speed interval, a message is printed that the initial rpm is on a decreasing load curve. Similarly, if the final speed is on an increasing load curve a corresponding message is printed. These messages indicate that the user may want to re-run the program and check either lower or higher speeds, respectively. These are in addition to loads for each mesh at each speed.

F. Nonplanetary Systems

1. Sun-Planet(s) Option

The original multiple mesh program simulated the sun-planet(s) option by the user inputting a trigger; SNPLBT = 1.0, which would set the compliance of the ring teeth to a very large value. The input now requires the system type trigger, K, be set to 4 for the sun-planet(s) option. This option is now solved exactly with the system equations given below.

The sun is the input pinion while the planets are the output gears as shown in the following figure:

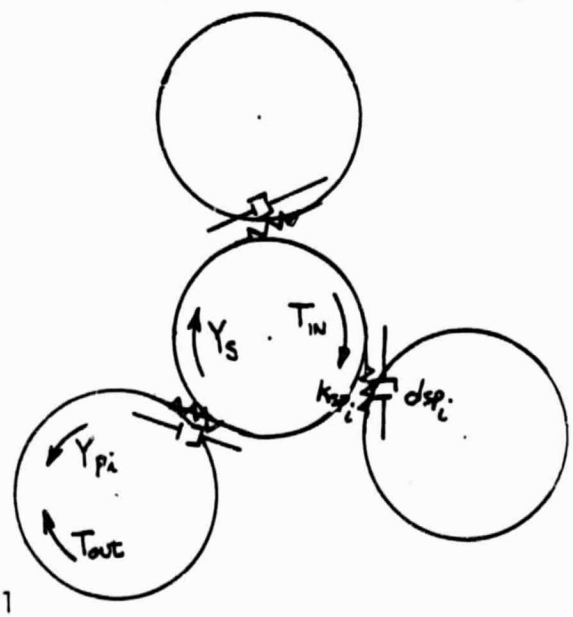

The following equilibrium equations can be written corresponding to the prior figure:

(Sun gear)

$$I_s \ddot{Y}_s + \sum_{i=1}^{n} d_{sp_i} \dot{Y}_{sp_i} + \sum_{i=1}^{n} k_{sp_i} Y_{sp_i} = \frac{T_{IN}}{R_{bs}} \tag{23}$$

(Planet gears)

$$I_{p_i} \ddot{Y}_{p_i} - d_{sp_i} \dot{Y}_{sp_i} - k_{sp_i} Y_{sp_i} = -\frac{T_{OUT_{p_i}}}{R_{bp_i}} \tag{24}$$

where d_{sp_i} and d_{rp_i} are the viscous damping terms, I_s and I_{pi} are the rotational inertias, k_{sp_i} and k_{rp_i} are tooth pair stiffness terms, T_{in} and T_{outpi} are input and output torques, and R_{bs} and R_{bpi} are gear involute base radii.

Subtracting (24) from (23) yields n relative motion equations:

$$\ddot{Y}_{sp_i} + \sum_{i=1}^{n} \frac{d_{sp_i}}{I_s} \dot{Y}_{sp_i} + \frac{d_{sp_i}}{I_{p_i}} \dot{Y}_{sp_i} + \sum_{i=1}^{n} \frac{k_{sp_i}}{I_s} + \frac{k_{sp_i}}{I_{p_i}} Y_{sp_i} = \frac{T_{IN}}{I_s R_{bs}} + \frac{T_{OUT}}{I_{p_i} R_{bp}} \tag{25}$$

where $Y_{sp} = Y_s - Y_{p_i}$

For a one planet system (n=1), equation (25) reduces to Richardson's equation[1] for a single external-external gear mesh as follows:

$$\ddot{Y}_{sp} + \left(\frac{1}{I_s} + \frac{1}{I_p}\right) d_{sp} \dot{Y}_{sp} + \left(\frac{1}{I_s} + \frac{1}{I_p}\right) k_{sp} Y_{sp} = \frac{T_{IN}}{I_s R_{bs}} + \frac{T_{OUT}}{I_p R_{bp}} \tag{26}$$

$$\frac{T_{IN}}{R_{bs}} = \frac{T_{OUT}}{R_{bp}} = L_o \tag{27}$$

$$\left(\frac{1}{I_s} + \frac{1}{I_p}\right) = \frac{1}{m_E} \tag{28}$$

$$\ddot{Y}_{sp} + \frac{d_{sp}}{m_E}\dot{Y}_{sp} + \frac{k_{sp}}{m_E}Y = \frac{L_o}{m_E} \tag{29}$$

where M_E is the meshing effective mass and L_0 is the static tooth load consistent with the gear torques.

For multiple planet cases equation 25 can be rewritten as:

$$\ddot{Y}_{sp_i} + \frac{1}{m_s}\sum_{1}^{\hat{n}} d_{sp_i}\dot{Y}_{sp_i} + \frac{d_{sp_i}}{m_{p_i}}\dot{Y}_{sp_i} + \frac{1}{m_s}\sum_{1}^{n} k_{sp_i}\bar{Y}_{sp_i} + \frac{k_{sp_i}}{m_{p_i}}\bar{Y}_{sp_i} = \frac{T_{IN}}{m_s R_{bs}} + \frac{T_{OUTp_i}}{m_{p_i} R_{bp_i}} \tag{30}$$

$$\bar{Y}_{sp_i} = Y_{sp_i} - e_{sp_{ji}} - \bar{X}^2_{sp_{ji}}\beta^2_{sp_{ji}} \tag{31}$$

Here e_{sp} and $\bar{x}^2_{sp}\,\beta^2_{sp}$ are the tooth spacing error and the involute profile modification terms, respectfully, of mesh i and tooth-pair j.

The tooth-pair meshing loads are

$$L_{sp_i} = \sum_{j=1}^{m}\left(\left[Y_{sp_i} - e_{sp_{ji}} - \bar{X}^2_{sp_{ji}}\beta^2_{sp_{ji}}\right] n_{sp_{ji}}\phi_{sp_{ji}}\right) \tag{32}$$

where m is the number of teeth in contact at mesh i, n_{sp} is the tooth pair stiffness and ϕ is a tooth-pair contact identity function.

Transform to 2n first-order equations of the following form as was done above for the flexible carrier and ring gear rim equations of motion:

$$\dot{X}_{sp_{i1}} + \frac{1}{m_s}\sum_{1}^{\hat{n}} d_{sp_i}X_{i1} + \frac{1}{m_{p_i}}d_{sp_i}X_{i1} + \frac{1}{m_s}\sum_{1}^{n} L_{sp_i} + \frac{1}{m_{p_i}}L_{sp_i} = \frac{T_{IN}}{m_s R_{bs}} + \frac{T_{OUTp_i}}{m_{p_i} R_{bp_i}} \tag{33}$$

$$\dot{X}_{sp_{i0}} = X_{sp_{i1}} \tag{34}$$

These equations are similar to the sun-planet equations of a star system, Reference 1, except there are no ring-planet terms or equations.

A test case was executed for spur gears using both the single-mesh program, which has a closed form solution, and the multiple-mesh program, which uses a numerical solution, with one planet. Table 1 contains the solutions from the multiple mesh program compared to the single mesh solution and the corresponding percent differences.

For a boundary condition tolerance of 0.5%, the differences between the closed form solution and the numerical solution maximum values were less than 2%. This comparison also verifies the validity of the numerical solution iteration parameters used in the multiple mesh program. Figures 7 and 8 show the single mesh loads and multiple mesh loads with the corresponding data sets, both for one mesh cycle, respectively.

2. Ring-Planet(s) Option

This ring-planet is input is similar to the sun-planet option in that the old trigger, SNPLBT = 2.0, would set the compliance of the sun teeth to a very large value. The input now required is that the system type trigger, K, be set to 5 for a ring-planet(s) mesh.

The planets act as the input pinions, with the input torque being per planet, while the ring acts as the output gear as shown below:

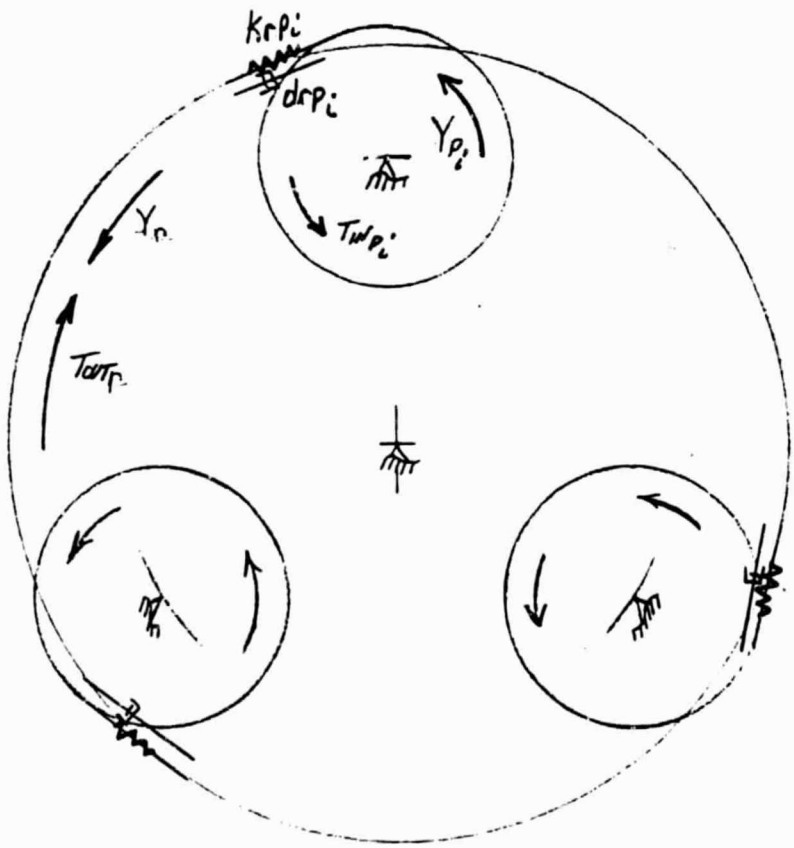

The equilibrium equations corresponding to the previous illustration can be written for the ring gears and planet gear as follows:

(Ring gear)

$$m_r \ddot{Y}_r - \sum_{i=1}^{n} d_{rp_i} \dot{Y}_{rp_i} - \sum_{i=1}^{n} k_{rp_i} Y_{rp_i} = -\frac{T_{OUT_r}}{R_{b_r}} \tag{35}$$

(Planet gears)

$$m_{p_i} \ddot{Y}_{p_i} + d_{rp_i} \dot{Y}_{rp_i} + k_{rp_i} Y_{rp_i} = \frac{T_{IN_{p_i}}}{R_{b_{p_i}}} \tag{36}$$

Subtracting (35) from (36) the following relative motion equations can be obtained:

$$\ddot{Y}_{rp_i} + \frac{1}{m_r} \sum_{1}^{n} d_{rp_i} \dot{Y}_{rp_i} + \frac{1}{m_r} d_{rp_i} \dot{Y}_{rp_i} + \frac{1}{m_r} \sum_{1}^{n} k_{rp_i} Y_{rp_i} + \frac{1}{m_{p_i}} k_{rp_i} Y_{rp_i} = \frac{T_{IN_{p_i}}}{m_{p_i} R_{b_{p_i}}} + \frac{T_{OUT_r}}{m_r R_{b_r}} \tag{37}$$

Equation (37) can be rewritten as

$$\ddot{Y}_{rp_i} + \frac{1}{m_r} \sum_{1}^{n} d_{rp_i} \dot{Y}_{rp_i} + \frac{1}{m_r} d_{rp_i} \dot{Y}_{rp_i} + \frac{1}{m_r} \sum_{1}^{n} L_{rp_i} + \frac{1}{m_{p_i}} L_{rp_i} = \frac{T_{IN_{p_i}}}{m_{p_i} R_{b_{p_i}}} + \frac{T_{OUT_r}}{m_r R_{b_r}} \tag{38}$$

where

$$L_{rp_i} = \sum_{j=1}^{m} \left(\left[Y_{rp_i} - e_{rp_{ji}} - \bar{X}^2_{rp_{ji}} \beta^2_{rp_{ji}} \right] n_{rp_{ji}} \phi_{rp_{ji}} \right) \tag{39}$$

Transform equation (38) to 2n first order equations:

$$\dot{X}_{rp_{i,1}} + \frac{1}{m_r} \sum_{1}^{n} d_{rp_i} X_{rp_{i,1}} + \frac{1}{m_{p_i}} d_{rp_i} X_{rp_{i,1}} + \frac{1}{m_r} \sum_{1}^{n} L_{rp_i} + \frac{1}{m_{p_i}} L_{rp_i} = \frac{T_{IN_{p_i}}}{m_{p_i} R_{b_{p_i}}} + \frac{T_{OUT_r}}{m_r R_{b_r}} \tag{40}$$

$$\dot{X}_{rp_{i,0}} = X_{rp_{i,1}} \tag{41}$$

These equations are similar to the ring-planet equations for a star system, Reference 1, with no sun-planet terms or equations.

A test case was run on both the single mesh and multiple mesh program for an internal-external mesh. The maximum values are presented in Table 2, along with the percent differences between the exact single mesh solutions and the numerical solutions of the multiple mesh program. The table is followed by the input data set for the multiple mesh program, Figure 9. Again there is excellent correlation, with the maximum difference being 3.85%. The higher percentage difference, compared to the sun-planet mesh, is due to a 1% convergence tolerance for boundary condition iterations, rather than 0.5% used for the sun-planet mesh.

3. Profile Modifications

In addition to the options eliminating the planet carrier and ring or sun gear, an additional input variable has been added for tooth profile modifications. The user can now specify the amounts of tooth tip and flank reliefs for each gear for a more comprehensive tooth profile modification table given in the program output.

III. EVALUATION OF PROGRAM

A. Introduction

Task II required evaluating the analytical method by comparing the program results with published test data and Hamilton Standard test data from a turboprop reduction gearbox. After extensive searching through engineering indexes via computer, and by hand for older publications, it was found that very little published test data of sufficient detail existed. An exception to this was a series of articles published in the Bulletin of the Japanese Society of Mechanical Engineers. They have published several articles which document their experimental investigations into dynamic tooth loading in planetary gears.

Another article, reference 4, was located that implied strain gauge data had been taken at Pratt & Whitney Aircraft of Canada on a planetary system. The author was contacted and asked to send test data. The data received was very limited in that only a small speed range was tested and there was little information as to the specific test procedure. Limited data was also the case with the Hamilton Standard test program for the turboprop gearbox. The strain gauge data on the gear teeth was limited due to the number of available monitoring channels.

B. Experimental and Modeling Characteristics

1. Japanese Stoeckicht 2K-H Planetary

Extensive testing was performed on a nonsynchronous meshing, three planet, planetary spur gear system. The basic characteristics are found in Table 3 and an illustration is given in Figure 10. Table 4 contains the characteristics of a similar test system that has synchronous meshing.

The nonsynchronous meshing system was designed for 20KW of transmitted power, a speed ratio of 6, and the working range of the higher speed shaft from 1800 to 7200 rpm. The synchronous meshing system has similar design features.

A power circulating type planetary gear testing machine was used to monitor the fillet strains in three sun gear teeth. Resistance wire strain gauges were placed on the compression side of the roots of tooth numbers 1, 5 and 10 of the sun gear. A tooth of the sun gear will engage 30 times with the

planet gears before returning to the same engaging position. Therefore, 90 pieces of fillet strain data, 30 per tooth, were used to obtain a mean dynamic load factor and coefficient of variation.

Typical input data sets are shown in Figure 11. The tooth geometry was obtained from the program geometric preprocessor as this information was not published. The program geometric preprocessor generates the basic tooth geometry using basic involute relationships given in Reference 1. A model damping ratio of 10% was used, corresponding to the 10% ratio used in the Japanese theoretical calculations. The equivalent mass for the planet carrier includes additional mass due to a low speed rotor in the test set-up.

2. First-Stage Reduction gear, Model A-27

The Pratt & Whitney epicyclic, first-stage reduction gear for the PT6 series of engines has 3 planets with synchronous meshing. The basic characteristics are shown in Table 5 and the system is illustrated in Figure 12. The input speed is 30,000 RPM or higher for normal operation[4].

Two strain gauges were placed in a fillet of the sun gear, each located 1/4 inch from the edge. The number of fillets monitored was not available. Data was taken for several different tangential load cases and for various sun gear rotational speeds.

An input data set is illustrated in Figure 13. The detailed tooth geometry was available for all the gears; thus, the geometric preprocessor was bypassed. Modal damping ratios of 20% were used for the various loads, and two load cases were also run with 10% damping ratios.

3. Hamilton Standard Turboprop Gearbox

The turboprop gearbox is a two-stage non-planetary system with characteristics found in Table 6 and a system diagram found in Figure 14. The tooth fillet strain gauge data available was for the first stage only. The gauges were located on an idler gear in a total of 6 fillets, 3 consecutive fillets on opposite sides of the gear, with 2 gauges located in the center of the width and 2 gauges each on both edges, as shown in Figure 15. Maximum stresses were observed for several loading conditions at various speeds; however, the maximum number of these gauges observed for a certain condition was four and the minimum two. This was due to a limited number of monitoring channels. For better load share between the two idler gears a floating input pinion (sun gear) was used for the design.

An example input data set can be found in Figure 16. Damping ratios of 5% and 10% were used. The geometry was directly input, bypassing the preprocessor, with the actual profile modifications being included for most of the cases, while one case was run with no modifications for load comparison.

C. Data & Results

1. Stoeckicht 2K-H Planetary

The test data for the Stoeckicht 2K-H planetary system was presented as a mean dynamic load factor and a coefficient of variation. The dynamic load factor is defined as the ratio of the dynamic strain to the static strain at corresponding positions, and the coefficient of variation is the standard deviation divided by the mean dynamic load. These data were then used to obtain the dynamic load range that included $\pm$ 2 standard deviations, or the range where approximately 95% of the loads would be expected to occur based on the experimental data. The test data used were the maximum fillet strains in a zone of single tooth contact.

Figure 17 illustrates the maximum dynamic loads for a static tangential tooth load of 130N (29.25 lbs.) for the nonsynchronous meshing case. The original effective masses are the same as the authors[5] used in their evaluation, with the carrier mass including the low speed rotor effective mass, as is the damping ratio of 10%. Variations of both of these parameters are also shown. The Japanese theoretical calculations were also presented as a mean dynamic load factor and a coefficient of variation, where the mean dynamic load factor is approximately 1. The upper limit of their theoretical variation (+2 standard deviations) appears on Figure 17 and includes the theoretical effect of tooth profile errors.

Figure 18 illustrates maximum dynamic loads for a static tangential load of 90N (20.25 lbs.), while Figure 19 shows results for a static tangential load of 50N (11.25 lbs.) Both figures are for nonsynchronous meshing and include computer runs for both with and without tooth spacing errors. Figure 19 also includes an effective mass variation for both with and without tooth spacing errors.

The synchronous meshing case is shown in Figure 20 in which the conditions are similar to those used in obtaining Figure 17. The tooth numbers and diametral pitch were adjusted while the pitch radii, pressure angle and speed ratio were kept constant. A case with a tooth error is also illustrated in Figure 20.

2. A-27 First-Stage Reduction Gears

The test data obtained for the PT-6 first-stage gear, model A-27, consisted of a plot of maximum peak sun gear dynamic stress vs. sun gear rotational speed for various constant transmitted loads. No information was available as to how many teeth were strain gauged, except a diagram indicating only two gauges on one tooth root and reference 4 indicating two sun gear teeth were strain gauged. Thus, the variation of stresses was not obtained experimentally.

Figure 21 contains the lower load cases, for transmitted loads of 445N, 890N and 1335N (100 lbs., 200 lbs., and 300 lbs.). All three cases were run

with a relatively high modal damping ratio of 20% and the 1335N (300 lbs.) load was also run at 10% damping. Similarly, Figure 22 illustrates the higher tangential load range. Loads of 1557N, 1668N, 1779N and 2002N (350 lbs., 375 lbs., 400 lbs. and 450 lbs.) were all run with 20% damping, and the 2002N case was also run with 10% damping.

Figure 23 shows maximum normal loads vs. speeds for several effective masses and for both sun-planet and ring-planet meshes. All load curves are for the 2002N (450 lbs.) tangential load case. The sun-planet mesh is shown to have two resonant speeds, while the ring-planet mesh has one major peak that occurs at a speed in between the two sun-planet peaks.

3. Hamilton Standard Turboprop First-Stage Reduction Gear

The strain gauge data taken on the turboprop reduction gear system was limited in applicability for comparison to the program results. One idler gear, which meshes with the input pinion had a total of 6 gauges in the tooth root area. For each run at various torque levels, different combinations of gauges and corresponding peak stresses were monitored. Gauges had been installed on the bull gear teeth also, but they were not monitored due to the lack of channels available. Thus, no data was available for the second-stage, only for the first-stage idler gear that meshes with the input pinion.

Figures 24 and 25 show the average of the experimental peak stresses and the average of the two theoretical input pinion-idler meshes. Cases were run with profile modifications, as the actual gears tested had profile modifications. The effects of different damping ratios are also illustrated.

Figures 26 through 29 show each load level individually, with maximum, minimum and average experimental peak stress points plotted. Different planet (idler) stresses calculated by the multiple mesh program, due to a fixed input shaft in the model and nonsynchronous meshing, are the boundaries for one theoretical band. Note: as discussed earlier, the program assumes fixed centers for the gears, whereas, the input pinion of the system is floating between the idlers. The other theoretical band arises from a nonuniform load distribution across the face width due to the location of the web. By use of finite element analysis done at Hamilton, the loads were found to be approximately 12% greater at the center of the face.

Figure 30 is a speed survey of idler gear load vs. input pinion speed for the 30% torque case which shows two speeds where resonance occurs. This also illustrates the unequal loads that can result due to the theoretical model of a fixed, rather than floating pinion. The differences between loads on a standard involute form and a tooth with a modified involute can also be seen.

D. Discussion of Results

1. Japanese Stoeckicht 2K-H

The Japanese authors performed extensive tests on the Stoeckicht planetary gear system. Two systems were tested, one synchronous meshing and one nonsynchronous meshing. The two systems were kept as similar as possible with the major changes being diametral pitch and number of teeth, in order to make a direct comparison between systems with the major difference being the planet phasing[6].

Figure 17 shows the nonsynchronous meshing system which parallels Figure 20 illustrating the synchronous meshing system. The range of experimental strain gauge results indicate a resonance near 2600 RPM, which is due to a resonance of the total torsional system resulting in torque variations[6]. The analytical program assumes constant torque, thus this resonance would not be predicted. The next resonance indicated experimentally is in the 5000 RPM vicinity. The theory predicts a resonant speed at 5200 RPM.

There is also an experimental resonance at approximately 7200 RPM, which for the synchronous case, is a multiple of the meshing frequency[6]. The experimental range in Figure 20 does not indicate this significantly; however, the in-phase theory predicts peak loads near this speed. Synchronous meshing will generally cause higher loads due to simultaneous meshing of the planets. This is shown by comparing Figures 17 and 20 where both the experimental and analytical loads are high for the synchronous meshing case at the resonant speeds.

Variation of the analytical effective mass has the effect of shifting the speed at which peak loads occur. The masses used for the majority of the theoretical calculations are the masses calculated for the Japanese theoretical evaluation[5]. The theoretical model of Reference 5 is very similar to that used here. The primary differences are that the Reference 5 model includes additional error terms and mass terms for rotor inertias but apparently did not include nonlinear tooth-pair meshing characteristics. Note: the selection of effective masses for the analytical model is not a trivial task in that it is difficult to decide on the amount of attached mass that should be included. These attached masses could be rotors, shafting, mounts, etc. A complete system dynamic analysis would be required to define the equivalent masses, which are frequency dependent. The planetary gear tested contained a high and low speed rotor which were modelled by adding the additional mass to the ring and planet carriers, respectively. However, the ring is fixed for a planetary system and, therefore, has zero rotational moment of inetia and correspondingly, zero effective mass. The actual system has a radially floating ring as well as a floating sun, neither of which is included in the theoretical model.

The shift in the speed at which the peak load occurs, due to altered effective mass, is illustrated in Figures 17 and 19. Figure 17 shows the theoretical peak shifting from about 5300 RPM to approximately 7400 RPM when all masses are divided in half. The half mass results seem to correlate with the experimental data better; however, there is insufficient information to verify either quantity as the actual effective mass. Figure 19 illustrates a lower transmitted load and correspondingly, the peaks are less pronounced. The flatter peaks make the distinction between the peaks less obvious, expecially in the cases with tooth errors where both bands have excellent correlation with the experimental range. The half effective masses seem to correlate with the experimental data better at speeds above 6000 RPM, primarily due to a shift in peak location similar to the one observed in Figure 17.

In addition to the case where all effective masses are halved, a case where only the planet carrier mass was decreased is also shown in Figure 17. There is a slight increase in loads and a slight shift in the main peak toward a higher speed. The differences in loads are less than 3%. Thus, in this case, the carrier effective mass is not the primary mass of the system even though it is the largest effective mass of the system.

Figure 17 also contains a few points at a much lower damping ratio of 5%. This increases the load at 5000 RPM by 26.5% and emphasizes the dynamic peak obtained near 5000 RPM. The Japanese theoretical calculations used a 10% damping ratio which apparently correlated well to the experimental test data.

The effects of tooth errors on the theoretical loads are illustrated in Figures 18 to 20. The loads plotted for the error cases are the minimum and maximum, although the maximum normally occurs in only one mesh and the average increase in loads for the error cases would be considerably lower. The manufacturing errors were estimated in reference 7. The pitch error, profile error and lead error were incorporated in a statistical total for a sun-planet mesh of magnitude .003388 mm (.00013338 in.) using $\sqrt{\Sigma_\mu e_\mu^2}$ from equation (14), Reference 8, where the e_μ's are the various types of tooth errors.

Figure 18 shows the theoretical results of having one tooth error in each of the three sun-planet meshes. At low speeds, the maximum loads predicted are less than 5% higher than the no error case. In the vicinity of the predicted resonance, the deviation increases to about 13% higher and 6% lower than the no error case as one would expect. The deviation decreases at speeds higher than resonance.

Figure 20 shows the synchronous meshing case and has the same magnitude of error applied to one tooth in all three sun-planet meshes, similar to the cases of Figure 18. The higher tangential load tends to decrease the effects of tooth spacing errors on dynamic loads, especially at higher speeds.

Figure 19 has the result of a different configuration of tooth errors plotted. The errors are of the same magnitude as in Figures 18 and 20, but they occur on five consecutive teeth and only one sun-planet mesh. In this case, which is for a very low transmitted load, the increase in load is fairly constant over the speed range, especially for the original mass. The half mass case shows more variation than the initial mass case throughout the speed range and seems to follow the experimental range better, except between 5000 and 7000 RPM where the theoretical band is considerably narrower than the experimental.

When the experimental and theoretical load ranges for the no tooth error and initial mass cases in Figures 17 through 19 are compared, it can be seen that for the highest static load case of 130N, the theoretical loads are near the upper boundary of the experimental range, for the 90N case they are more toward the center of the range, and for the lowest load of 50N, the theoretical loads are near the lower boundary.

2. PT6 First-stage, Model A-27

The strain gauge data for the first-stage A-27 was obtained from Pratt & Whitney of Canada in the form of a plot of stress vs. speed for several transmitted loads. This data is reproduced on Figures 21 and 22.

The results plotted in Figure 21 are for 20% damping and predict stresses higher than the experimental data for the 890N (200 lbs.) and 1335N (300 lbs.). The 890N theoretical case predicts stresses from 17% to 58% higher at 18,800 RPM and 21,800 RPM, respectively. The 1335N theoretical case predicts stresses from 28% to 139% higher at 28,600 and 22,500 RPM. The lowest load, 445N (100 lb.) has the best magnitude correlation, especially at lower speeds -- up to about 23,000 RPM the difference is less than 10%. However, at 30,000 RPM the theoretical stress is 58% lower the experimental stress. The 10% damping case emphasizes any peaks and thus increases the maximum differences and decreases the minimum differences to 155% and 21% for the 1335N (300 lbs.) case. Strain gauge size and placement can significantly affect the results. No static tooth load calibration was made on the gauges; therefore, the gauge data can only be used to indicate tooth load trends. In fact, if the experimental data is normalized, then the correlation is good with theory.

Figure 22 illustrates the higher transmitted load cases. The experimental data indicates a resonance occuring between 28,000 and 31,000 RPM. The minimum deviations for the 20% damping cases range from 27% to 64% corresponding to the loads ranging from 1557N (350 lbs.) to 2002N (450 lbs.). Similarly, the maximum deviations range from 184% to 66% for loads of 1557N to 2002N. The 10% damping case indicates smaller deviations of about 51% near the experimental resonance, however the theoretical peak occurs at a lower speed at which insufficient test data is available.

The experimental data is strange in that the maximum stresses vary by less than 9% near resonance, while the applied tangential load increases by 29%. It may be that the damping of the system is load dependent. The theory predicts stresses that increase in a similar manner to the increase in applied load, with the overall stress increasing by approximately 29%, for assumed constant damping.

The resonance indicated by the experimental data near 29,000 RPM could have been due to the influence of the ring-planet mesh or a system resonance. The theory predicts resonances for tooth-pair meshing, but is not set up to predict overall system responses or shaft responses. The sharp load peak for the ring-planet mesh shown in Figure 23 indicates a strong ring-planet resonance that would be likely to be picked up in experimental test results. As there is no strain gauge data for the ring or elsewhere, it is impossible to differentiate where in the system the resonance is occuring.

The theoretical stresses on Figures 21 and 22 are for standard spur gear teeth with no profile modifications and include no tooth spacing errors. Experimentally, one possible reason for the measured stresses being nearly independent of the applied loads could be due to the effects of inherent manufacturing gear tooth errors.

Figure 23 vividly illustrates the importance of the calculated effective mass used for the analytical model and the effect of varying the effective masses. As the masses are decreased, the peak responses shift to higher speeds. There are two resonant speeds for the sun-planet mesh predicted theoretically; however, experimentally only a small range of speeds was tested which includes only one resonance between 28,000 and 31,000 RPM. This could correspond to either of the peaks theoretically predicted for the sun-planet mesh or could correspond to the one resonance predicted for the ring-planet mesh.

Figure 23 also shows the result of a lower modal damping ratio. As the damping ratio is reduced, the peaks become much more pronounced. One side effect of reduced damping ratios in running the program is generally a larger number of convergence iterations for boundary conditions. Therefore, in most cases, lower damping ratios will require more CPU time than higher damping ratios.

3. Hamilton Standard Turboprop Reduction Gearbox

The test program for the turboprop gearbox involved strain gauging the gear rims, webs, and tooth roots. At different torque levels, various combinations of gauges were monitored. Thus, the peak stress data from some of the gauges located in the fillets, see Figure 15 for locations, were compared to the maximum stress results from the multiple-mesh program.

Figures 24 and 25 illustrate the average of the experimental data points for each speed and the averages of the two theoretical idler (planet) stresses. The experimental data was averaged to eliminate the data scatter. The experimental data scatter is a result of gear runout, tooth spacing errors, tooth geometric tolerances, and strain gauge placement. Some of this data was actively available that could have been used but contract funding was limited and, therefore, beyond the scope of the study. The theoretical data was averaged between the two idlers (planets) because of unequal load share. The actual experimental setup had a vertically floating input pinion which resulted in equal idler load share in the test setup.

Based on the averages, the two lower load cases, Figure 24, have good correlation at lower speeds, and reasonable correlation at the higher speeds. For the two higher load cases in Figure 25, theoretically predicted stresses are considerably higher than the experimental stresses for the lower speeds. The correlation at higher speeds is excellent with an 8.3% difference between the 90% torque case using 5% damping at 21,100 RPM. The 68% torque case had only two speeds at which experimental data was taken, thus comparison may be based on the trends of the other load cases.

The theoretical data shows an increase in stress for speeds higher than the tested range with a peak appearing at about 24,000 RPM. If the theoretical effective masses were increased, shifting the peak to a lower speed, more of the experimental ranges would have paralleled the theoretical stress bands. The higher torque cases, Figures 28 and 29, show the theory being conservative and predicting stresses higher than the experimental data, especially for the lower speeds. If the peaks were shifted, the differences would again be decreased, yielding better correlation between test and theory.

The effect of modal damping is shown in Figure 24. For the 50% torque case, the stresses vary by about 10% for an increase in the damping ratio from 5% to 10%. The largest difference occurs as the pinion speed approaches resonance, as would be expected.

Figures 26 through 29 show the minimum and maximum experimental data points, as well as the average experimental stress and theoretical ranges. However, there are extremely large variations in the experimental stresses, especially for the 30% and 50% torque cases which also had more experimental data points. As mentioned, much of the variation can be attributed to gearmount, tooth spacing errors, tooth tolerances and strain gauge placement. At the lower loads, all of these effects excluding gauge placement are much more influential that at the higher loads because the gear tooth deflections are smaller for lower loads. The tooth errors and tolerance differences are a larger portion of the tooth deflections.

One theoretical band on Figures 26 to 29 represents the stress distribution across the tooth face due to a web located at the center of the face. Studies were conducted using finite element analyses to determine the effect the web had on the load distribution. The result of that study indicated a 12% increase in the center of the face and a 12% decrease near the edges. This variation was applied to the theoretical average to obtain the dashed band on Figures 26 to 29.

Figure 30 is a theoretical speed survey for the lowest torque case, illustrating the effect of profile modifications. The modifications have little effect on the maximum loads at a resonant speed. However, the minimum loads prior to the resonant peak are larger for the modified profile than for the standard involute form.

Theoretical unequal load sharing is also illustrated in Figure 30. In the operating range, the loads are fairly equal. At resonant speeds, however, the loads vary by as much as $\pm$ 26% . The variation is less than $\pm$ 6% for speeds of 25,000 RPM and above. The variation is due to the fixed pinion mathematical model, which does not allow for a floating pinion present in the actual system.

IV. CONCLUSIONS

1. The variable coefficient of friction modifications lead to more accurately predicted flash temperatures.

2. Modifications to make the program user friendly assist the user in setting up the input data via three levels of input, and they aid in interpreting the output.

3. The dynamic side band option allows the user to investigate the simulated effect of a runout error on the input pinion of a single external-external mesh. The number of error solutions calculated is equivalent to the number of teeth on the input pinion, simulating runout for a full mesh cycle. The load data can be used to obtain the frequency spectrum to evaluate the sideband phenomenon.

4. A speed survey option allows the user to obtain load variations from speed range and to determine more readily the speeds where resonances are likely to occur.

5. The addition of nonplanetary, sun-planet(s) and ring-planet(s), systems not only allows for single-mesh equivalent systems, but also allows for multiple planet systems with no planet carriers, and results in one universal analysis program.

6. Comparison of spur gear single mesh configurations in the multiple mesh program to the single mesh program, which has a closed form solution, indicates the numerical solution used for solving the differential equations in the multiple mesh program is accurate.

7. The flexible planet carrier or ring gear rim options resulted in some numerical instabilities. The system equations have been verified by the eigenvalue solution so the problem most likely exists in the numerical solution routines.

8. The comparison of the Stoeckicht 2K-H planetary system data with theory showed the loads correlated well. The other two systems evaluated had stress data rather than load data, which did not correlate as well with theory. In addition, the Stoeckicht load data was presented statistically rather than with absolute measurements and, therefore, corresponded more realistically to theoretical results.

9. The program predicted the general location of the natural frequencies of the three systems, even though the meshing action of the teeth is nonlinear.

10. All three test systems showed a better correlation to theory at higher applied static load levels, while the program tended to underestimate the dynamic loads or stresses for lower static load levels. This is a result of the relative displacements of the tooth pair under load compared to tooth spacing errors. At low loads the spacing errors can significantly affect the dynamic loads. Therefore, for lightly loaded gears the tooth-spacing errors should be carefully defined and analyzed.

11. All three test systems were shown to be very dependent on the equivalent masses and damping ratio input, with respect to resonant speeds and load magnitudes, respectively. This phenomenon is typical of lowly damped systems to vibratory loads. Usually a range of effective mass is studied for sensitivity of dynamic response.

V. REFERENCES

1. Interactive Multiple Spur Gear Mesh Dynamic Load Program, James A. Pike, CR-165514, December, 1981.

2. "Documentation for the Expansion of the Dynamic Load Solution for Multiple Planet Spur Gearing to Helical Gearing", James A. Pike, September, 1983, (Dennis Townsend, NASA-Lewis program monitor).

3. "Instantaneous Coefficients of Gear Tooth Friction", G. H. Benedict and B. W. Kelley, ASLE Transactions 4, 59-70 (1961).

4. "Vibration Measurements on Planetary Gears of Aircraft Turbine Engines", M. Botman, Paper 79-7012 at the 4th International Symposium on Airbreathing Propulsion, Orlando, FL, April 1-6, 1979, AIAA Special Publication.

5. "Analysis of Dynamic Tooth Load on Planetary Gear", Teruaki Hidaka, Yoshio Terauchi & Makoto Fujii, Bulletin of the JSME, Vol. 23, No. 176, Feb. 1980.

6. "Dynamic Behavior of Planetary Gear (6th Report, Influence of Meshing - Phase)", Teruaki Hidaka, Yoshio Terauchi and Kazuteru Nagamura, Bulletin of the JSME, Vol. 22, No. 169, July 1979.

7. ""Dynamic Behavior of Planetary Gear (1st Report Load Distribution in Planetary Gear)", Terauki Hidaka and Yoshio Terauchi, Bulletin of the JSME, Vol. 19, No. 132, June 1976.

8. "Dynamic Tooth Loads and Stressing for High Contact Ratio Spur Gears", R. W. Cornell and W. W. Westervelt, Journal of Mechanical Design, Jan. 1978.

9. "Dynamic Behavior of Planetary Gear (4th Report, Influence of The Transmitted Tooth Load on The Dynamic Increment Load)", Teruaki Hidaka, Yoshio Terauchi, and Kunio Ishioka, Bulletin of the JSME, Vol. 22, No. 167, June, 1979.

VI. BIBLIOGRAPHY

- Benedict, G. H. and Kelley, B. W., "Instantaneous Coefficients of Gear Tooth Friction", ASLE Transactions 4, 59-70 (1961).

- Botman, M., "Epicyclic Gear Vibrations", Journal of Engineering for Industry, August, 1976.

- Botman, M., "Vibration Measurements on Planetary Gears of Aircraft Turbine Engines", AIAA Special Publication, Paper 79-7012 at the 4th International Symposium on Airbreathing Propulsion, Orlando, FL, April 1-6, 1979.

- Cornell, R. W. and Westervelt, W. W., "Dynamic Tooth Loads and Stressing for High Contact Ratio Spur Gears", Journal of Mechanical Design, January, 1978.

- Hidaka, Teruaki and Terauchi, Yoshio, "Dynamic Behavior of Planetary Gear (1st Report, Load Distribution in Planetary Gear)", Bulletin of JSME, Vol. 19, No. 132, June 1976.

- Hidaka, Teruaki; Terauchi, Yoshio; and Fujii, Makoto, "Analysis of Dynamic Tooth Load on Planetary Gear", Bulletin of the JSME, Vol. 23, No. 176, February, 1980.

- Hidaka, Teruaki; Terauchi, Yoshio; and Ishioka, Kunio, "Dynamic Behavior of Planetary Gear (4th Report, Influence of the Transmitted Tooth Load on the Dynamic Increment Load)", Bulletin of the JSME, Vol. 22, No. 167, June 1979.

- Hidaka, Teruaki; Terauchi, Yoshio; and Nagamura, Kazuteru, "Dynamic Behavior of Planetary Gear (6th Report, Influence of Meshing - Phase)", Bulletin of JSME, Vol. 22, No. 169, July 1979.

- Pike, James A., "Documentation for the Expansion of the Dynamic Load Solution for Multiple Planet Spur Gearing to Helical Gearing", September, 1983, (Dennis Townsend, NASA-Lewis program monitor).

- Pike, James A., Interactive Multiple Spur Gear Mesh Dynamic Load Program, December, 1981, CR-165514.

TABLE 1: SUN-PLANET OPTION

	Single Mesh		Multiple Mesh		Difference (%)	
	Sun	Planet	Sun	Planet	Sun	Planet
K_t	1.4430	1.4030	1.44353	1.40281	0.037	0.035
Maximum Hertz Stress (psi)	103322	103322	103503.	103503.	0.175	0.175
Maximum Hertz Stress at PD (psi)	97690.	97690	96735	96735	0.98	0.98
Maximum Bending Stress (psi)	6733.	7213.	6748	7125	.22	1.2
Maximum Bending Stress at PD (psi)	6341.	7162.	6218	7023	1.94	1.94
Maximum Dynamic PV (psi $*10^{-6}$ ft/min.)	53.	53.	52.7	52.7	.62	.62
Maximum Normal Load (lbs)	472.	472.	470.	470.	.42	.42
Maximum Hertz Stress (MPa)	712.4	712.4	713.6	713.6	.17	.17
Maximum Hertz Stress at PD (MPa)	673.5	673.5	667.0	667.0	.97	.97
Maximum Bending Stress (MPa)	46.4	49.7	46.5	49.1	.22	1.2
Maximum Bending Stress at PD (MPa)	43.7	49.4	42.9	48.4	1.8	2.0
Maximum Dynamic PV ($Pa*10^{-9}*m/s$)	1.86	1.86	1.84	1.84	1.1	1.1
Maximum Normal Load (KN)	2.10	2.10	2.09	2.09	.48	.48

TABLE 2: RING-PLANET OPTION

	Single Mesh		Multiple Mesh		Difference (%)	
	Planet	Ring	Planet	Ring	Planet	Ring
K_t	1.4716	1.6036	1.4499	1.5685	1.5	2.2
Maximum Hertz Stress (psi)	19896.	19896.	19785.	19785.	0.56	0.56
Maximum Hertz Stress at PD (psi)	15927.	15927.	16022.	16022.	0.59	0.59
Maximum Bending Stress (psi)	566.	664.	575.	657.	1.6	0.99
Maximum Bending Stress at PD (psi)	384.	246.	399.	253.	3.9	2.8
Maximum Dynamic PV ($psi*10^{-6}*ft/min$)	6.00	6.00	6.03	6.03	0.51	0.51
Maximum Normal Load (lbs)	30.	30.	29.4	29.4	2.0	2.0
Maximum Hertz Stress (MPa)	137.2	137.2	136.4	136.4	0.58	0.58
Maximum Hertz Stress at PD (MPa)	109.8	109.8	110.5	110.5	0.64	0.64
Maximum Bending Stress (MPa)	3.90	4.58	3.96	4.53	1.5	1.1
Maximum Bending Stress at PD (MPa)	2.65	1.70	2.75	1.74	3.8	2.4
Maximum Dynamic PV ($Pa*10^{-6}*m/s$)	210.	210.	211.	211.	0.48	0.48
Maximum Normal Load (N)	133.	133.	131.	131.	1.5	1.5

TABLE 3: STOECKICHT 2K-H NONSYNCHRONOUS PLANETARY CHARACTERISTICS

Number of Planets	3
Diametral Pitch	1/3
Pressure Angle	22.5°
Module	3

	SUN	PLANET	RING	CARRIER
Number of Teeth	14	28	70	--
Face Width (in.)	1.18	1.18	1.42	--
Equivalent Mass (lbs.)	.0562	0.155	--	28.9
Accumulative pitch error (in x 10^{-3})	.118	1.10	--	--
Tooth Profile error (in x 10^{-3})	.118	0.197	--	--
Lead error (in x 10^{-3})	.158	0.276	--	--
Backlash Tolerance (in.)	.0075			
Face Width (mm)	30.	30.	36.	--
Equivalent Mass (kg)	.0255	.0704	0.0	13.12
Accumulative pitch error (/, m)	3.	28.	--	--
Tooth profile error (m)	3.	5.	--	--
Lead error (m)	4.	7.	--	--
Backlash Tolerance (mm)	.19			

TABLE 4: STOECKICHT 2K-H SYNCHRONOUS PLANETARY CHARACTERISTICS

Number of Planets	3
Diametral Pitch	0.5
Pressure Angle	22.5°
Module	2.

	SUN	PLANET	RING	CARRIER
Number of Teeth	21.	42.	105.	--
Face Width (in.)	1.18	1.18	1.18	--
Equivalent Mass (lbs)	0.0562	0.155	0.0	28.9
Accumulative pitch error (in.)	0.118	1.10	--	--
Tooth Profile error (in.)	0.118	0.197	--	--
Lead error (in.)	0.158	0.276	--	--
Backlash Tolerance (in.)	0.0050			
Face Width (mm)	30.	30.	30.	--
Equivalent Mass (Kg.)	.0255	.0704	0.0	13.12
Accumulative pitch error (m)	3.	28.	--	--
Tooth Profile error (m)	3.	5.	--	--
Lead error (m)	4.	7.	--	--
Backlash Tolerance (mm)	.127			

TABLE 5: A-27 FIRST-STAGE REDUCTION GEAR CHARACTERISTICS

Number of Planets	3
Diametral Pitch	19.2
Pressure Angle	22.5°
Module	0.0521

	Sun	Planet	Ring	Carrier
Number of teeth	27	45	117	--
Relative Radius of Gyration	.254	.294	1.096	.599
Relative Mass	.269	.362	1.0	1.092
Face Width (in.)	1.2220	1.2220	0.945	--
Root Diameter, maximum (in.)	1.2946	2.1940	6.2340	--
Tip Diameter, maximum (in.)	1.5184	2.3663	5.990	--
Fillet Radius, maximum (in.)	.0223	.0220	.0160	--
Tooth Thickness, nominal (in.)	.0851	.0740	.0830	
Face Width (mm)	31.0	31.0	24.0	--
Root Diameter, maximum (mm)	32.9	55.7	158.	--
Tip Diameter, maximum (mm)	38.6	60.1	152.	--
Fillet Radius, maximum (mm)	0.566	0.559	0.406	--
Tooth Thickness, nominal (mm)	2.16	1.88	2.11	--

TABLE 6:

HAMILTON STANDARD FIRST STAGE TURBOPROP GEARBOX CHARACTERISTICS

Number of Idlers	2
Diametral Pitch	11.0099
Pressure Angle	25°
Module	0.0908

	Input Pinion (sun)	Idlers (planets)
Number of Teeth	24	77
Face Width (in.)	2.22	1.90
Effective Mass (lb.)	0.0033804	.017106
Root Diameter, maximum (in.)	1.9703	6.7288
Tip Diameter, maximum (in.)	2.3820	7.1499
Fillet Radius, maximum (in.)	.0410	.0370
Tooth Thickness, nominal (in.)	.1534	.1319
Face Width (mm)	56.4	48.3
Effective Mass (Kg)	.00153	.00776
Root Diameter, maximum (mm)	50.0	171.
Tip Diameter, maximum (mm)	60.5	182
Fillet Radius, maximum (mm)	1.04	0.940
Tooth Thickness, nominal (mm)	3.90	3.35

Figure 1. Coefficient of Friction vs. Benedict-Kelley Parameter

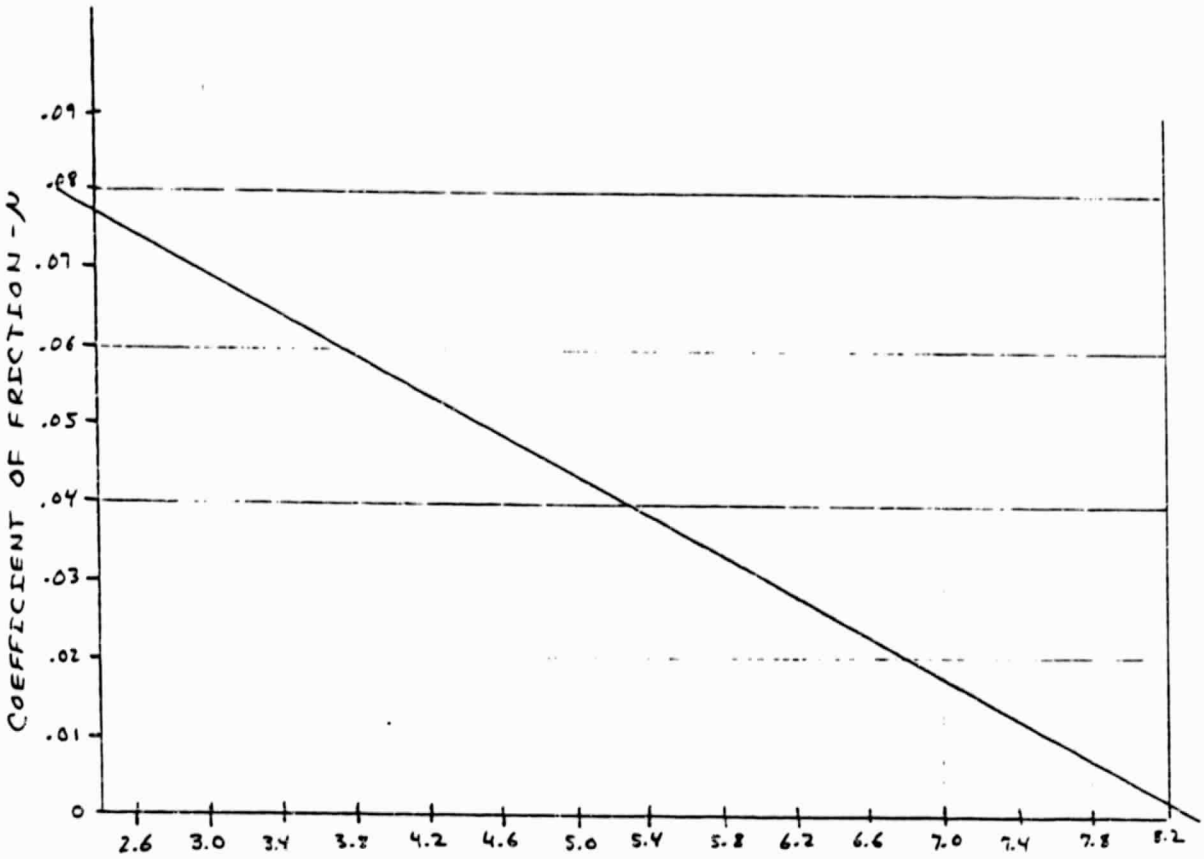

$$X = \log_{10}\left\{\frac{\mu_o V_s V_T^2}{L/w}\right\}$$

$$\mu = -.0130556\,X + .1093333$$

Figure 2. Specific Gravity vs. Temperature

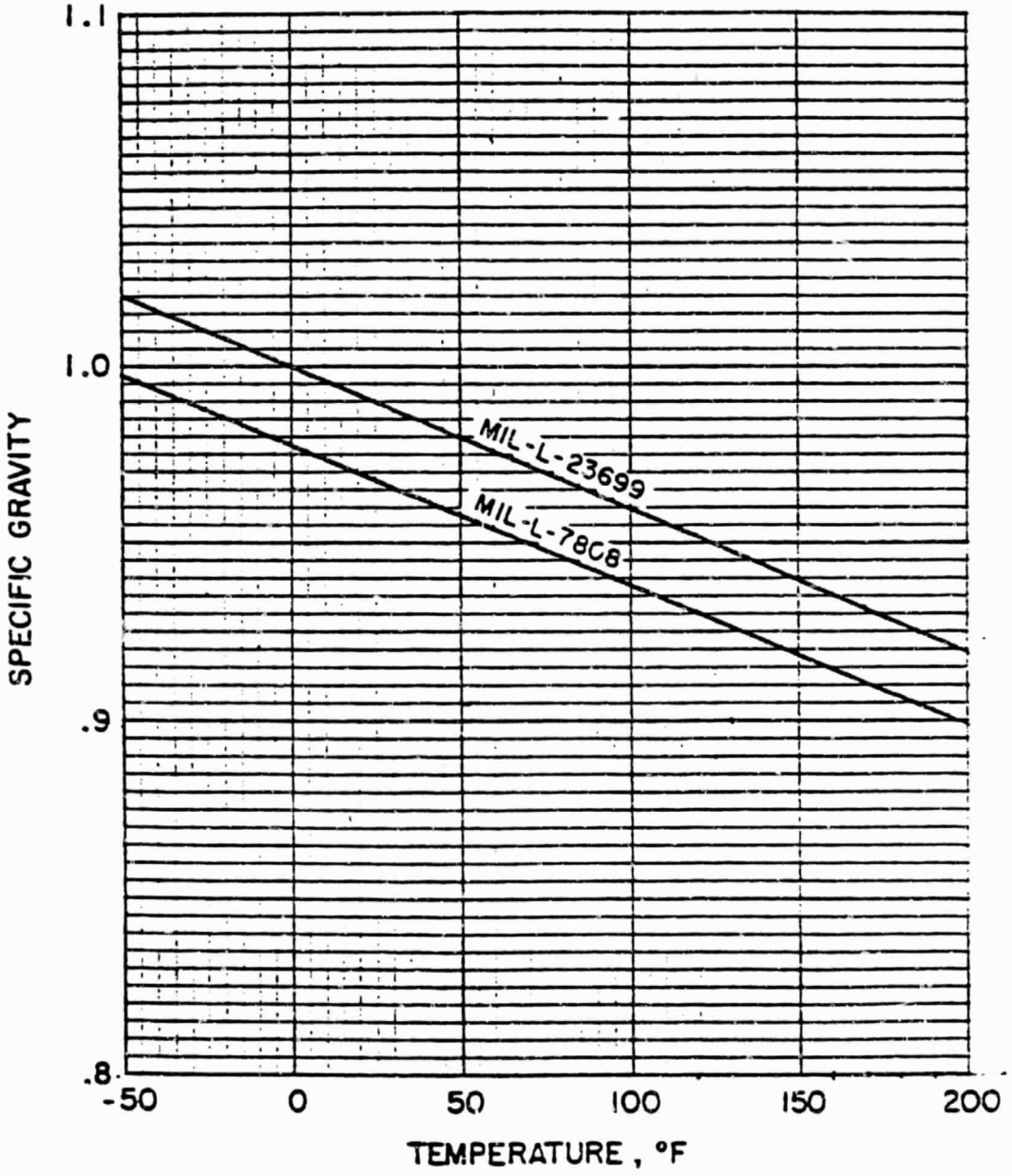

Figure 3. Kinematic Viscosity vs. Temperature

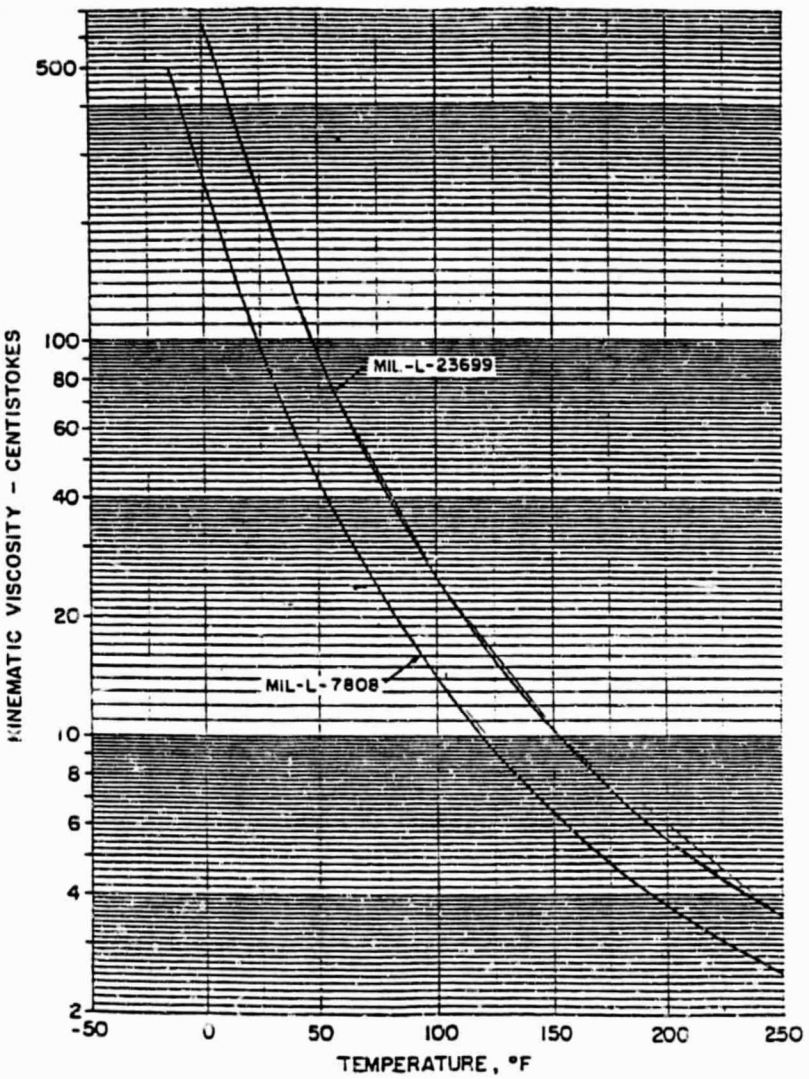

Figure 4. Flash Temperature, Before and After Variable Friction Modifications to Single Mesh Program

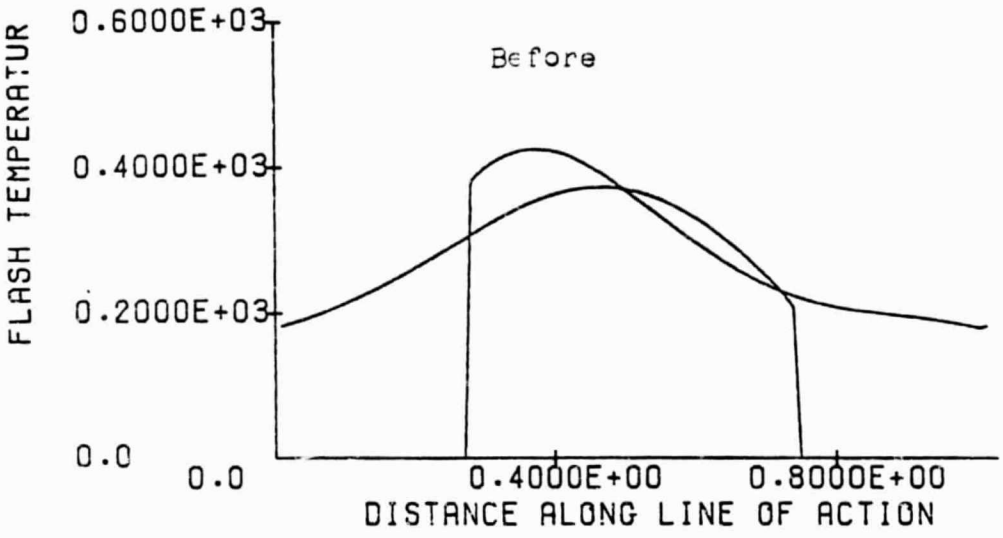

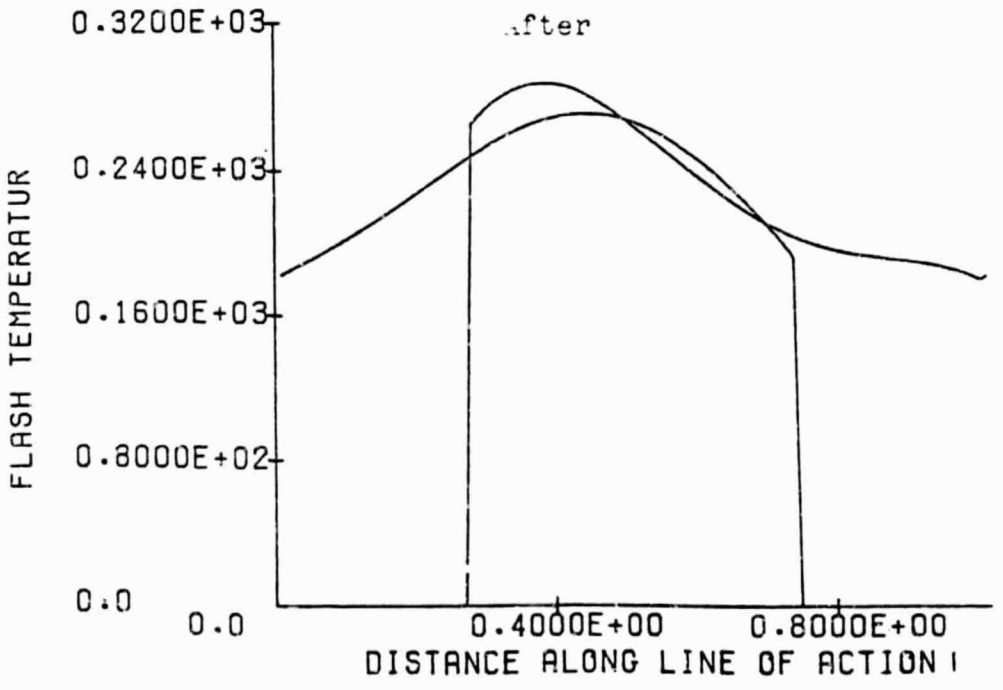

Figure 5. Schematic of Dynamic Model for Flexible Carrier and Ring Rim

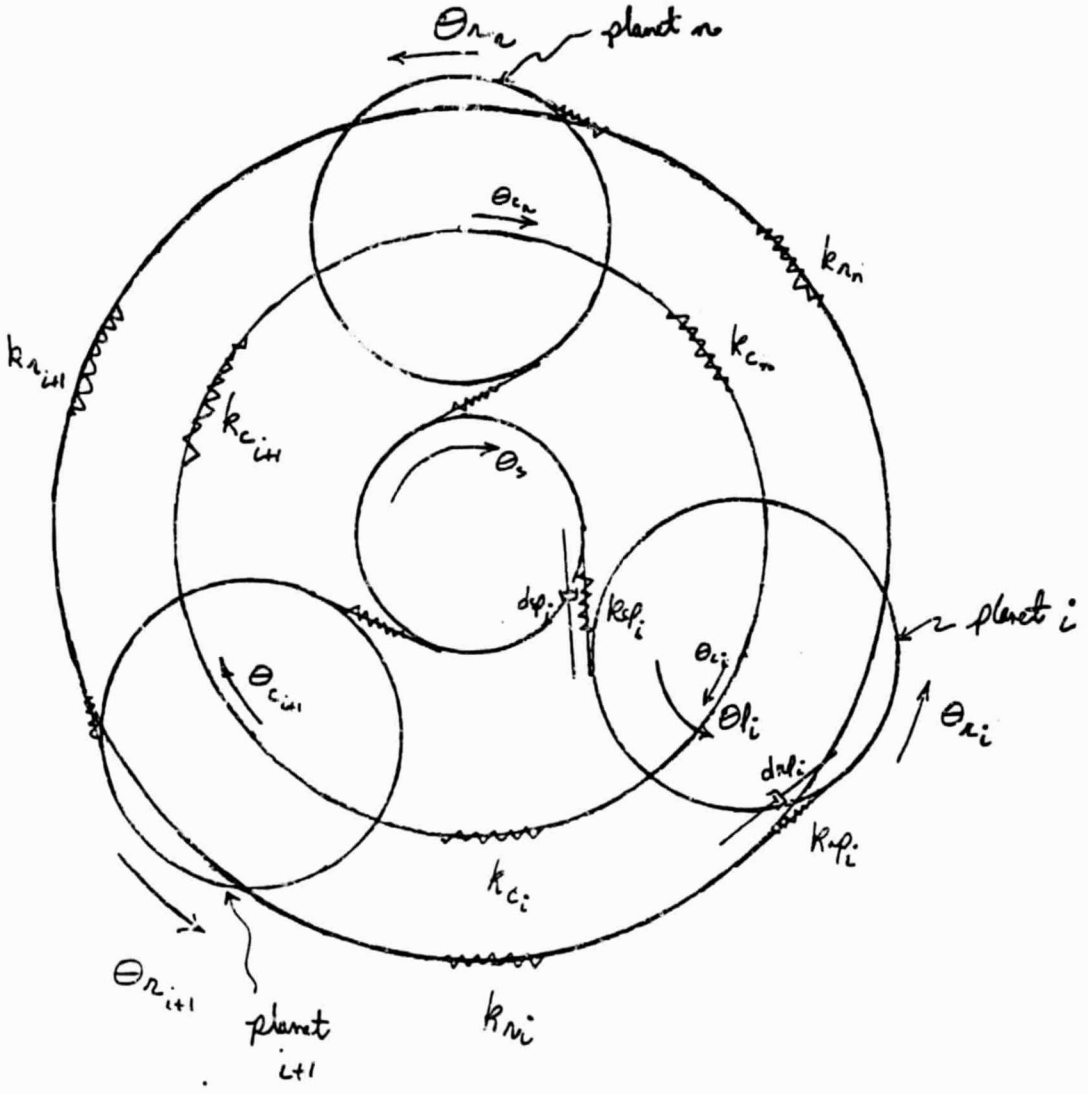

Figure 6a: Runout Loads vs. Angular Location on Pinion

14 Tooth Planet

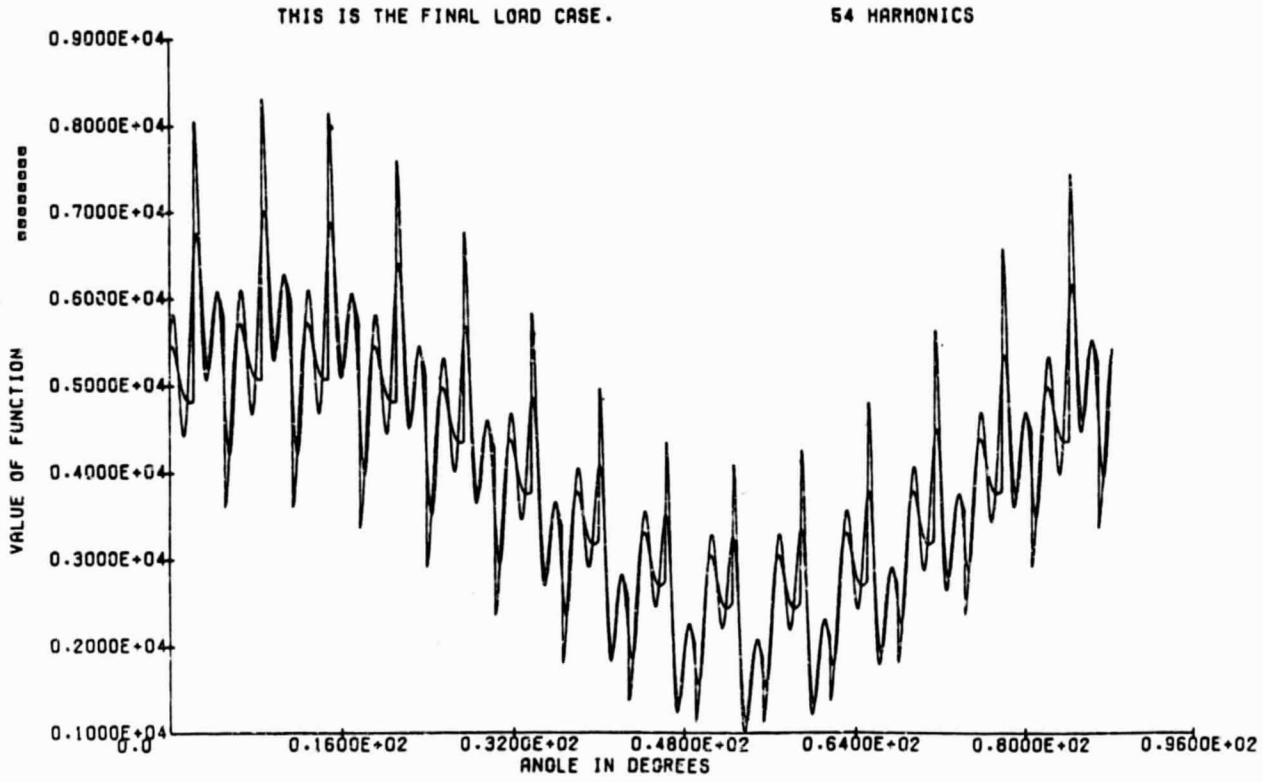

Figure 6b: Fourier Transformed Loads vs. Order of Harmonics

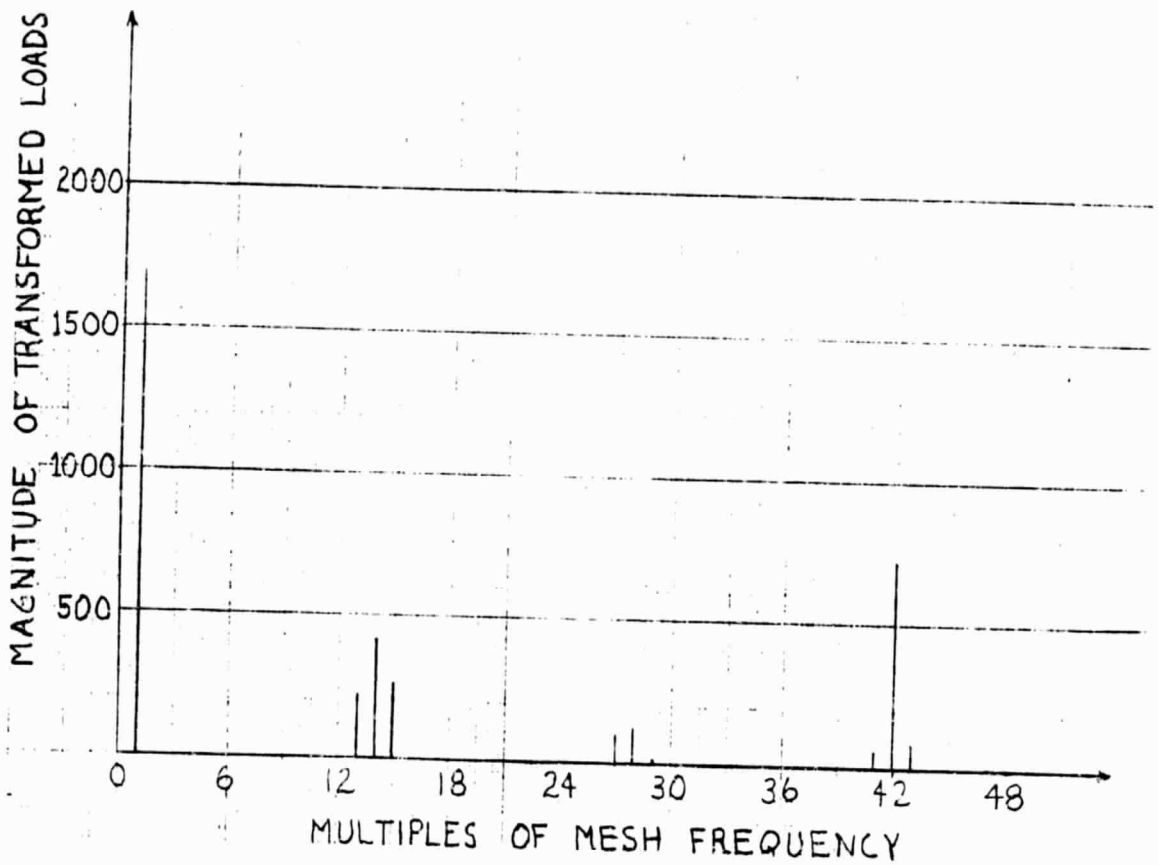

Mesh Frequency = 14

Figure 7. Single Mesh Loads and Input Data Set

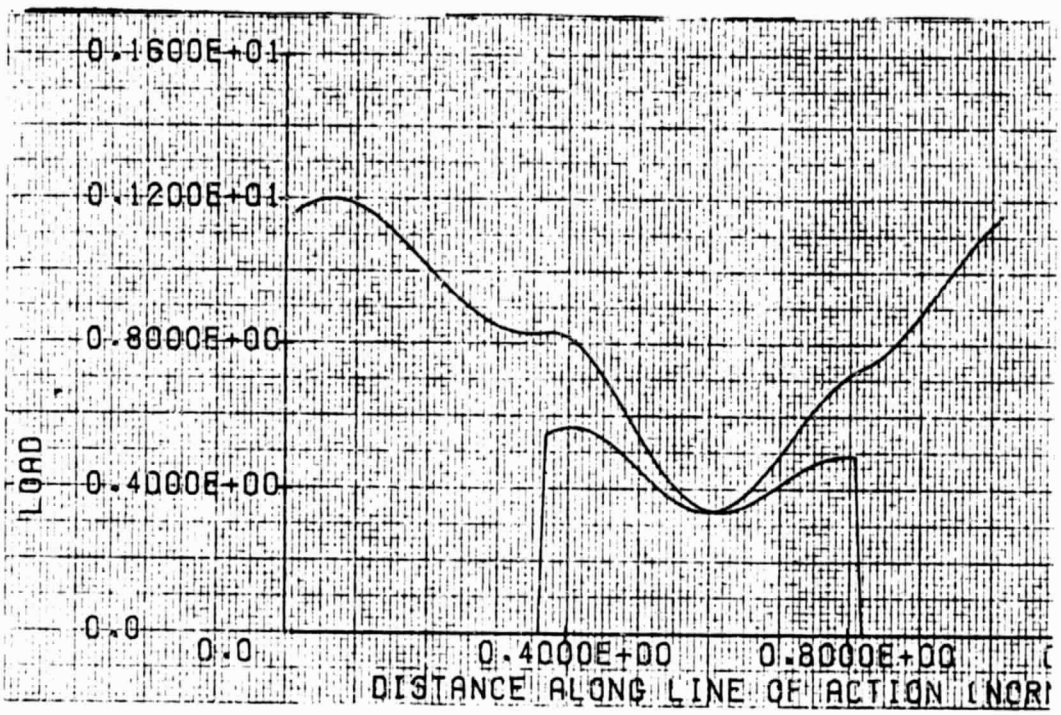


```
COMPARE P354 TO MULTIPLE MESH, K = 4
5          1.       8.4667        22.5          14.          28.        1.1811
5          6.       1.1811         300.        3000.        30.0         30.0
2         11.          .3            .3
2         32.       .04123           .1
5         36.                        1.
3         41.          25.          25.         180.
1         46.        .0528
0-1.
```

Figure 8. Multiple Mesh, Sun-Planet Loads and Input Data Set

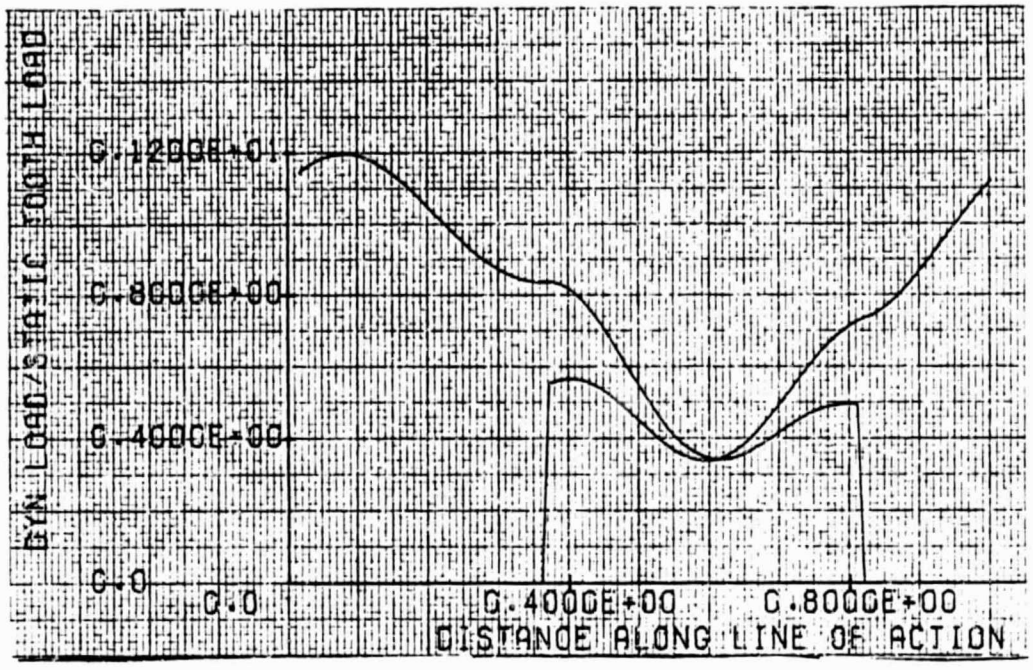


```
TEST CASE FOR SUN AND PLANET
3          1.          2.        8.4667        22.5
5          6.         14.          28.          0.       1.1011       1.1811
3         12.          1.           4.        300.
3         15.       3000.        3000.          1.
4         28.     .056167           0.          0.       .15507
2         52.          .1           .1
3        140.         25.         180.       .0528
2        150.         .005         20.
1        601.          1.
0-1.
```

Figure 9. Input Data for Multiple-Mesh, Ring-Planet Option

```
TEST FOR RING-PLANET OPTION
5          1.          2.       8.4667        22.5          0.          0.
5          6.          0.         28.         70.           0.       1.1811
4         11.       1.1811          1.          5.          70.
3         15.        3000.        3000.         1.
5         30.         12.       .15507
2         52.          .1           .1
1        120.          0.
3        140.         25.         180.        .0528
2        150.         .01          20.
1        167.       .0075
1        501.    .0000105
1        541       -.00330
1        699.          0.
0-1
```

Figure 10. Stoeckicht 2K-H Planetary System Diagram

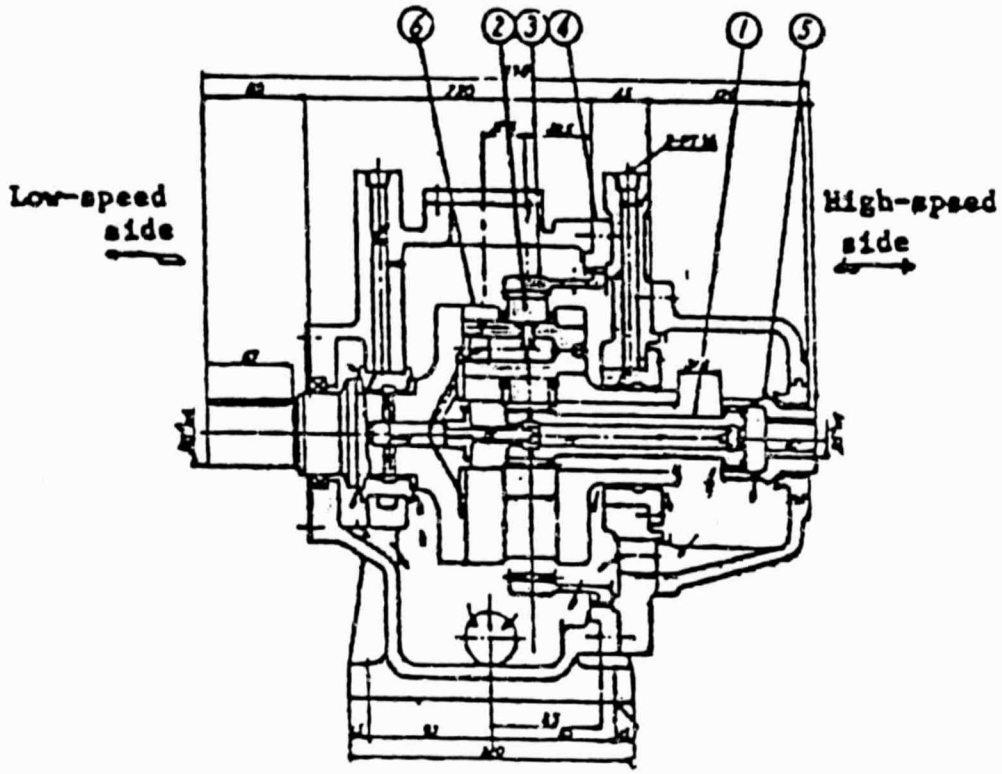

1 sun gear
2 planet gear
3 ring gear
4 coupling retainer
5 high-speed gear coupling
6 planet carrier

Reference 7

Figure 11. Input Data Set for Stoeckicht 2K-H System

```
STOECKICHT GEAR
5          1.          2.        8.4667        22.5          0.          0.
5          6.         14.          28.          70.      1.1811      1.1811
4         11.      1.4184          3.           1.        25.8
3         15.        1000.        6000.          5.
5         28.      .056167     28.8987          0.      .15507      .15507
1         33.      .15507
2         52.          .1          .1
1        120.          0.
3        140.         25.         180.       .0528
2        150.         .01          20.
1        167.       .0075
3        421.          0.      .6666667    .3333333
3        441.          .5     .1666667    .8333333
1        699.          0.
0-1
```

Figure 12. A-27 System Diagram

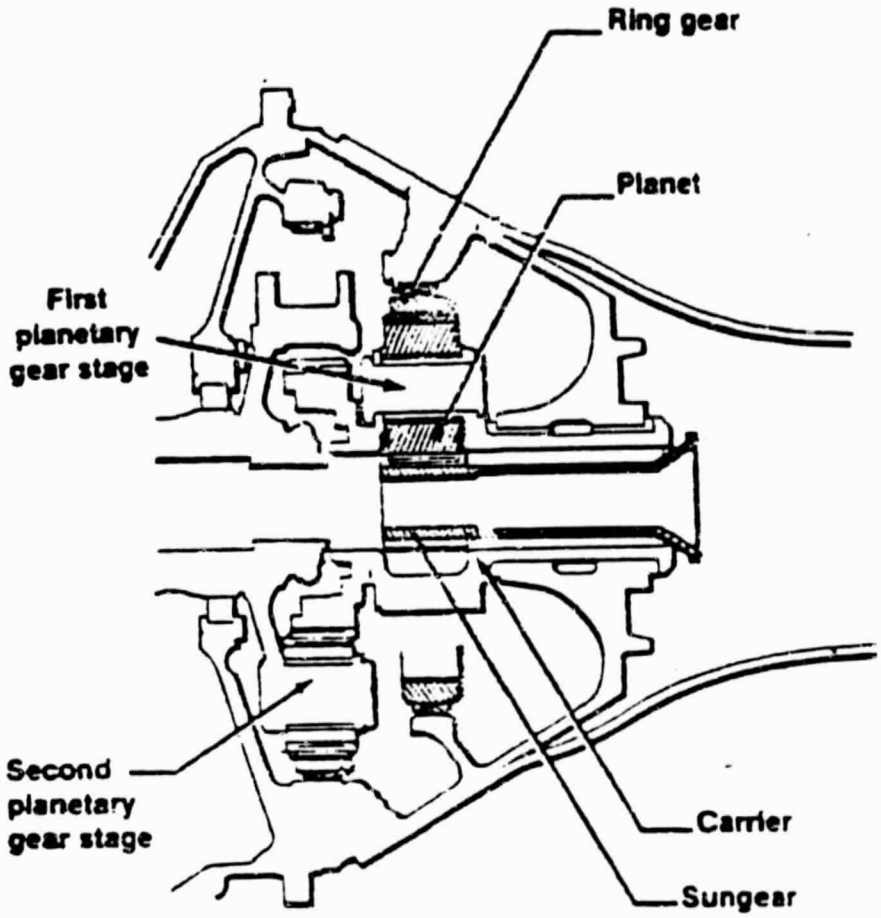

Reference 4

Figure 13. A-27 Input Data Set

```
FIRST STAGE, PW&C
3          1.          3.          19.2        22.5
5          6.          27.         45.         117.        1.222       1.222
3          11.         .945        3.          1.
4          14.         949.2525    36000.      36000.      1.
5          28.         .001567     .004317     0.          .001017     .001017
1          33.         .001017
2          52.         .20         .20
5          120.        1.          .6473       1.097       3.117       .7592
5          125.        1.18315     2.993       .0851       .074        .083
3          130.        .0223       .022        .016
3          140.        25.         180.        .0528
2          150.        .02         30.
0-1.
```

Figure 14: Gearbox System Diagram

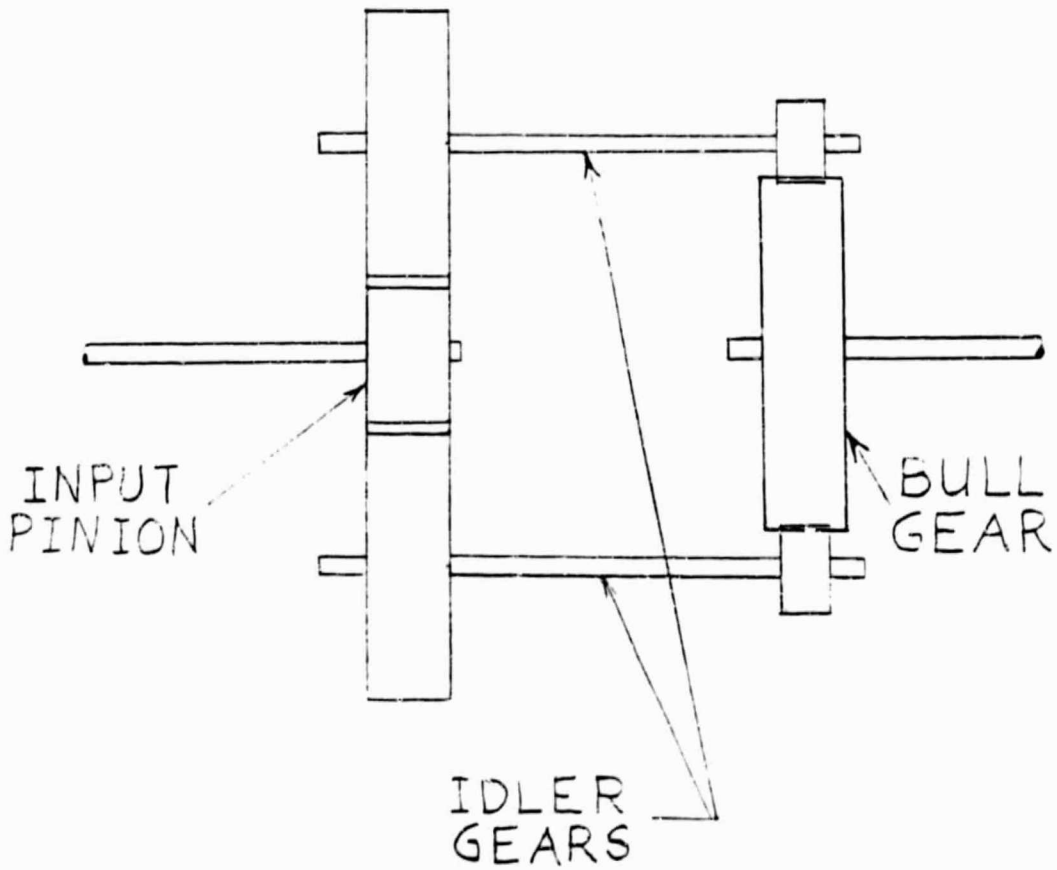

Figure 15: Idler Gear Gauge Locations

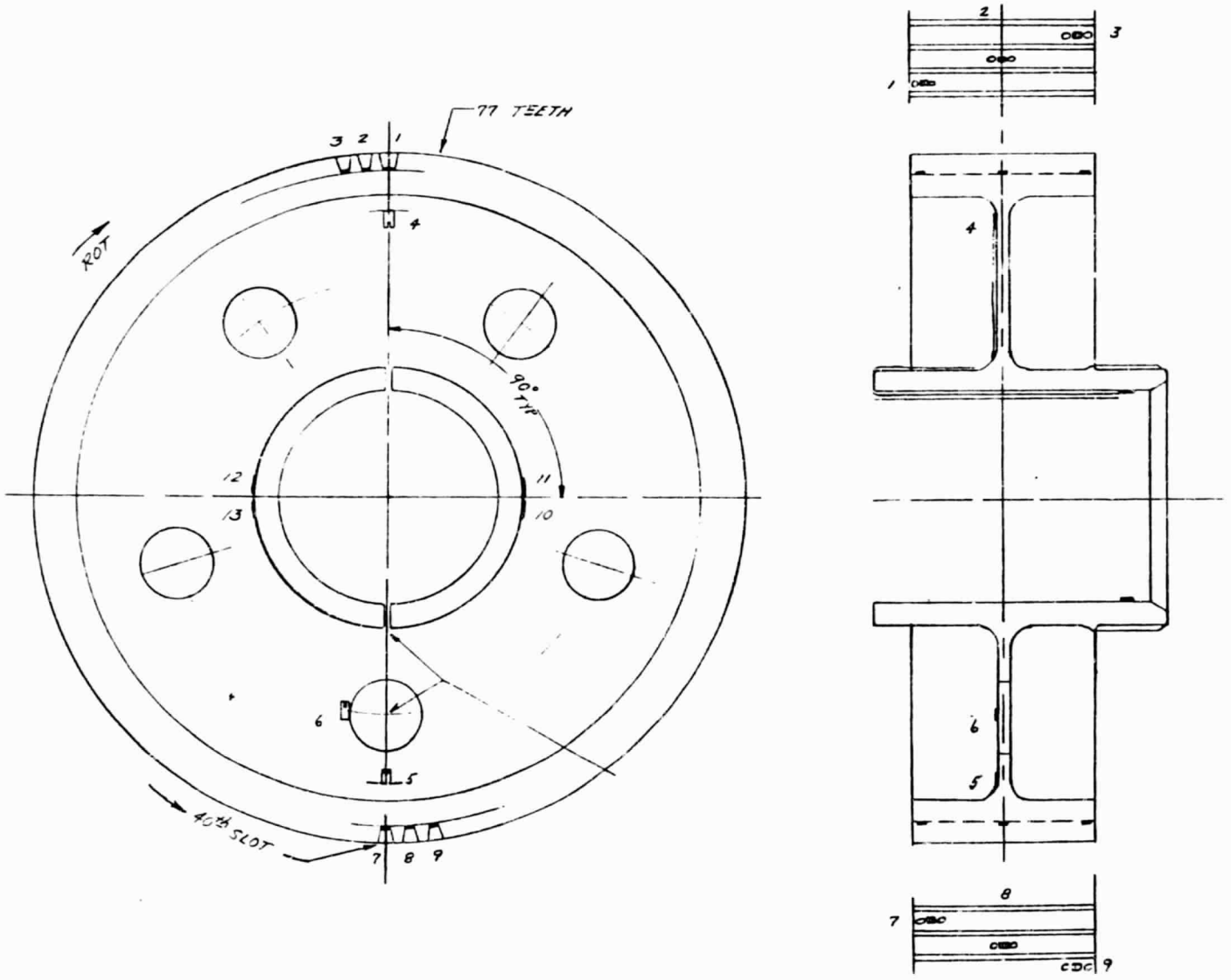

Figure 16: Gearbox Input Data Set

```
GEARBOX, INPUT PINION & GEAR K
3          1.          2.      11.0099         25.
5          6.         24.         77.          0.       2.220          1.90
2         12.          2.          4.
4         14.       1682.      23000.      23000.          1.
5         28.  .0033804          0.          0.      .017106       .017106
1         52.        .10
4         60.       75.4        71.5       .0006       .0006
3         66.      15.35       84.65       .0002
1         78.      .0007
5        120.         1.       .98515     3.36440          0.      1.19225
4        125.    3.57620          0.       .1534       .1319
2        130.       .041        .037          0.
3        140.         20.        120.       .0528
2        150.       .005         20.
2        421.         0.   .18838665
0-1.
```

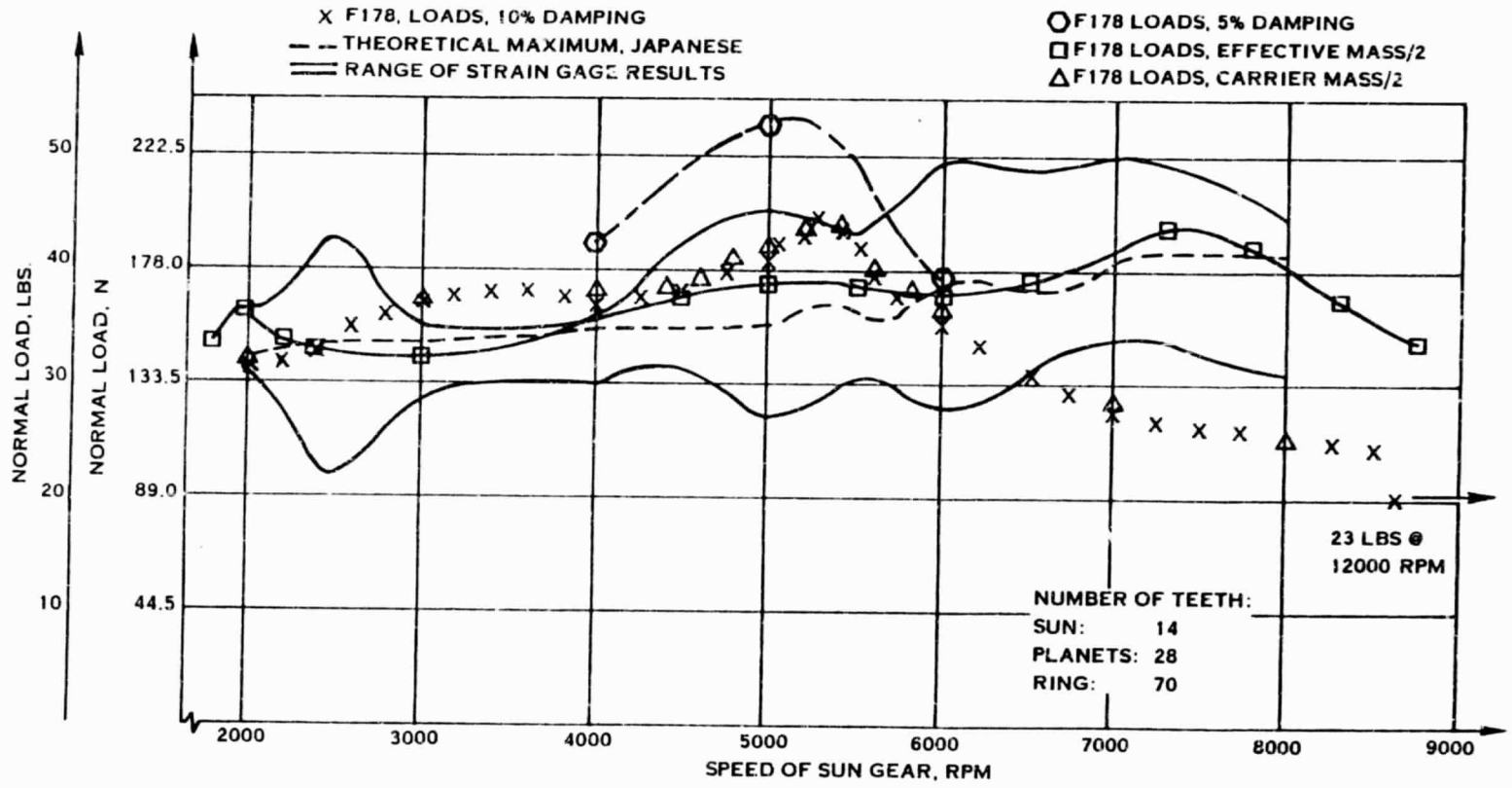

FIGURE 17. STOECKICHT 2K-H PLANETS NONSYNCHRONOUS STATIC LOAD = 130N (29.25 LBS)

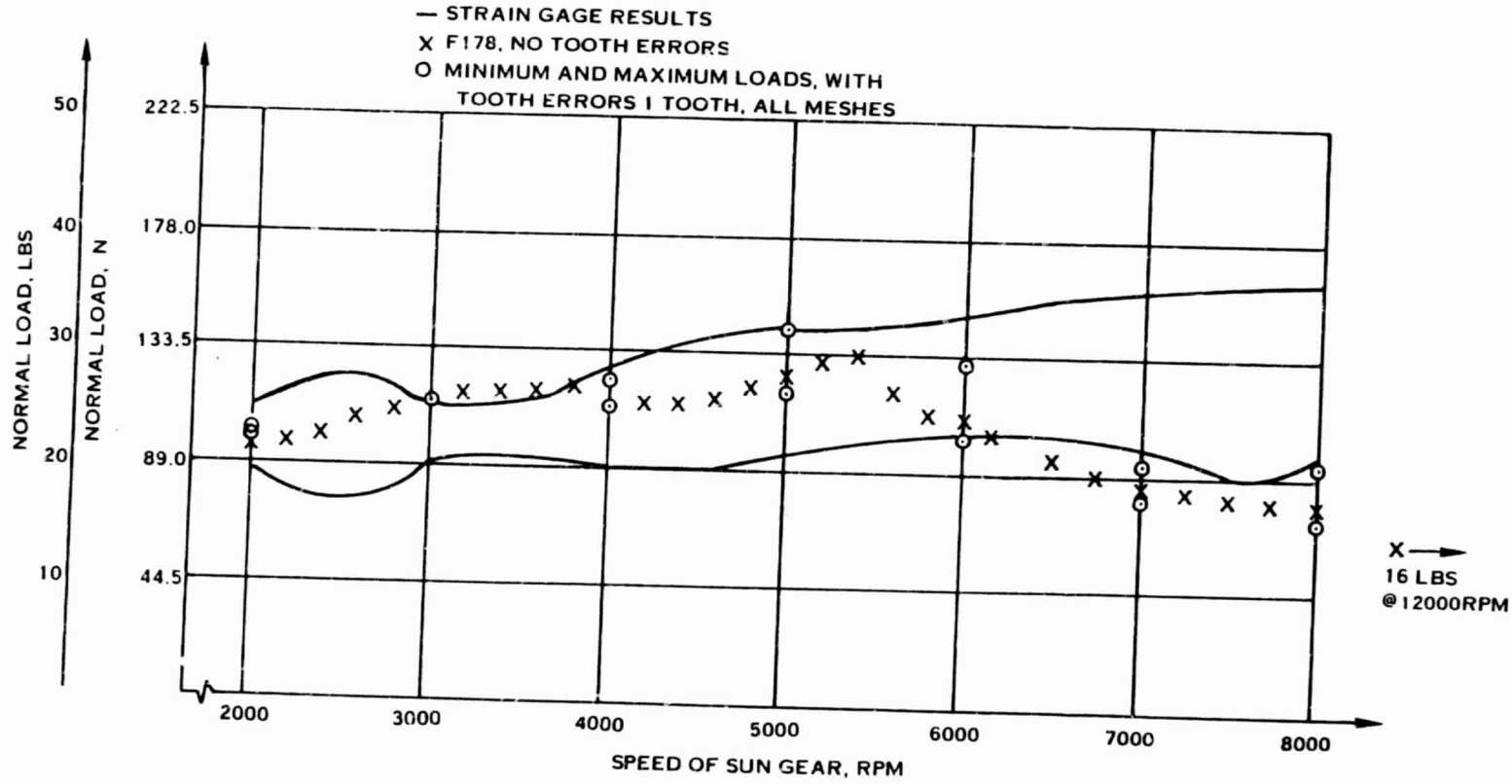

FIGURE 18. STOECKICHT 2K-H PLANETS NONSYNCHRONOUS STATIC LOAD = 90 N (20.25 LBS)

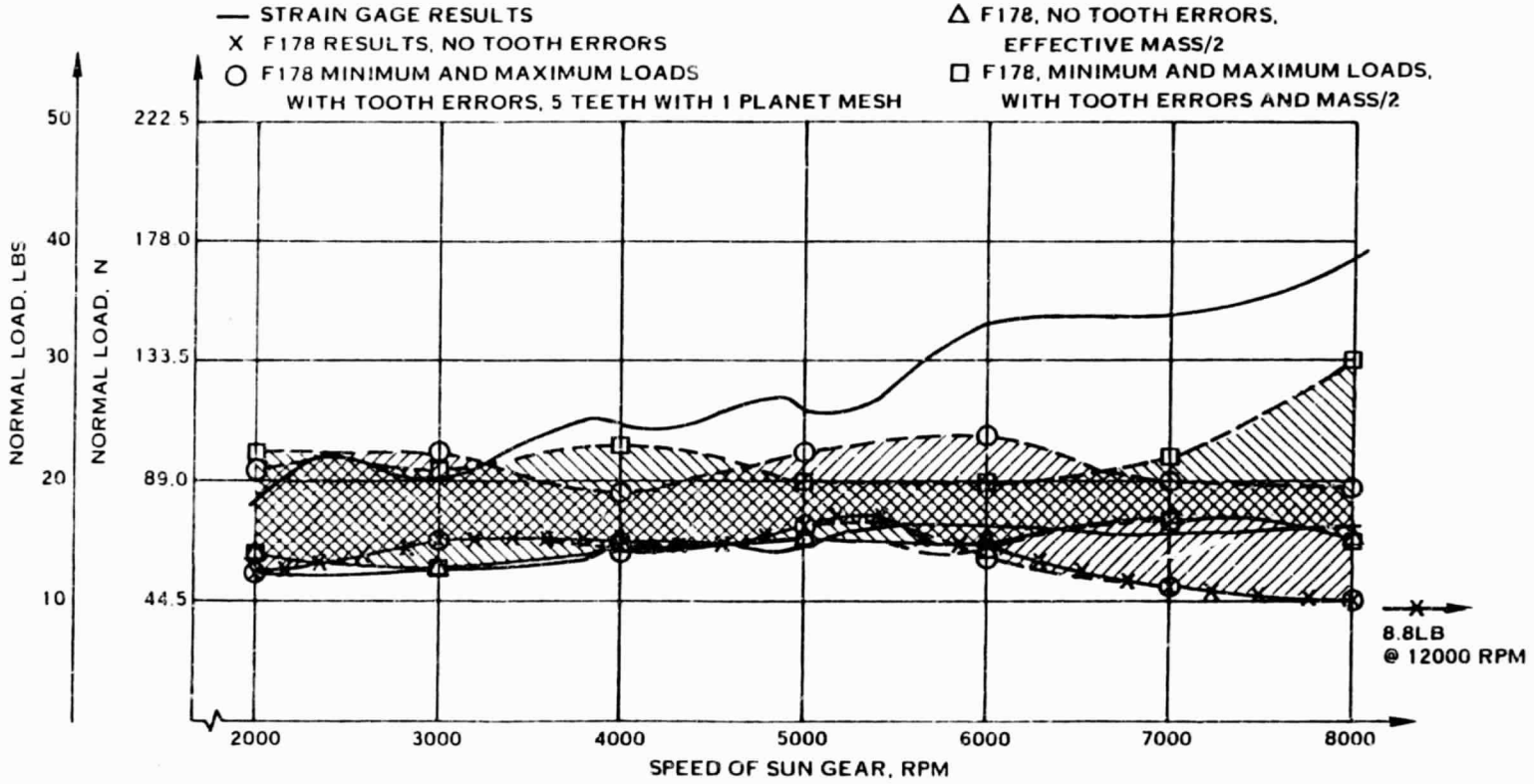

FIGURE 19. STOECKICHT 2K-H PLANETS NONSYNCHRONOUS STATIC LOAD = 50N (11.25 LBS)

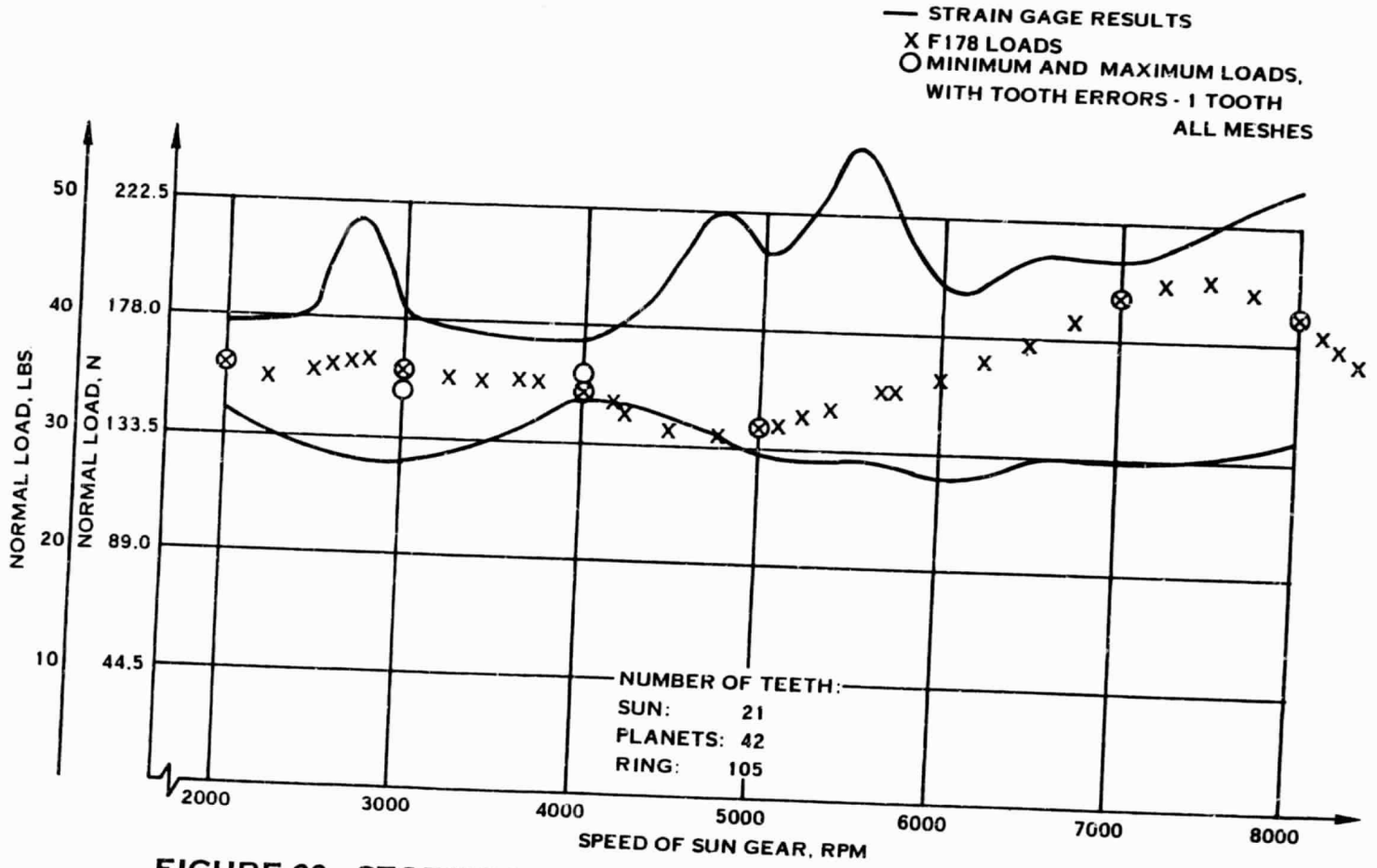

FIGURE 20. STOECKICHT 2K-H PLANETS SYNCHRONOUS STATIC LOAD = 130N (29.25 LBS.)

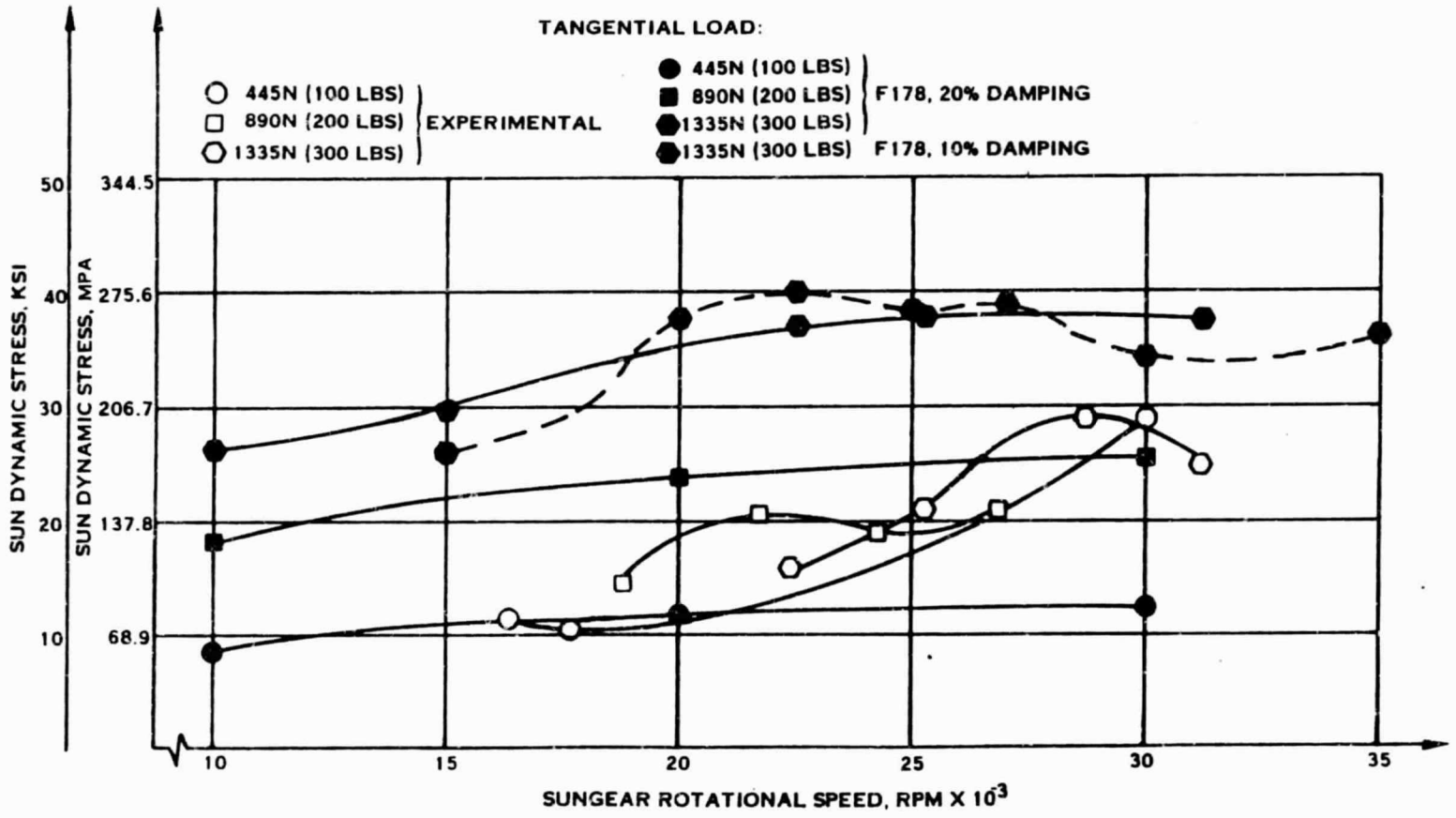

FIGURE 21: MODEL A-27, STRESS VS. SPEED LOWER TANGENTIAL LOADS

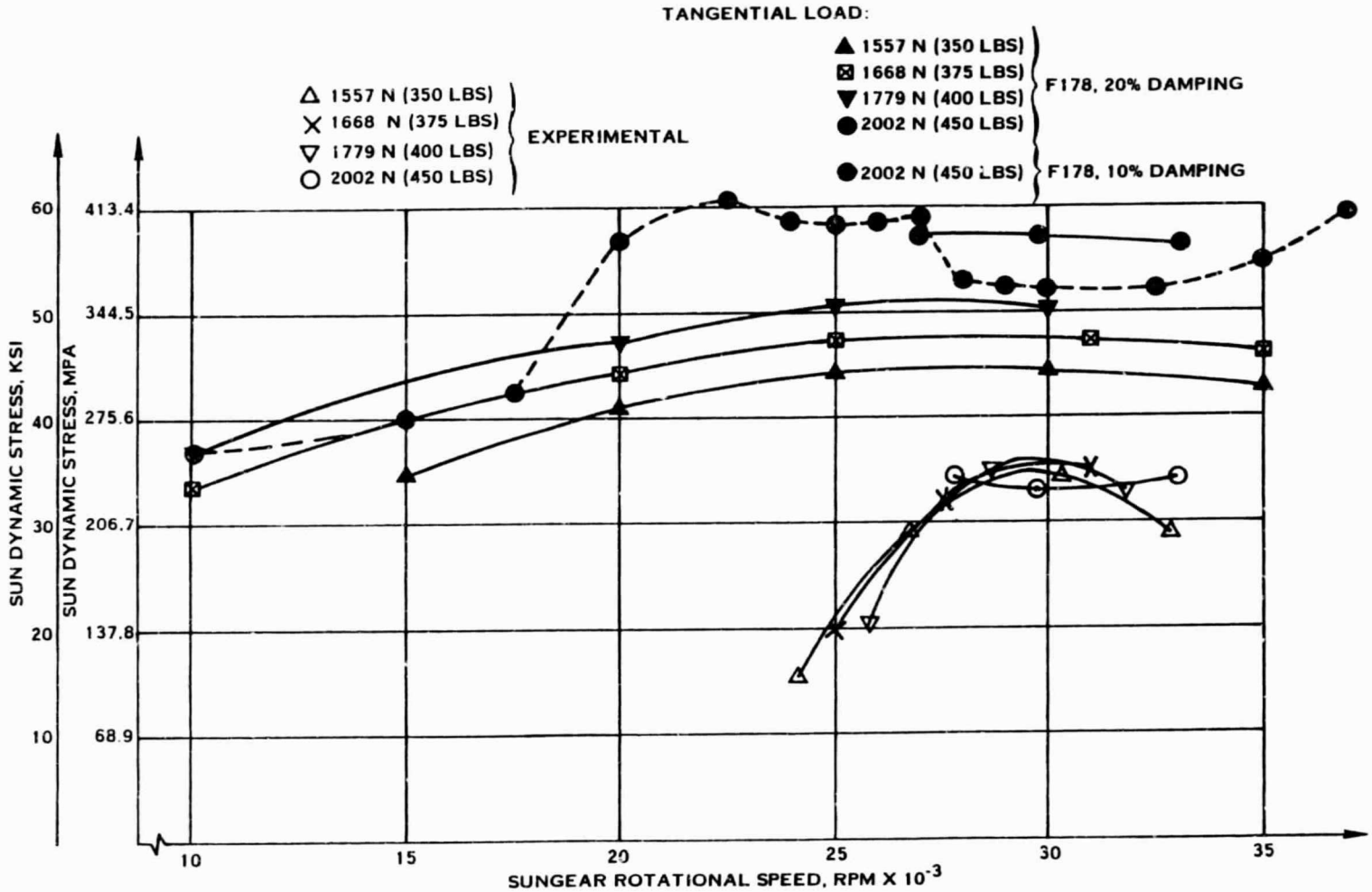

FIGURE 22. MODEL A-27, STRESS VS. SPEED HIGHER TANGENTIAL LOADS

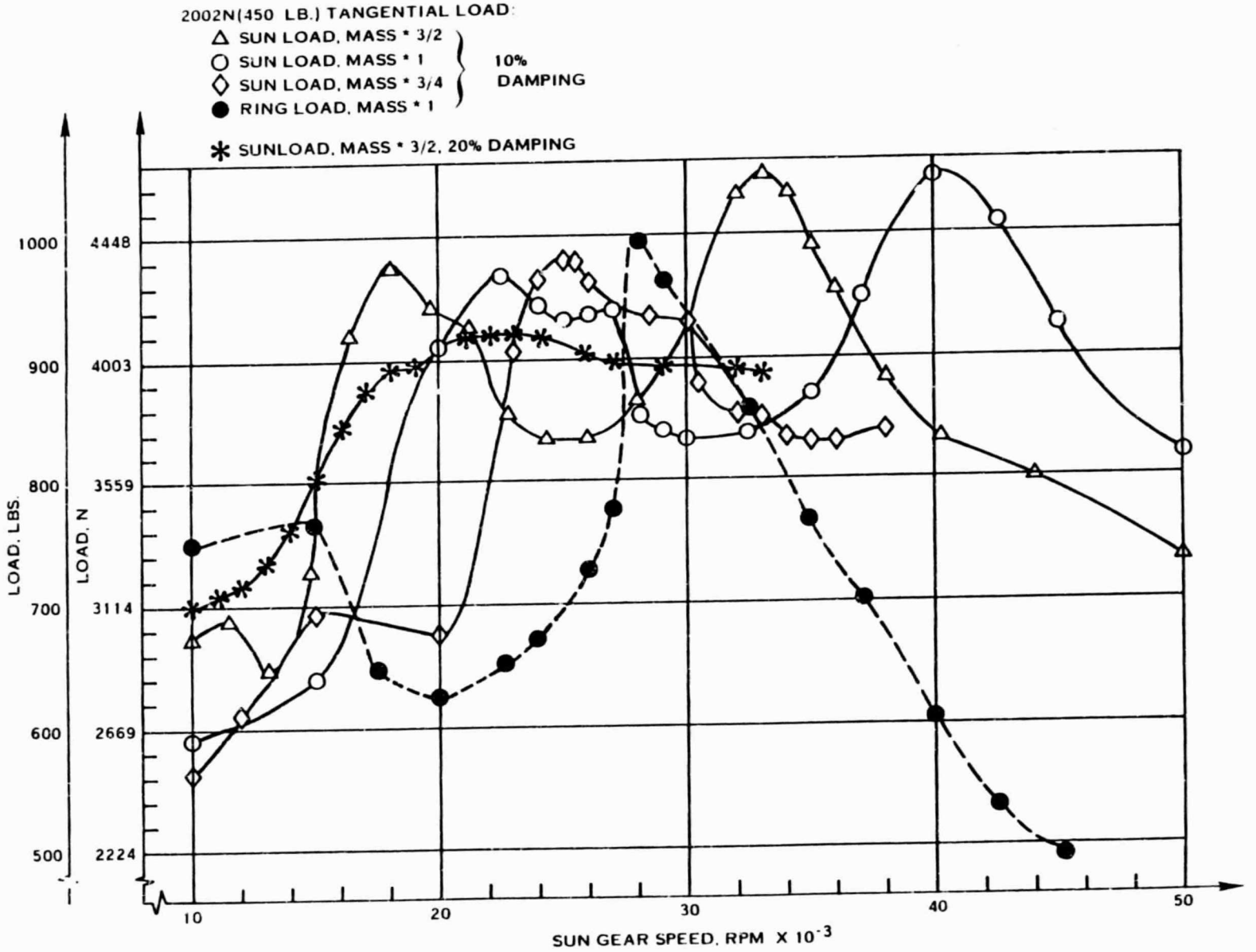

FIGURE 23: MODEL A-27, SPEED SURVEY

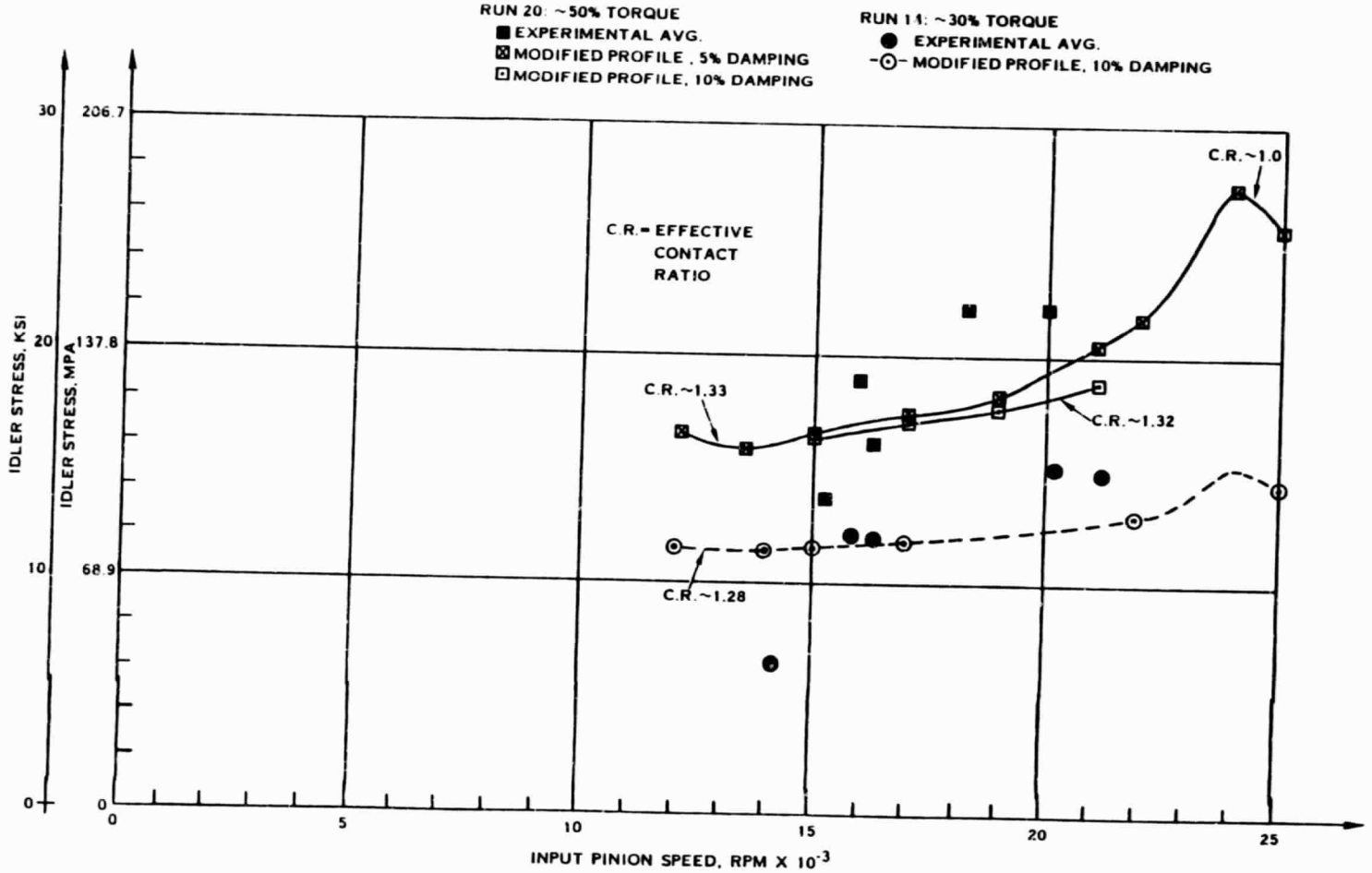

FIGURE 24. HAMILTON STANDARD GEARBOX FIRST STAGE IDLER STRESS

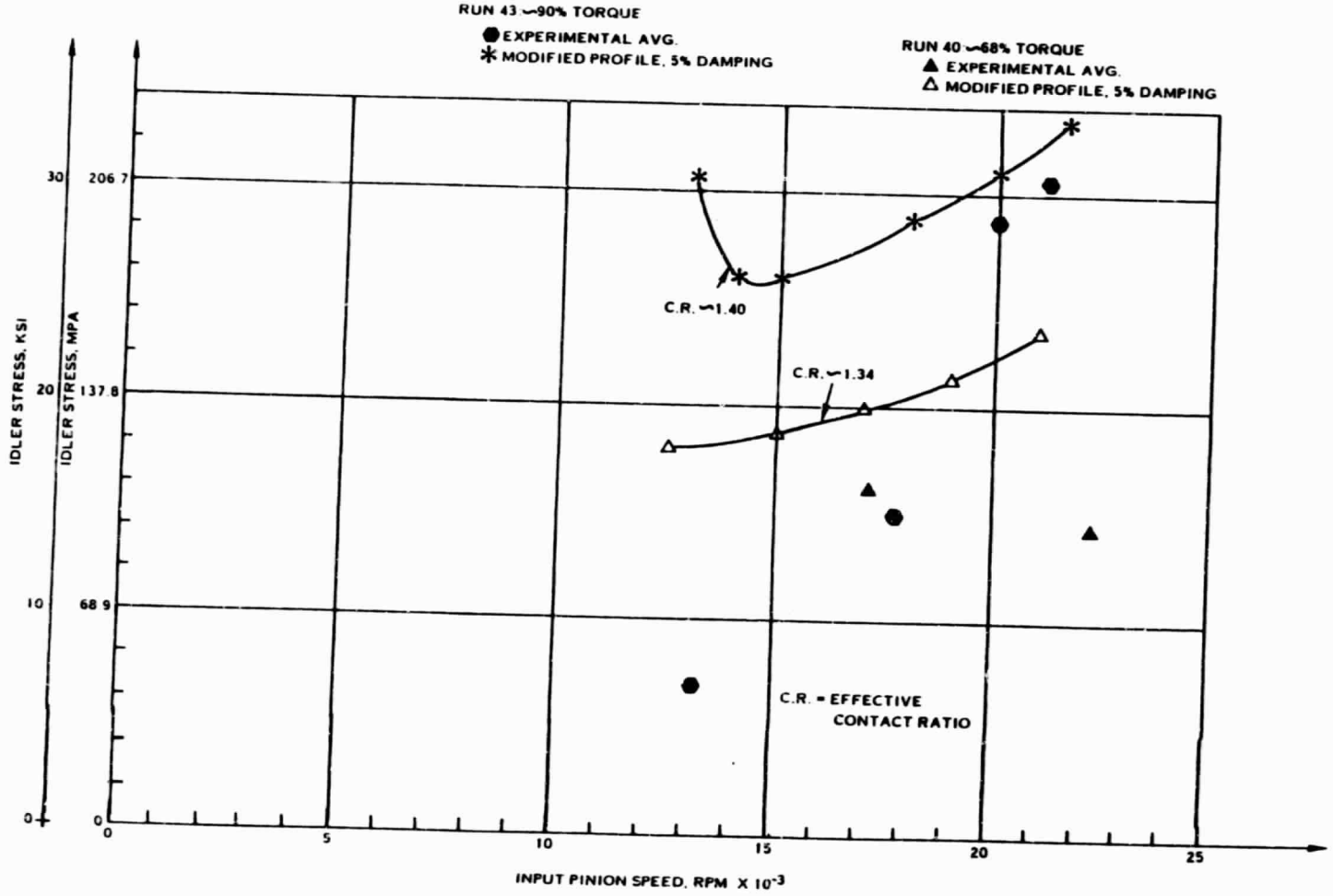

FIGURE 25. HAMILTON STANDARD GEARBOX FIRST STAGE IDLER STRESS

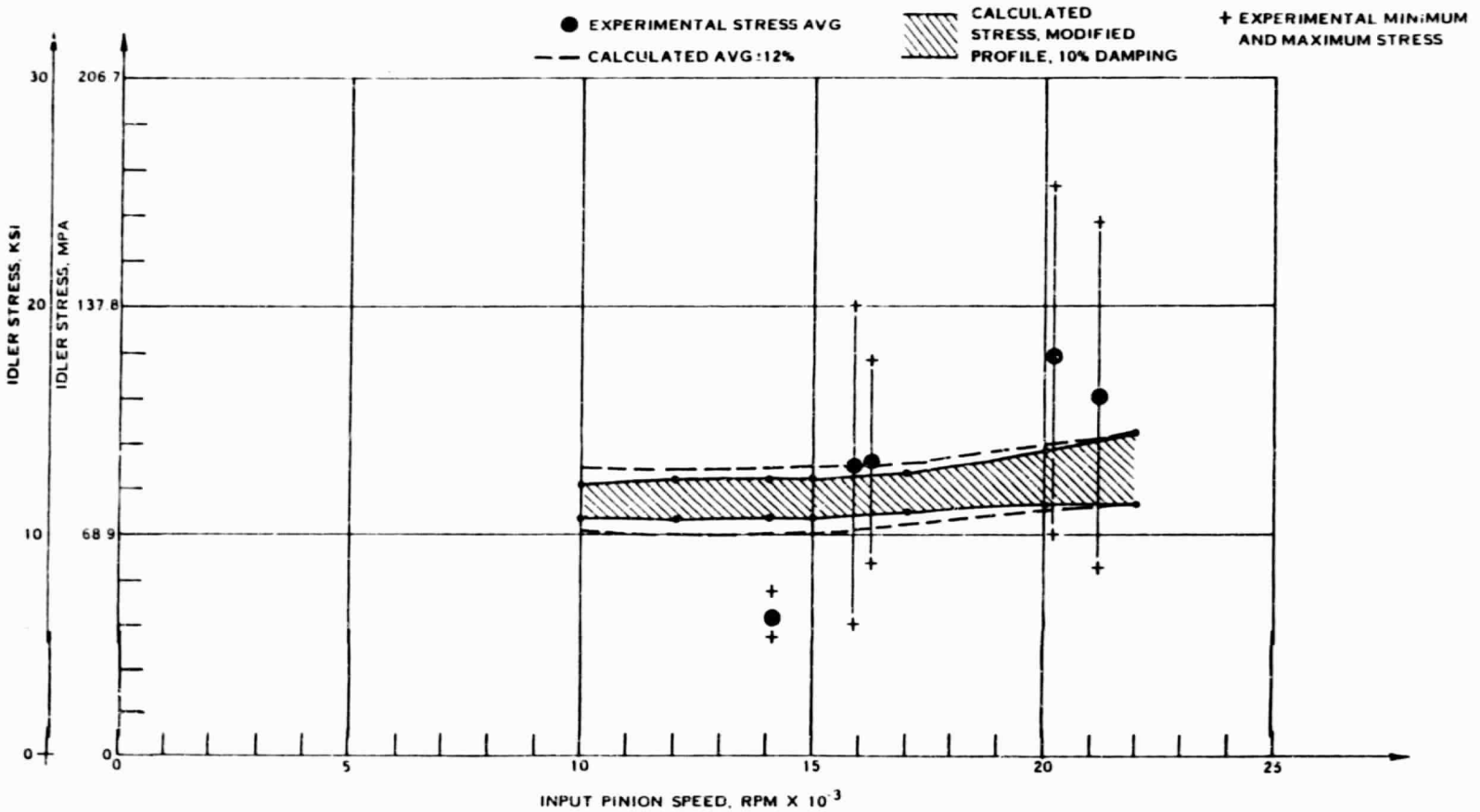

FIGURE 26. HAMILTON STANDARD GEARBOX, IDLER STRESSES~30 % TORQUE CASE

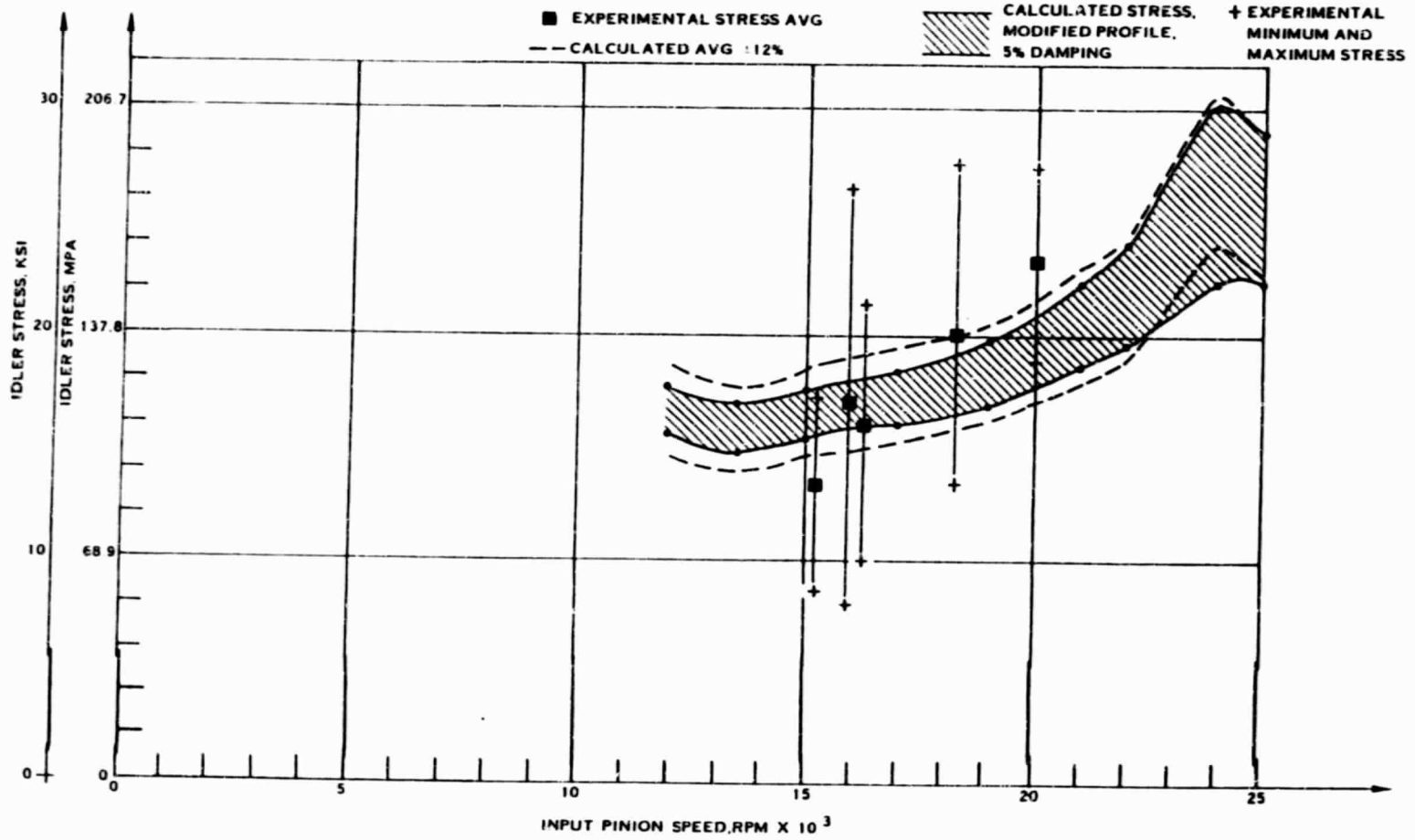

FIGURE 27. HAMILTON STANDARD GEARBOX, IDLER STRESSES ~ 50% TORQUE CASE

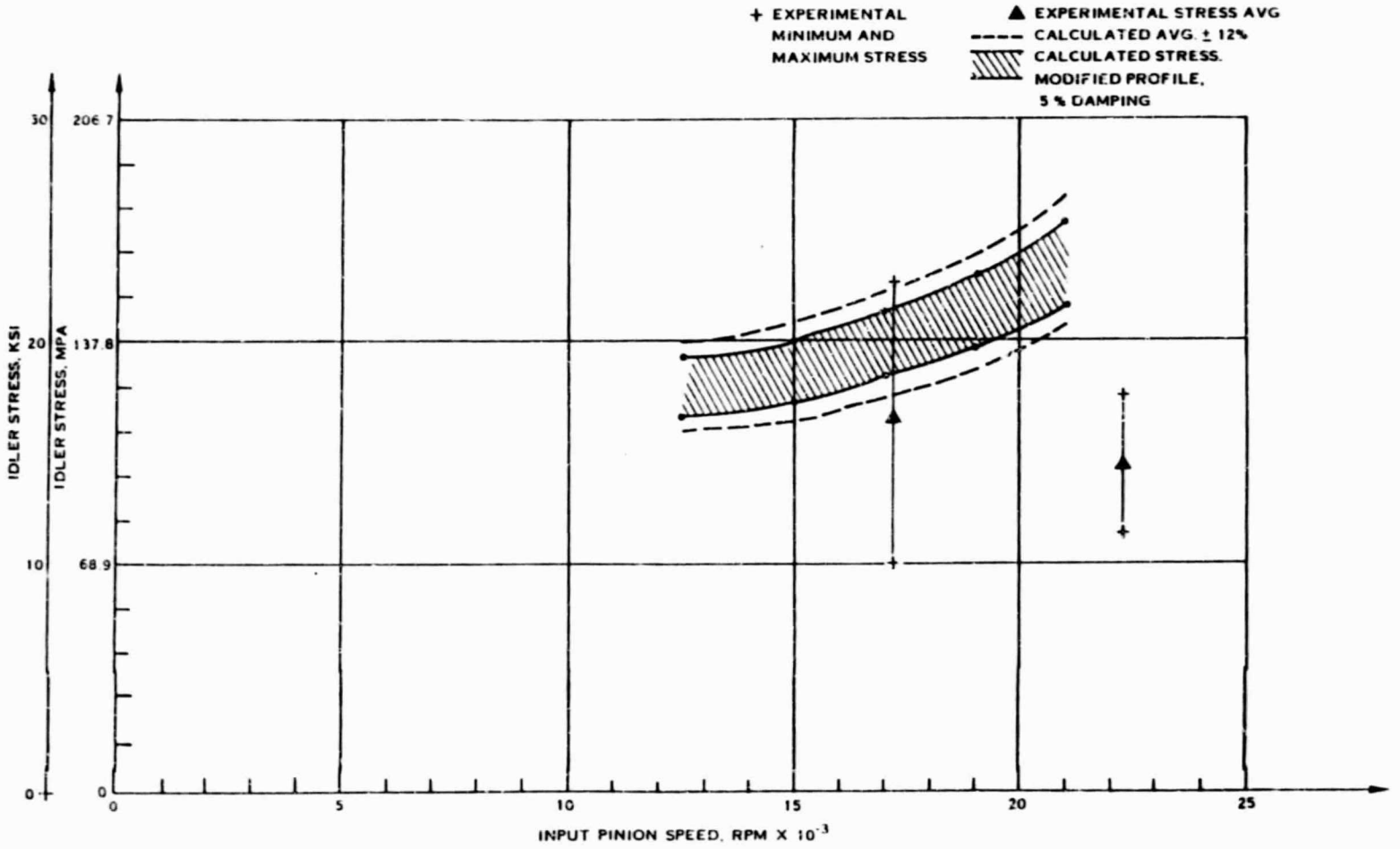

FIGURE 28. HAMILTON STANDARD IDLER STRESSES~68% TORQUE CASE

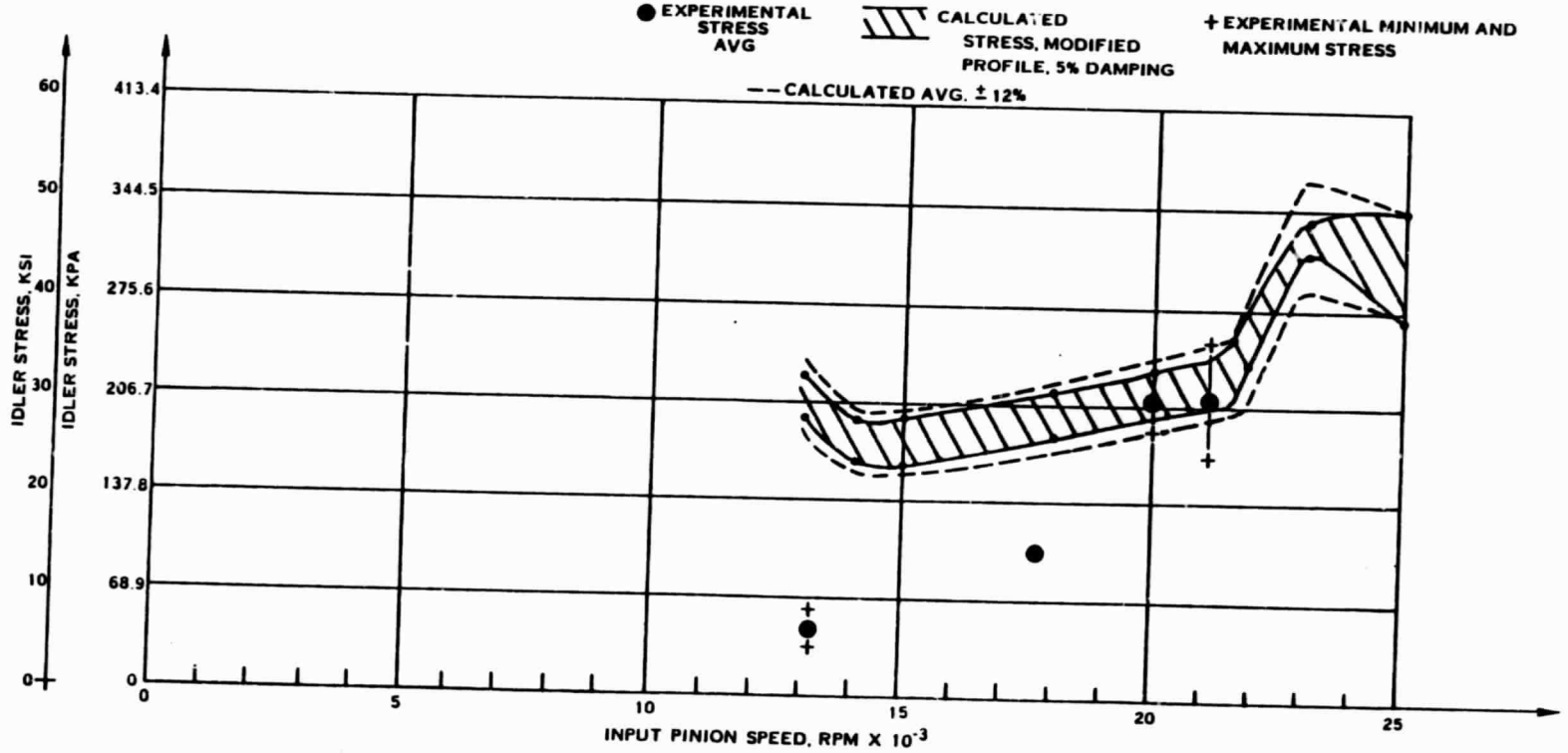

FIGURE 29. HAMILTON STANDARD GEARBOX, IDLER STRESSES ~ 90% TORQUE CASE

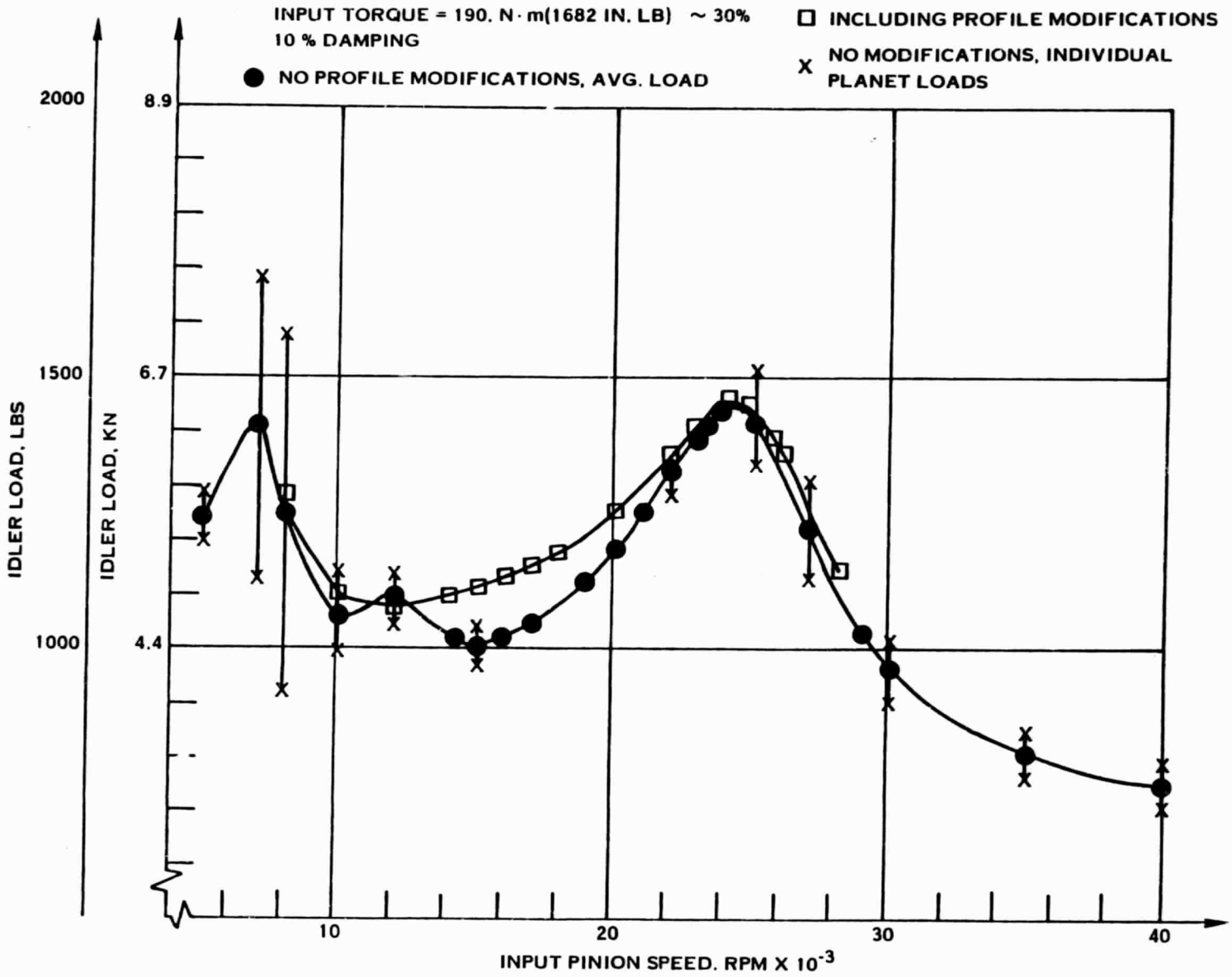

FIGURE 30. HAMILTON STANDARD GEARBOX, SPEED SURVEY OF LOADS

APPENDIX A: USER'S MANUAL

```
* * * * * * * * * * * * * * * * * * * * * * * * * * * * * * * * * * *
* * * * * * * * * * * *   F 1 7 8   * * * * * * * * * * * * * * * * * *
* * * * * * * * * * * * * * * * * * * * * * * * * * * * * * * * * * *
* *  U S E R ' S   M A N U A L   F O R   M U L T I P L E   M E S H  *
* *  S P U R   A N D   H E L I C A L   G E A R   S Y S T E M S  * * *
* * * * * * * * * * * * * * * * * * * * * * * * * * * * * * * * * * *
* * * * * * * * * *     AUG  1984     * * * * * * * * * * * * * * * *
* * * * * * * * * * * * * * * * * * * * * * * * * * * * * * * * * * *
```

* * * * * * * * * PROGRAM RESTRICTIONS * * * * * * * * * * * * * *

1. MAXIMUM PLANETS FOR SPUR AND SINGLE HELICAL GEARING IS 20
2. MAXIMUM PLANETS FOR DOUBLE HELICAL GEARING IS 10
3. MAXIMUM ITERATIONS FOR SOLUTION CONVERGENCE IS 20
4. MAXIMUM TEETH WITH TOOTH SPACING ERRORS IS 5
5. 10 TEETH ARE CHECKED FOR DYNAMICS DURING TOOTH ERROR PASS
6. MAXIMUM INVOLUTE CONTACT RATIO IS 3.0
7. MAXIMUM NUMBER OF SUN TEETH IS 50 FOR RUNOUT OPTION

* *
* * *INPUT DATA FOR MULTIPLE MESH SPUR AND HELICAL GEAR PROGRAM * * *

NOTE: ALL GEOMETRIC INPUT DATA IS IN THE ROTATIONAL PLANE AND ALL DEFAULT VALUES ARE 0.0 UNLESS OTHERWISE NOTED.

ANGLES ARE IN DEGREES
FORCES ARE IN POUNDS (#)
LENGTHS ARE IN INCHES (IN)
MASSES ARE IN (#-SEC**2/IN)
STRESSES ARE IN (#/IN**2)
TEMPERATURES ARE IN DEGREES FAHRENHEIT

THE DATA SET REQUIRED TO RUN THE MULTIPLE MESH PROGRAM IS DESCRIBED BELOW AND AN EXAMPLE DATA SET WITH CORRESPONDING EXAMPLE PROBLEM ARE IN APPENDIX C. A LIST OF GEAR SYSTEM PARAMETERS WITH DESCRIPTIONS, LOCATION NUMBERS, AND SOME NONZERO DEFAULT VALUES FOLLOWS THE INPUT DESCRIPTION.

CARD 1: TITLE CARD—CONTAINS CASE TITLE AND/OR DESCRIPTIVE INFORMATION. AT LEAST ONE COLUMN FROM 1 TO 40 MUST BE NONBLANK.

DATA CARDS: CARDS CONTAIN DATA IN THE FORM SHOWN IN FIGURE 1, NUMBER OF DATA ITEMS ON CARD, LOCATION NUMBER OF FIRST DATA ITEM IN LINE (SEE GEAR SYSTEM PARAMETERS SECTION FOR PARAMETER DESCRIPTION AND CORRESPONDING LOCATION NUMBERS), AND DATA ITEMS ARE IN 5 FIELDS OF 12 SPACES.

CASE TERMINATION CARD: TO TERMINATE A CASE THE LAST LINE MUST CONTAIN 0-1. IN COLUMNS 1-4.

SUBSEQUENT CASES: ANOTHER DATA SET OF THE SAME FORMAT—TITLE CARD, DATA CARD, AND CASE TERMINATION CARD—MAY FOLLOW THE CASE TERMINATION CARD.

JOB TERMINATION CARD: AFTER THE LAST SUBSEQUENT CASE TERMINATION CARD, A BLANK CARD (LINE) MUST BE INCLUDED.

** NOTE ** ALL NUMBERS MUST BE REAL EXCEPT THE NUMBER OF ITEMS, THAT IS, A DECIMAL POINT MUST BE INCLUDED. IT IS NOT NECESSARY TO INPUT ZERO VALUES AS THEY WILL DEFAULT TO ZERO UNLESS OTHERWISE SPECIFIED.

A BRIEF DESCRIPTION OF OUTPUT FOLLOWS THE GEAR SYSTEM PARAMETER SECTION.

FOR EXAMPLE, IN APPENDIX C THE TITLE CARD READS 'EXAMPLE DATA SET'. THE NEXT LINE IN THE DATA SET CONTAINS 5 PIECES OF DATA, STARTING AT LOCATION #1., FOLLOWED BY THE LEVEL (2.), THE DIAMETRAL PITCH (8.4667), THE PRESSURE ANGLE (22.5), COAST SIDE PRESSURE ANGLE AND HELIX ANGLE (BOTH = 0. FOR STANDARD SPUR GEARS, THESE WOULD DEFAULT TO 0 IF LEFT BLANK AND THE NUMBER OF ITEMS IN THE LINE WERE CHANGED TO 3.)

MOST OF THE INPUT VARIABLES HAVE SUFFICIENT EXPLANATION IN THE GEAR SYSTEM PARAMETERS SECTION, HOWEVER THE FOLLOWING PARAMETERS SHOULD BE CALCULATED AS FOLLOWS.

*** EQUIVALENT MASSES:

SUN EQUIVALENT MASS = J / (BASE RADIUS OF SUN)**2

WHERE J IS THE MASS MOMENT OF INERTIA FOR THE SUN. THE OTHER COMPONENTS ARE CALCULATED SIMILARLY, USING THE CORRESPONDING MOMENTS AND BASE RADII.

*** PHASING CONSTANTS:

FOR EQUALLY SPACED PLANETS THE SUN PHASING CONSTANTS ARE DETERMINED BY ASSUMING THE FIRST PLANET MESH HAS A PHASING CONSTANT OF ZERO. THE REMAINING SUN-PLANET PHASING CONSTANTS ARE DETERMINED BY:

(PLANET # - 1)*THE FRACTIONAL REMAINDER FROM DIVIDING THE NUMBER OF SUN TEETH BY THE TOTAL NUMBER OF PLANETS

WHERE THE 'FRACTIONAL REMAINDER' INDICATES THE SPACING DIFFERENCE BETWEEN PLANETS.

THE PHASING CONSTANTS FOR THE RING-PLANET MESHES ARE DETERMINED THE SAME WAY IF THE PLANET HAS AN ODD NUMBER OF TEETH, USING THE NUMBER OF RING TEETH. IF THE PLANETS HAVE AN EVEN NUMBER OF TEETH THE CONSTANTS ARE CALCULATED FOR THE SUN MESHES THEN 0.5 IS ADDED TO EACH TO OBTAIN THE RING-PLANET MESH PHASING CONSTANTS (KRP), DUE TO THE RING GEAR BEING .5 OFFSET FROM THE SUN GEAR.

EXAMPLE CORRESPONDING TO APPENDIX C:

SUN PLANET MESH— 14/3 = 12 2/3

PLANET 1, KSP(1) = 0.

PLANET 2, (2-1)*(2/3) = .6666667
KSP(2) = .6666667

PLANET 3, (3-1)*(2/3)=1.3333333
KSP(3) = .3333333

RING PLANET MESH— (EVEN NUMBER OF PLANET TEETH)

PLANET 1, KRP(1) = KSP(1) + .5 = .5

PLANET 2, KSP(2) + .5 = 1.1666667
KRP(2) = .1666667

PLANET 3, KSP(3) + .5 = .8333333

KRP(3) = .8333333

*** BOUNDARY CONDITIONS:

AN INITIAL ESTIMATE FOR DISPLACEMENT BOUNDARY CONDITIONS MAY BE OBTAINED BY DIVIDING THE STATIC TOOTH LOAD AT THE PITCH RADIUS BY THE TOOTH SPRING RATE AT THE PITCH RADIUS.

***** LEVELS OF INPUT

LEVEL I INPUT
THE FIRST INPUT ITEM WILL BE THE LEVEL DESIRED, FOLLOWED BY ITEMS 2 THROUGH 51 AND WHERE NOTED. THE OTHER VALUES WILL DEFAULT. THE MATERIAL PROPERTIES, LOCATIONS 22 TO 27, DEFAULT FOR STEEL. THE TOLERANCES ARE SET TO ZERO OR DEFAULT VALUES BELOW, ERRORS ARE SET TO 0. THERE ARE NO PROFILE MODIFICATIONS. OTHER NONZERO DEFAULT VALUES ARE: SURFACE ROUGHNESS = 25, OIL TEMPERATURE = 180 F, MATERIAL CONSTANT = 0.0528, DAMPING = .02, AND OIL TYPE MIL-L-23699. ANY DESIRED PLOTS CAN BE OBTAINED, SEE LOC G01-G08,

AND A CHECK ON INPUT DATA CAN BE MADE, # 699. IF CONTACT RATIO IS HIGH (GREATER THAN 2) IT MUST BE INPUT IN LOC 54 & 55.

LEVEL II INPUT
LEVEL 2 REQUIRES THE ITEMS REQUIRED FOR LEVEL 1 PLUS ALL OTHER ITEMS EXCEPT LOCATIONS 64, 65, 91-100, AND 175-192. THE MINIMUM INPUT FOR THIS LEVEL WOULD BE LEVEL 1 DATA PLUS DAMPING, FLASH TEMPERATURE DATA, SOLUTION ITERATION DATA, AND PHASING CONSTANTS. DEFAULT VALUES ARE ZERO UNLESS INDICATED OTHERWISE BELOW.

LEVEL III INPUT
LEVEL 3 REQUIRES ALL ITEMS TO BE INPUT, UNLESS DEFAULT VALUES ARE INDICATED. THE MINIMUM INPUT FOR THIS LEVEL WOULD BE LEVEL 2 DATA.

**** NOTE: FOR HIGH CONTACT RATIO GEARS (CR > 2.), THE USER MUST INPUT THE CR (LOC 54 AND 55). PROGRAM CALCULATES RATIO IF CR < 2.

*** G E A R S Y S T E M P A R A M E T E R S ******************

LOC	NAME	DESCRIPTION
1	LEVEL	TRIGGER FOR LEVEL OF INPUT DATA
2	DP	DIAMETRAL PITCH (NORMAL PLANE)
3	PSANG	SUN-PLANET DRIVE SIDE PRESSURE ANGLE @ PD RING-PLANET COAST SIDE PRESSURE ANGLE @ PD
4	PSANGB	SUN-PLANET COAST SIDE PRESSURE ANGLE @ PD RING-PLANET DRIVE SIDE PRESSURE ANGLE @ PD ** 0.0 IF PRESSURE ANGLES FOR DRIVE & COAST SIDES EQUAL
5	PSIO	HELIX ANGLE @ PD ** 0.0 FOR SPUR GEARS
6	N1	NUMBER OF TEETH ON SUN GEAR
7	N2	PLANET GEARS
8	N3	RING GEAR
9	FW1	AXIAL FACE WIDTH OF SUN GEAR
10	FW2	PLANET GEARS
11	FW3	RING GEAR
12	N	NUMBER OF PLANET GEARS
13	K	IF K=1 PLANETARY SYSTEM, I.E., RING GEAR FIXED IF K=2 STAR SYSTEM, I.E., PLANET CARRIER FIXED ** IF K=4 NON PLANETARY, I.E., NO RING AND NO CARRIER SUN-INPUT, PLANET-OUTPUT IF K=5 NON PLANETARY, I.E., NO SUN AND NO CARRIER, PLANET INPUT, RING OUTPUT * IF K=6 PLANETARY SYSTEM WITH FLEXIBLE PLANET CARRIER * IF K=7 STAR SYSTEM WITH FLEXIBLE RING GEAR RIM

******* K = 6 AND K = 7 CURRENTLY NOT AVAILABLE *********

* IF K=6 OR K=7 LOC 89 IS REQUIRED FOR PLANET CARRIER OR RING GEAR RIM STIFFNESS VALUE ALONG THE LINE-OF-ACTION.
** FOR K=4 AND RUNOUT ERROR, INPUT LOC 200.

14	TORQ	AXIAL INPUT TORQUE ON SUN GEAR (OR PLANET IF K=5)
15	RPM	INITIAL AXIAL ROTATIONAL SPEED OF SUN GEAR (OR PLANET IF K=5)
16	RPMF	FINAL AXIAL ROTATIONAL SPEED OF SUN GEAR FOR SPD RANGE
17	INTVL	NUMBER OF MAIN INTERVALS THE SPEED RANGE DIVIDED INTO ** FOR ONE RPM ONLY, RPM=RPMF AND INTVL=1.** STEP SIZE =(RPMF - RPM)/INTVL, WILL BE DIVIDED BY 5 IN AREAS OF PEAK LOADS

******* GEAR MATERIAL PROPERTIES *********************************

22	E1	YOUNGS MODULUS * E-06 OF SUN GEAR	(DEFAULT = 30.)
23	E2	PLANET GEARS	" " "
24	E3	RING GEAR	" " "
25	MU1	POISSONS RATIO OF SUN GEAR	(DEFAULT = .30)
26	MU2	PLANET GEARS	" " "
27	MU3	RING GEAR	" " "

******* GEAR EQUIVALENT MASSES ***********************************

28	MS	EQUIVALENT MASS OF SUN GEAR ABOUT ROTATIONAL AXIS
29	MC	PLANET CARRIER
30	MR	RING GEAR
31-50	MP(I)	PLANET GEARS

*** NOTE: FOR K=6 OR K=7,CARRIER OR RING MASSFOR TOTAL UNIT, NOT SEGMENTS.

******* TRIGGER FOR DOUBLE HELICAL GEARING *********************

51	DBHEL	IF = 0.0 SINGLE HELICAL GEARING IF PSIO .NE. 0.0 IF = 1.0 DOUBLE HELICAL GEARING IF PSIO .NE. 0.0

* *
END OF LEVEL 1 INPUT (UNLESS HIGH CONTACT RATIO)
* *

```
******* GEAR MESHING DAMPING RATIOS ****************************

   52   ZSP      DAMPING RATIO OF SUN-PLANET MESHES
   53   ZRP        "       "     " RING-PLANET MESHES
 * * * NOTE:  IF CONTACT RATIO > 2, CRSP AND CRRP MUST BE INPUT, BUT
       IF ZERO IS INPUT THE PROGRAM WILL CALCULATE FOR CR < 2 ONLY.
   54   CRSP     INVOLUTE CONTACT RATIO OF SUN-PLANET MESHES
   55   CRRP       "         "      "   "  RING-PLANET MESHES

******* ACTIVE FACE WIDTH VALUES *******************************

  **NOTE:  LOC 56 - 59 FOR HELICAL GEARS ONLY

   56   L1SP     INACTIVE SUN-PLANET FACE WIDTH ON LEFT
   57   L2SP        "     "    "     "     "   "  RIGHT
   58   L1RP     INACTIVE RING-PLANET FACE WIDTH ON LEFT
   59   L2RP        "     "    "     "     "   "  RIGHT

******* SUN-PLANET PROFILE MODIFICATION INPUT DATA *************

   60   PCTSOD  SD AS A PERCENT OF SOD (%)
   61   PCTSOE  SE AS A PERCENT OF SOE (%)
   62   DELD    DISENGAGEMENT TIP RELIEF (IN.), MINIMUM
   63   DELE    ENGAGEMENT TIP RELIEF    (IN.), MINIMUM
   **NOTE:  SIGN CONVENTION—POSITIVE INPUT, MATERIAL REMOVED

 * * * * * * XNVDX AND XNVEX ARE NOT REQUIRED FOR LEVEL 2 * * * *
   64   XNVDX   DISENGAGEMENT PROFILE MODIFICATION SHAPE FACTOR
   65   XNVEX      ENGAGEMENT
 * * * * * * * * * * * * * * * * * * * * * * * * * * * * * * * * *

   66   PMODSP  PERCENT OF TIP RELIEF ON SUN GEAR, ENGAGEMENT
   67   PMDSPD  PERCENT OF TIP RELIEF ON SUN GEAR, DISENGAGEMENT
                  = % TIP RELIEF ON PLANET
   68   DLSP    TOLERANCE AT START OF PROFILE MODIFICATION
   78   DLTOL   TOTAL TIP RELIEF TOLERANCE (SUN + PLANET
                AND/OR RING + PLANET, DEPENDING ON SYSTEM TYPE)
        SOD = LENGTH OF DISENGAGEMENT PART OF THE LINE OF ACTION
        SOE =   "    "  ENGAGEMENT     "   "   "    "   "     "
        SD & SE ARE THE SEGMENTS OF THE SOD & SOE THAT ARE USED, WHEN
         PROFILE MODIFICATIONS ARE MADE.

******* RING-PLANET PROFILE MODIFICATION INPUT DATA ************

   69   PTSOD3  SD AS A PERCENT OF SOD
   70   PTSOE3  SE AS A PERCENT OF SOE
   71   DELD3   DISENGAGEMENT TIP RELIEF
   72   DELE3   ENGAGEMENT TIP RELIEF
```

```
* * * * * LOCATION 73 AND 74 NOT REQUIRED FOR LEVEL 2 * * * * *
  73    XNVDX3  DISENGAGEMENT PROFILE MODIFICATION SHAPE FACTOR
  74    XNVEX3  ENGAGEMENT PROFILE MODIFICATION SHAPE FACTOR
* * * * * * * * * * * * * * * * * * * * * * * * * * * * * * * *

  75    PMODRP  PERCENT OF TIP RELIEF ON PLANET GEAR, ENGAGEMENT
  76    PMDRPD  PERCENT OF TIP RELIEF ON PLANET GEAR, DISENGAGEMENT
                - % TIP RELIEF ON RING GEAR
  77    DLRP    TOLERANCE AT START OF PROFILE MODIFICATION
  78    DLTOL   TOTAL TIP RELIEF TOLERANCE, FOR BOTH SUN+PLANET
                AND/OR RING + PLANET

****** MESH MODIFICATION DUE TO FACE WIDTH CROWNING ***********

  80    LECSP   LENGTH OF FACE WIDTH CROWN OF ENGAGEMENT FOR SP MESH
  81    LDCSP     "    "   "     "    "   "  DISENGAGEMENT FOR SP MESH
  82    DLECSP  ENGAGEMENT EDGE RELIEF FOR SP MESH
  83    DLDCSP  DISENGAGEMENT EDGE RELIEF FOR SP MESH

  84    LECRP   LENGTH OF FACE WIDTH CROWN OF ENGAGEMENT FOR RP MESH
  85    LDCRP     "    "   "     "    "   "  DISENGAGEMENT FOR RP MESH
  86    DLECRP  ENGAGEMENT EDGE RELIEF FOR RP MESH
  87    DLDCRP  DISENGAGEMENT EDGE RELIEF FOR RP MESH

****** FLEXIBLE PLANET CARRIER OR RING GEAR RIM DATA **********

  88    ZCR     IF K=6, PLANET CARRIER DAMPING RATIO
                IF K=7, RING GEAR RIM DAMPING RATIO

  89    CARRK   IF K=6 PLANET CARRIER STIFFNESS ALONG-THE-LINE-OF-
                ACTION (#/IN)
                IF K=7 RING GEAR RIM STIFFNESS ALONG-THE-LINE-OF-
                ACTION (#/IN)

****** TOOTH PAIR COMPLIANCE DATA ****************************

  90    WIOK    IF = 0.0 PREPROCESSOR CALULATES TOOTH PAIR COMPLIANCE
                IF = 1.0 INPUT COMPLIANCE DATA IN LOCATIONS 91-101

* * * * * 91 - 100 NOT REQUIRED FOR LEVEL 2 * * * * * * * * * * *

  91    SPKSP   SINGLE TOOTH PAIR SPRINGRATE OF SUN-PLANET MESHES
  92    COMASP  COMPLIANCE CONSTANT (S/SO)**1 OF SUN-PLANET MESHES
  93    COMBSP                              2
  94    COMCSP                              3
  95    COMDSP                              4

  96    SPKRP   SINGLE TOOTH PAIR SPRINGRATE OF RING-PLANET MESHES
  97    COMARP  COMPLIANCE CONSTANT (S/SO)**1 OF RING-PLANET MESHES
```

```
 98   COMBRP                                  2
 99   COMCRP                                  3
100   COMDRP                                  4

    WHERE S - IS THE LENGTH ALONG THE LINE OF ACTION TO THE POINT
     OF ENGAGEMENT
    AND SO - THE LENGTH OF THE LINE OF ACTION

* * * * * * * * * * * * * * * * * * * * * * * * * * * * * * * * * * * * *

101   HRTZSP  HERTZ STRESS FOR COMPLIANCE CALCULATION FOR SUN-PLANET
102   HRTZRP                                                 RING-PLANET
      ** THE PROGRAM WILL USE 101 AND 102 AS CONSTANTS FOR THE COM-
         PLIANCE CALCULATIONS IF INPUT.  DEFAULT WILL USE CALCULATED
         STRESS THROUGH MESH.
103   XPSPSP  IF - 0.0 PLANE STRESS IS ASSUMED FOR SUN-PLANET
              IF - 1.0 PLANE STRAIN IS ASSUMED FOR SUN-PLANET
104   XPSPRP  IF - 0.0       STRESS                  RING-PLANET
              IF - 1.0       STRAIN                  RING-PLANET

111   CONVEK  IF - 0.0 HELICAL TOOTH IS DIVIDED INTO 10 INDEPENDENT
                   AXIAL SEGMENTS
              IF - 1.0 CONVECTIVE COMPLIANCE MATRIX MUST BE INPUT
                  IN LOCATIONS 701 TO 800

******* TOOTH PAIR GEOMETRIC DATA ******************************

120   BYPASS IF - 0.0 GEOMETRIC PREPROCESSOR IS USED
             IF - 1.0 GEOMETRIC DATA MUST BE INPUT IN LOCATIONS
                      121-132

121   RADTOS MAX. RADIUS TO BASE OF FILLET OF SUN GEAR        (ROOT
122   RADTOP                                  PLANET GEARS  RADIUS)
123   RADTOR                                  RING GEAR

124   RADTIS MAX. RADIUS TO TIP OF TOOTH OF SUN GEAR
125   RADTIP                                PLANET GEARS
126   RADTIR                                RING GEAR

127   TOOTHS NOMINAL TOOTH THICKNESS AT PD OF SUN GEAR
128   TOOTHP                                  PLANET GEARS
129   TOOTHR                                  RING GEAR

130   RADFIS MAX. FILLET RADIUS OF SUN GEAR
131   RADFIP                        PLANET GEARS
132   RADFIR                        RING GEAR
```

```
****** FLASH TEMPERATURE DATA **********************************

 140   SROU    SURFACE ROUGHNESS (RMS, MICROINCHES)
 141   TOIL    OIL INLET TEMPERATURE
 142   CFMAT   MATERIAL CONSTANT
 143   OILTYP  TYPE OF OIL IN GEARBOX
                1 FOR MIL-L-23699
                2 FOR MIL-L- 7808
                3 TO BE DETERMINED
                4 TO BE DETERMINED
                (0 DEFAULTS TO TYPE 1)

******* SOLUTION ITERATION DATA *********************************

 150   TOLER   ITERATION TOLERANCE FOR BOUNDARY CONDITION CONVERGENCE
                 (% * 100, DEFAULT FOR LEVEL 1 = .01)
 151   NLOOP   NUMBER OF ITERATIONS FOR BOUNDARY CONDITION CONVERGENCE
               NLOOP MAXIMUM = 20, DEFAULT = 20.

****** TOOTH PAIR GEOMETRIC TOLERANCE DATA ********************

 160   DLROS   TOLERANCE ON TIP RADIUS OF SUN GEAR    (DEFAULT = .002)
 161   DLROP                              PLANET GEARS    "    "   "
 162   DLROR                              RING GEAR       "    "   "
 163   BSE     EDGE BREAK ON TOPLAND OF ALL GEARS     (DEFAULT = .010)
 164   DLRR    ROOT RADIUS TOLERANCE OF ALL GEARS     (DEFAULT = .005)
 165   DLCDN   CENTER DISTANCE TOLERANCE (TOWARD TIGHT MESH)ALL GEARS
 166   DLCDP   CENTER DISTANCE TOLERANCE (AWAY FROM TIGHT MESH)
 167   DLMBT   MACHINE BACKLASH TOLERANCE ALL GEARS   (DEFAULT = .002)

NOTE:THE TOOTH ROOT FILLET RADIUS TOLERANCE = .005 IN THE PREPROCESSOR

******* 3-DIMENSIONAL FACTORS FOR SPUR GEARS ONLY **************

* * * * * 175 - 192 NOT REQUIRED FOR LEVEL 2 * * * * * * * * * * * * *

 175   SPRNBS  IF = 0. RIM BENDING EFFECTS NOT INCLUDED IN SUN GEAR
                   (DEFAULT = 10.E+10)
               IF > 0. BENDING SPRINGRATE(IN-#/RAD) OF SUN RIM
 176   SPRNBP  IF = 0. RIM BENDING EFFECTS NOT INCLUDED IN PLANET GEAR
                   (DEFAULT = 10.E+10)
               IF > 0. BENDING SPRINGRATE(IN-#/RAD) OF PLANET RIM
 177   SPRNBR  IF = 0. RIM BENDING EFFECTS NOT INCLUDED IN RING GEAR
                   (DEFAULT = 10.E+10)
               IF > 0. BENDING SPRINGRATE(IN-#/RAD) OF RING RIM
 178   SPRNLS  RADIUS FROM RIM TO PD (REQUIRED WITH SPRNBS) SUN
 179   SPRNLP  RADIUS FROM RIM TO PD (REQUIRED WITH SPRNBP) PLANET
 180   SPRNLR  RADIUS FROM RIM TO PD (REQUIRED WITH SPRNBR) PLANET
```

181 EFWD1S EFFECTIVE SUN FACE WIDTH FACTOR AT TOOTH TIP
IF = 0. (DEFAULT = 1.0)
182 EFWD2S EFFECTIVE SUN FACE WIDTH FACTOR AT FILLET
IF = 0. (DEFAULT = 1.0)
183 EFWD1P EFFECTIVE PLANET FACE WIDTH FACTOR AT TOOTH TIP
IF = 0. (DEFAULT = 1.0)
184 EFWD2P EFFECTIVE PLANET FACE WIDTH FACTOR AT FILLET
IF = 0. (DEFAULT = 1.0)
185 EFWD1R EFFECTIVE RING FACE WIDTH FACTOR AT TOOTH TIP
IF = 0. (DEFAULT = 1.0)
186 EFWD2R EFFECTIVE RING FACE WIDTH FACTOR AT FILLET
IF = 0. (DEFAULT = 1.0)
187 STRSES STRESS DISTRIB. FACTOR FOR END EFFTS AT SUN WIDTH EDGE
IF = 0. (DEFAULT = 1.0)
188 STRSCS STRESS DISTRIB. FACTOR FOR END EFFTS AT SUN WIDTH CENT
IF = 0. (DEFAULT = 1.0)
189 STRSEP STRESS DISTRIB. FACTOR FOR END EFFTS AT PLAN WDTH EDGE
IF = 0. (DEFAULT = 1.0)
190 STRSCP STRESS DISTRIB. FACTOR FOR END EFFTS AT PLAN WDTH CENT
IF = 0. (DEFAULT = 1.0)
191 STRSER STRESS DISTRIB. FACTOR FOR END EFFTS AT RING WDTH EDGE
IF = 0. (DEFAULT = 1.0)
192 STRSCR STRESS DISTRIB. FACTOR FOR END EFFTS AT RING WDTH CENT
IF = 0. (DEFAULT = 1.0)

******* HELIX ANGLE ERRORS **********

195 DELPSP HELIX ANGLE ERROR FOR SUN-PLANET MESH

196 DELPRP " " " " RING-PLANET MESH

197 DELPS2 IF DBHEL = 0.0 DELPS2 = 0.0
IF DBHEL = 1.0 DELPS2 = HELIX ANGLE ERROR OF RIGHT
HALF OF SUN-PLANET DOUBLE HELICAL GEARS
198 DELPR2 IF DBHEL = 0.0 DELPR2 = 0.0
IF DBHEL = 1.0 DELPR2 = HELIX ANGLE ERROR OF RIGHT
HALF OF RING-PLANET DOUBLE HELICAL GEARS

******* TOOTH PAIR SPACING ERRORS **********

200 DR SUN RUNOUT ERROR FOR EXTERNAL-EXTERNAL SINGLE MESH ONLY
(K=4), DISPLACEMENT ERROR OF SUN CENTER

**NOTE: FOR DOUBLE HELICAL GEARS (DBHEL = 1.0) THE FIRST 10
VALUES OF I IN THE E(I,J) ARRAYS ARE FOR THE LEFT HALF
OF THE DOUBLE HELICAL GEARS AND THE LAST 10 LOCATIONS
ARE FOR THE RIGHT HALF OFTHE DOUBLE HELICAL GEARS,
WHERE I = THE PLANET NUMBER.

```
  221 TO 240   ESP(I,1)SUN-PLANET ERROR ARRAY FOR TOOTH 1
  241 TO 260   ESP(I,2)                                  2
  261 TO 280   ESP(I,3)                                  3
  281 TO 300   ESP(I,4)                                  4
  301 TO 320   ESP(I,5)                                  5

  321 TO 340   ERP(I,1)RING-PLANET ERROR ARRAY FOR TOOTH 1
  341 TO 360   ERP(I,2)                                  2
  361 TO 380   ERP(I,3)                                  3
  381 TO 400   ERP(I,4)                                  4
  401 TO 420   ERP(I,5)                                  5

******* PLANET GEARS PHASING CONSTANTS *************************

  421 TO 440  KSP(I)   SUN-PLANET PHASING CONSTANTS ARRAY
  441 TO 460  KRP(I)  RING-PLANET PHASING CONSTANTS ARRAY

******* INITIAL BOUNDARY CONDITIONS ****************************

  481 TO 500  XOSP(I)  SUN-PLANET INITIAL DISPLACEMENT BOUNDARY COND
  501 TO 520  XORP(I) RING-PLANET INITIAL DISPLACEMENT BOUNDARY COND
  521 TO 540  X1SP(I)  SUN-PLANET INITIAL VELOCITY BOUNDARY COND
  541 TO 560  X1RP(I) RING-PLANET INITIAL VELOCITY BOUNDARY COND

******* PROGRAM PLOT SELECTIONS FOR SPUR GEARS ONLY ************

  601    PLTLD    IF = 0.0
                  IF = 1.0 LOAD PLOTS, NORMALIZED LOAD--DYNAMIC/STATIC
  602    PLTPV    IF = 0.0
                  IF = 1.0 PV   PLOTS, PRESSURE SLIDING VELOCITY
  603    PLTHS    IF = 0.0
                  IF = 1.0 HERTZ STRESS PLOTS
  604    PLTFT    IF = 0.0
                  IF = 1.0 FLASH TEMPERATURE PLOTS
  605    PLTSS    IF = 0.0
                  IF = 1.0 SUN GEAR HEYWOOD STRESS PLOTS
  606    PLTPSS   IF = 0.0
                  IF = 1.0 SUN-PLANET PLANET GEAR HEYWOOD STRESS PLOTS
  607    PLTPRS   IF = 0.0
                  IF = 1.0 RING-PLANET PLANET GEAR HEYWOOD STRESS PLOTS
  608    PLTRPS   IF = 0.0
                  IF = 1.0 RING GEAR HEYWOOD STRESS PLOTS
```

******* PROGRAM CHECK RUN **

```
699    CHECK    IF = 0.0 REGULAR RUN TO COMPLETION
                IF = 1.0 EXITS PROGRAM BEFORE DYNAMIC SOLUTION
                         TO ALLOW CHECKING OF INPUT DATA AND THE
                         PREPROCESSOR RESULTS
```

******* CONVECTIVE COMPLIANCE MATRIX FOR HELICAL GEARING *******

** CURRENTLY NOT AVAILABLE WITHOUT PROGRAM ALTERATIONS, IE. COMMENT STATEMENTS MUST BE REMOVED

```
701 TO 709  LL=1 TO  9    L=1
711 TO 719  LL=1 TO  9    L=2
721 TO 729  LL=1 TO  9    L=3
731 TO 739  LL=1 TO  9    L=4
741 TO 749  LL=1 TO  9    L=5
751 TO 759  LL=1 TO  9    L=6
761 TO 769  LL=1 TO  9    L=7
771 TO 779  LL=1 TO  9    L=8
781 TO 789  LL=1 TO  9    L=9
```

* *

***** OUTPUT DESCRIPTION

THE FOLLOWING LIST INDICATES THE INFORMATION AND RESULTS THAT MAY APPEAR IN THE OUTPUT, IN THE ORDER THEY WILL APPEAR.

CASE TITLE—THE TITLE AND/OR OTHER INFORMATION INPUT ON THE FIRST DATA CARD.

TIP MODIFICATION—IF THERE IS INSUFFICIENT TIP CLEARANCE, AN ADJUSTMENT IS MADE INTERNALLY AND A MESSAGE OUTPUT UNTIL SUFFICIENT CLEARANCE IF OBTAINED.

INVOLUTE MODIFICATION TABLE—SHOWS THE PROCESSED RESULTS OF ANY INPUT PROFILE MODIFICATIONS. TABLES ARE PRINTED FOR ENGAGEMENT AND DISENGAGEMENT WHICH INCLUDE MINIMUM AND MAXIMUM INVOLUTE MODIFICATIONS, DIAMETER AND CORRESPONDING ROLL ANGLE FOR THE MODIFIED PORTION OF THE PROFILE. THIS WILL BE OUTPUT FOR THE SUN-PLANET MESH AND/OR RING-PLANET MESH IN CONJUNCTION WITH THE CORRESPONDING INPUT DATA.

INPUT DATA—THE INPUT DATA AND PREPROCESSED GEOMETRIC DATA IS PRINTED FOR SUN-PLANET MESH AND/OR RING-PLANET MESH.

FLEXIBILITY—IF THE FLEXIBLE PLANET CARRIER OPTION IS IN EFFECT A MESSAGE APPEARS THAT INDICATES THIS.

ADDITIONAL INPUT DATA—NUMBER OF PLANETS, EQUIVALENT MASSES, ETC.

COMPLIANCE CONSTANTS—CALCULATED CONSTANTS FOR FOURTH ORDER COMPLIANCE EQUATION.

ITERATED BOUNDARY CONDITIONS—BOUNDARY CONDITIONS PRINTED, FOLLOWED BY THE CURRENT SPEED BEING EXAMINED AND CORRESPONDING MAXIMUM LOADS (FOR SUN-PLANET AND/OR RING-PLANET MESHES).

IF A SPEED SURVEY WAS RUN, THE SPEED CORRESPONDING TO THE OVERALL MAXIMUM LOAD FROM THE RANGE CALCULATED IS OUTPUT WITH THE MAXIMUM LOAD. THIS IS THE SPEED USED FOR THE REMAINING CALCULATIONS, I.E. STRESS.

MAXIMUM VALUES—TABLE(S) OF MAXIMUM VALUES CALCULATED ARE PRINTED FOR EACH SUN-PLANET MESH AND/OR RING-PLANET MESH. THESE WILL APPEAR FOR THE NO ERROR SOLUTION AND EACH ERROR SOLUTION. TWO ABBREVIATIONS APPEAR—PV=PRESSURE SLIDING VELOCITY AND PD=PITCH DIAMETER.

ERROR MATRIX—IF TOOTH SPACING ERRORS ARE INPUT, OR GENERATED FOR RUNOUT SOLUTION, A TABLE OF ERRORS IS PRINTED BEFORE THE TABLES OF MAXIMUM VALUES.

EXAMPLE PROBLEM

Diametral Pitch = 8.4667

Pressure Angle = 22.5°

Number of Sun Teeth = 14

Number of Ring Teeth = 70

Number of Planet Teeth = 28

Face Width, Sun & Planets = 1.1811 in.

Face Width, Ring = 1.4184 in.

Input Torque = 30 in. lb.

Input RPM = 7000 rpm

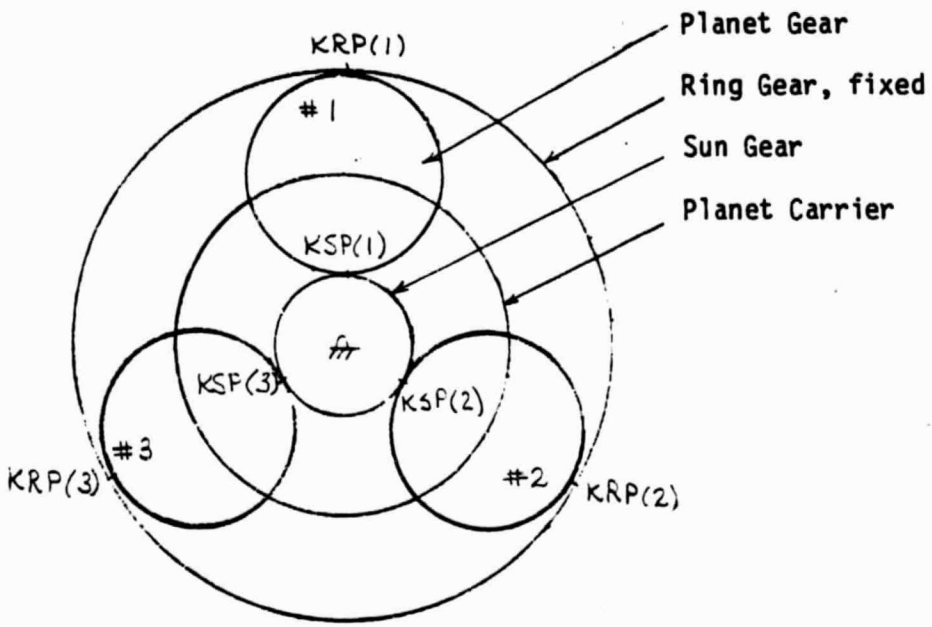

Example Data Set

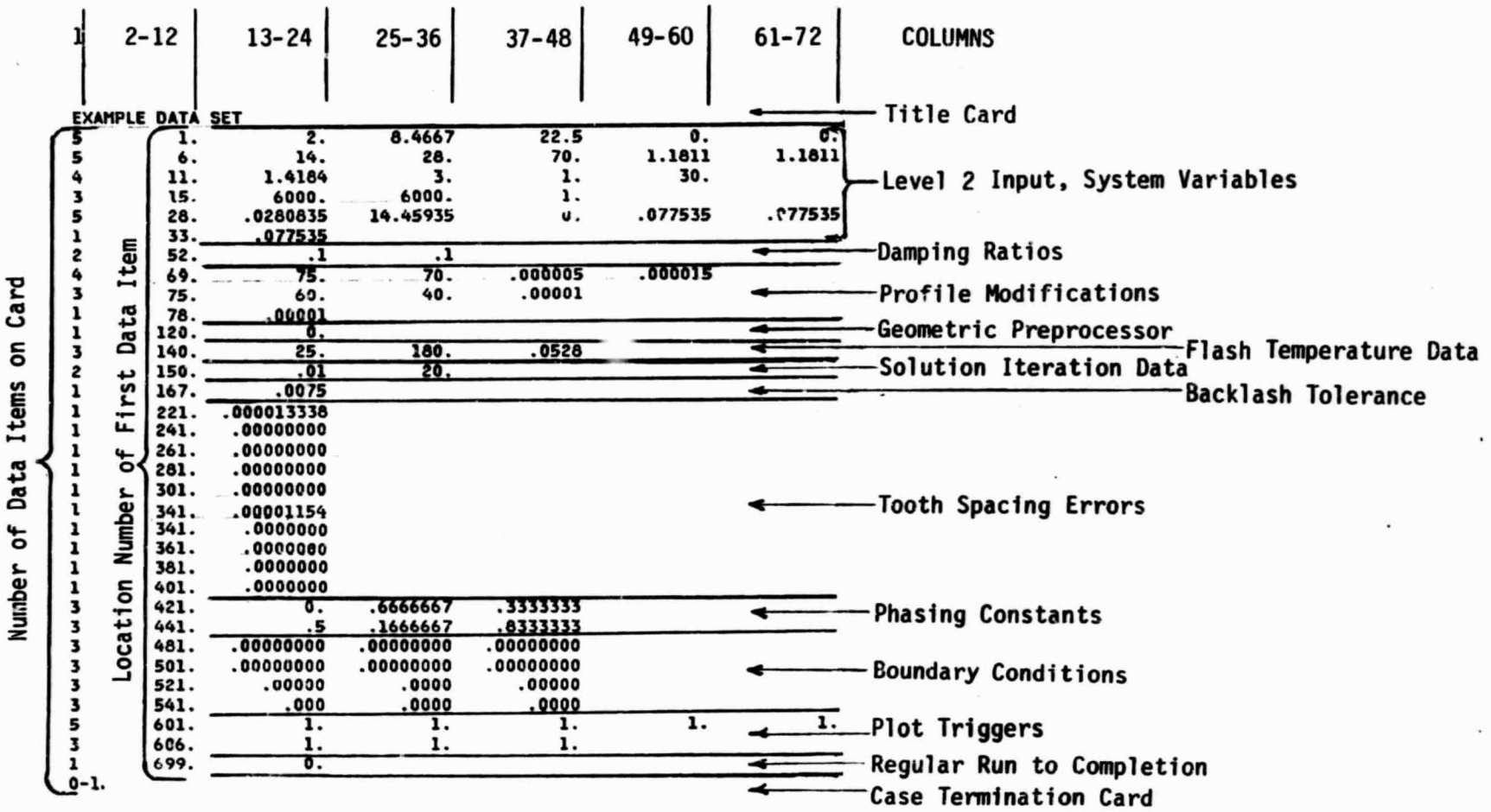

PROGRAM FEATURES OF THE AUG 1984 VERSION

1. CALCULATES DYNAMIC LOAD RESPONSE FOR
   A. SINGLE MESH SPUR GEARING
   B. MULTIPLE MESH SPUR GEARING,
      STAR OR PLANETARY
   C. SINGLE MESH HELICAL GEARING
   D. MULTIPLE MESH HELICAL GEARING
   E. DOUBLE HELICAL GEARING

2. GEOMETRIC PREPROCESSOR CAN BE USED FOR
   A. INVOLUTE SPUR AND HELICAL TOOTH FORMS
   B. INVOLUTE BUTTRESSED TOOTH FORMS
   C. EXTERNAL AND INTERNAL TOOTH FORMS
   D. MEASUREMENT OVER WIRES DATA
   E. TOLERANCE AND INTERFERENCE CHECKING
   F. INVOLUTE MODIFICATION TABLES

3. STRESS POSTPROCESSOR CAN BE USED FOR
   A. DYNAMIC LOAD SUMMARY
   B. MODIFIED HEYWOOD STRESS SENSITIVITY
   C. HERTZ STRESSING
   D. FLASH TEMPERATURE SUMMARY
   E. PRESSURE-SLIDING VELOCITY(PV) SUMMARY

4. DYNAMIC LOAD SOLUTION ASSUMPTIONS
   A. CIRCUMFERENTIALLY STIFF RING GEAR
   B. CIRCUMFERENTIALLY STIFF PLANET CARRIER
   C. EQUILIBRIUM EQUATIONS DO NOT INCLUDE FRICTION
   D. INPUT TORQUE IS CONSTANT

5. GEOMETRIC DATA IN ROTATIONAL PLANE UNLESS NOTED
   A. ANGLES ARE IN DEGREES
   B. FORCES ARE IN POUNDS(#)
   C. LENGTHS ARE IN INCHES(IN)
   D. MASSES ARE IN (#-SEC**2/IN)
   E. STRESSES ARE IN PSI(#/IN**2)
   F. TEMPERATURES ARE IN DEGREES FAHRENHEIT

6. THE PLANET CARRIER OR RING GEAR RIM FLEXIBILITIES
   ALONG THE RESPECTIVE LINES-OF-ACTION CAN BE
   ACCOUNTED FOR IN THE DYNAMIC LOAD SOLUTION

THIS PROGRAM WAS DEVELOPED AT HAMILTON STANDARD DIVISION OF UNITED TECHNOLOGIES , WINDSOR LOCKS , CONN. BY J. PIKE, R. CORNELL, W. WESTERVELT, AND L. BOYD. FUNDING WAS GIVEN UNDER CONTRACT BY NASA-LEWIS , CLEVELAND AND MONITORED BY D. TOWNSEND.

CASE TITLE = EXAMPLE DATA SET

* * * * * * * * * * NOT ENOUGH TIP CLEARANCE -0.0001 CHANGE RA1P BY .005

* * * * * * * * * * NOT ENOUGH TIP CLEARANCE 0.0047 CHANGE RA1P BY .005

SUN-PLANET MESH

ROTATIONAL PLANE
INVOLUTE MODIFICATIONS
****

(ENGAGEMENT)

PINION					GEAR			
LOC.	INV. MODIFIC. MIN.	MAX.	DIA.	ROLL ANG.	INV. MODIFIC. MIN.	MAX.	DIA.	ROLL ANG.
0.0	0.0	0.0	1.6535	23.7326	0.0	0.0	3.3071	23.7326
0.1	0.0	0.0	1.6372	22.0813	0.0	0.000000	3.3242	24.5583
0.2	0.0	0.0	1.6219	20.4299	0.0	0.000000	3.3418	25.3839
0.3	0.0	0.0	1.6076	18.7785	0.0	0.000001	3.3598	26.2097
0.4	0.0	0.0	1.5945	17.1271	0.0	0.000002	3.3784	27.0353
0.5	0.0	0.0	1.5824	15.4757	0.0	0.000002	3.3974	27.8611
0.6	0.0	0.0	1.5715	13.8242	0.0	0.000004	3.4169	28.6866
0.7	0.0	0.0	1.5618	12.1728	0.0	0.000005	3.4368	29.5124
0.8	0.0	0.0	1.5532	10.5217	0.0	0.000006	3.4572	30.3380
0.9	0.0	0.0	1.5459	8.8704	0.0	0.000008	3.4780	31.1638
1.0	0.0	0.0	1.5397	7.2190	0.0	0.000010	3.4993	31.9894

(DISENGAGEMENT)

PINION					GEAR			
LOC.	INV. MODIFIC. MIN.	MAX.	DIA.	ROLL ANG.	INV. MODIFIC. MIN.	MAX.	DIA.	ROLL ANG.
0.0	0.0	0.0	1.6535	23.7326	0.0	0.0	3.3071	23.73261
0.1	0.0	0.0	1.6755	25.8061	0.0	0.000000	3.2863	22.69581
0.2	0.0	0.0	1.6989	27.8793	0.0	0.000000	3.2664	21.65921
0.3	0.0	0.0	1.7238	29.9527	0.0	0.000001	3.2472	20.62241
0.4	0.0	0.0	1.7501	32.0261	0.0	0.000002	3.2289	19.58591
0.5	0.0	0.0	1.7778	34.0994	0.0	0.000002	3.2115	18.54921
0.6	0.0	0.0	1.8066	36.1728	0.0	0.000004	3.1949	17.51251
0.7	0.0	0.0	1.8368	38.2462	0.0	0.000005	3.1791	16.47581
0.8	0.0	0.0	1.8680	40.3195	0.0	0.000006	3.1643	15.43911
0.9	0.0	0.0	1.9004	42.3928	0.0	0.000008	3.1504	14.40231
1.0	0.0	0.0	1.9338	44.4663	0.0	0.000010	3.1374	13.36561

INPUT DATA

NO.TEETH - SUN	14.0000
NO.TEETH - PLANET	28.0000
PRESSURE ANGLE (DEGREES) DRIVE SIDE	22.5000
DIAMETRAL PITCH	8.4667
TOOTH TIP RADIUS TOL. (INCH)	0.0020
EDGE BREAK ON TOPLAND (INCH)	0.0100
MACHINED BACKLASH TOL.(INCH)	0.0075
ROOT RADIUS TOL. (INCH)	0.0050
FACE WIDTH - SUN (INCH)	1.1811
FACE WIDTH - PLANET (INCH)	1.1811
YOUNGS MOD.*E-6 - SUN (LB/SQ.INCH)	30.0000
YOUNGS MOD.*E-6 - PLANET (LB/SQ.INCH)	30.0000
POISSONS RATIO - SUN	0.3000
POISSONS RATIO - PLANET	0.3000
SURFACE ROUGHNESS-MAX (AA)	25.0000
OIL INLET TEMPERATURE (DEG.F)	180.0000
INITIAL RPM OF RANGE	6000.0000
FINAL RPM OF RANGE	6000.0000
NUMBER OF INTERVALS	1.0000
TORQUE INPUT (IN-LBS)	30.0000
TOTAL INV.PROFILE MODIFICATION,ENGAGE (INCH)	0.0
TOTAL INV.PROFILE MODIFICATION,DISENG (INCH)	0.0
INV.PROFILE MOD.LOCATION-% OF SOE	0.0
INV.PROFILE MOD.LOCATION-% OF SOD	0.0
INV.PROFILE MOD.TOTAL TOLERANCE	0.0000
+C.D.TOL. (OUT OF MESH) (INCH)	0.0
-C.D.TOL. (INTO MESH) (INCH)	0.0
CONTACT RATIO INPUT	0.0
HERTZ CONSTANT FOR COMPLIANCE	28761.
CENTER DISTANCE,THEO. (INCH)	2.4803
CENTER DISTANCE,MAX. (INCH)	2.4803
CENTER DISTANCE,MIN. (INCH)	2.4803
CIRCULAR PITCH (INCH)	0.3711
CIRCULAR BASE PITCH (INCH)	0.3428
MAX.OPERATING PRESS. ANGLE (DEG) DRIVE	22.5000
MIN.OPERATING PRESS. ANGLE (DEG) DRIVE	22.5000
NOMINAL CONTACT RATIO AT C.D.-THEO.	1.4485
MINIMUM CONTACT RATIO AT C.D.-MAX.	1.3182
MATERIAL CONSTANT	0.0528
CODE FOR TYPE OF OIL	0.0

		SUN	PLANET
NUMBER OF TEETH		14.0000	28.0000
PITCH DIAMETER	(INCH)	1.6535	3.3071
BASE CIRCLE DIA. DRIVE SIDE	(INCH)	1.5277	3.0553
TOOTH TIP DIAMETER,MAX.	(INCH)	1.9338	3.4993
TOOTH TIP DIAMETER,MIN.	(INCH)	1.9298	3.4953
EFFECTIVE TOOTH TIP DIA	(INCH)	1.9098	3.4753
ROOT DIAMETER,MAX.	(INCH)	1.4303	3.0078
ROOT DIAMETER,MIN.	(INCH)	1.4203	2.9978
TRUE INV.FORM DIA.	(INCH)	1.5397	3.1374
TOPLAND WIDTH,MIN.	(INCH)	0.0460	0.0720
ROOT FILLET RADIUS,MIN.	(INCH)	0.0576	0.0633
MACHINE BACKLASH,MAX.	(INCH)	0.0080	0.0080
MACHINE BACKLASH,MIN.	(INCH)	0.0005	0.0005
CIRCULAR TOOTH THICKNESS	(INCH)	0.2038	0.1673
MACH.CIRC.TOOTH THKNS.MAX.	(INCH)	0.2033	0.1668
MACH.CIRC.TOOTH THKNS.MIN.	(INCH)	0.1958	0.1593
TIP/ROOT CLEAR.MIN AT CD MIN.	(INCH)	0.0155	0.0095
ROLL ANGLE AT TOOTH TIP DIA.	(DEG)	44.4662	31.9895
ROLL ANGLE	(DEG)	23.7326	23.7326
AT ADD.INV.MODIFICATION DIA.	(INCH)	1.6535	3.3071
ROLL ANGLE AT PITCH DIA.	(DEG)	23.7326	23.7327
ROLL ANGLE	(DEG)	23.7326	23.7326
AT DED.INV.MODIFICATION DIA.	(INCH)	1.6535	3.3071
ROLL ANGLE AT TIFD	(DEG)	7.2188	13.3657
INSPECTION WIRE/BALL DIA.	(INCH)	0.2000	0.2350
MAX.MEASUREMENT OVER 2 WIRE/BALL	(INCH)	1.9554	3.6531
MIN.MEASUREMENT OVER 2 WIRE/BALL	(INCH)	1.9411	3.6375
EFFECTIVE WIDTH AT TOOTH TIP		1.1811	1.1811
EFFECTIVE WIDTH AT START OF FILLET		1.1811	1.1811
RADIUS TO BASE OF FILLET INPUT (INCH)		0.0	0.0
OUTSIDE RADIUS INPUT (INCH)		0.0	0.0
FILLET RADIUS INPUT (INCH)		0.0	0.0
DAMPING RATIO INPUT		0.1000	0.1000

RING-PLANET MESH

ROTATIONAL PLANE
INVOLUTE MODIFICATIONS
****

(ENGAGEMENT)

PINION

LOC.	INV. MODIFIC. MIN.	MAX.	DIA.	ROLL ANG.
0.0	0.0	0.000010	3.1554	14.7805
0.1	0.000000	0.000010	3.1503	14.3969
0.2	0.000000	0.000010	3.1454	14.0132
0.3	0.000001	0.000010	3.1406	13.6293
0.4	0.000001	0.000011	3.1359	13.2457
0.5	0.000002	0.000011	3.1314	12.8620
0.6	0.000003	0.000012	3.1270	12.4784
0.7	0.000004	0.000012	3.1227	12.0948
0.8	0.000006	0.000013	3.1185	11.7111
0.9	0.000007	0.000014	3.1145	11.3275
1.0	0.000009	0.000015	3.1106	10.9438

GEAR

INV. MODIFIC. MIN.	MAX.	DIA.	ROLL ANG.
0.0	0.000010	8.0970	20.1517
0.000000	0.000010	8.0903	19.9983
0.000000	0.000010	8.0835	19.8447
0.000001	0.000010	8.0769	19.6913
0.000001	0.000010	8.0702	19.5379
0.000001	0.000010	8.0637	19.3843
0.000002	0.000010	8.0571	19.2309
0.000003	0.000010	8.0506	19.0775
0.000004	0.000010	8.0442	18.9240
0.000005	0.000010	8.0378	18.7705
0.000006	0.000010	8.0315	18.6170

(DISENGAGEMENT)

PINION

LOC.	INV. MODIFIC. MIN.	MAX.	DIA.	ROLL ANG.
0.0	0.0	0.000010	3.4782	31.1703
0.1	0.000000	0.000010	3.4845	31.4183
0.2	0.000000	0.000010	3.4909	31.6662
0.3	0.000000	0.000010	3.4973	31.9140
0.4	0.000000	0.000009	3.5038	32.1621
0.5	0.000001	0.000009	3.5103	32.4100
0.6	0.000001	0.000009	3.5168	32.6579
0.7	0.000001	0.000008	3.5234	32.9058
0.8	0.000001	0.000007	3.5300	33.1538
0.9	0.000002	0.000007	3.5366	33.4017
1.0	0.000002	0.000006	3.5433	33.6497

GEAR

INV. MODIFIC. MIN.	MAX.	DIA.	ROLL ANG.
0.0	0.000010	8.4274	26.70771
0.000000	0.000010	8.4330	26.80691
0.000000	0.000010	8.4386	26.90601
0.000000	0.000010	8.4443	27.00521
0.000000	0.000010	8.4499	27.10441
0.000001	0.000010	8.4556	27.20351
0.000001	0.000010	8.4613	27.30271
0.000001	0.000010	8.4669	27.40181
0.000002	0.000009	8.4727	27.50111
0.000002	0.000009	8.4784	27.60021
0.000003	0.000009	8.4841	27.69941

INPUT DATA

NO.TEETH - PLANET(EXTERNAL GEAR)	28.0000
NO.TEETH - RING (INTERNAL GEAR)	70.0000
PRESSURE ANGLE (DEGREES) DRIVE SIDE	22.5000
DIAMETRAL PITCH	8.4667
TOOTH TIP RADIUS TOL. (INCH)	0.0020
EDGE BREAK ON TOPLAND (INCH)	0.0100
MACHINED BACKLASH TOL.(INCH)	0.0075
ROOT RADIUS TOL. (INCH)	0.0050
FACE WIDTH - PLANET (INCH)	1.1811
FACE WIDTH - RING (INCH)	1.4184
YOUNGS MOD.*E-6 - PLANET (LB/SQ.INCH)	30.0000
YOUNGS MOD.*E-6 - RING (LB/SQ.INCH)	30.0000
POISSONS RATIO - PLANET	0.3000
POISSONS RATIO - RING	0.3000
SURFACE ROUGHNESS-MAX (AA)	25.0000
OIL INLET TEMPERATURE (DEG.F)	180.0000
INITIAL RPM OF RANGE	6000.0000
FINAL RPM OF RANGE	6000.0000
NUMBER OF INTERVALS	1.0000
TORQUE INPUT (IN-LBS)	30.0000
TOTAL INV.PROFILE MODIFICATION,ENGAGE (INCH)	0.0000
TOTAL INV.PROFILE MODIFICATION,DISENG (INCH)	0.0000
INV.PROFILE MOD.LOCATION-% OF SOE	70.0000
INV.PROFILE MOD.LOCATION-% OF SOD	75.0000
INV.PROFILE MOD.TOTAL TOLERANCE	0.0000
+C.D.TOL. (OUT OF MESH) (INCH)	0.0
-C.D.TOL. (INTO MESH) (INCH)	0.0
CONTACT RATIO INPUT	0.0
HERTZ CONSTANT FOR COMPLIANCE	13893.
CENTER DISTANCE,THEO. (INCH)	2.4803
CENTER DISTANCE,MAX. (INCH)	2.4803
CENTER DISTANCE,MIN. (INCH)	2.4803
CIRCULAR PITCH (INCH)	0.3711
CIRCULAR BASE PITCH (INCH)	0.3428
MAX.OPERATING PRESS. ANGLE (DEG) DRIVE	22.5000
MIN.OPERATING PRESS. ANGLE (DEG) DRIVE	22.5000
NOMINAL CONTACT RATIO AT C.D.-THEO.	1.7660
MINIMUM CONTACT RATIO AT C.D.-MAX.	1.5845
MATERIAL CONSTANT	0.0528
CODE FOR TYPE OF OIL	0.0

		PLANET	RING
NUMBER OF TEETH		28.0000	70.0000
PITCH DIAMETER	(INCH)	3.3071	8.2677
BASE CIRCLE DIA. DRIVE SIDE	(INCH)	3.0553	7.6383
TOOTH TIP DIAMETER,MAX.	(INCH)	3.5433	8.0355
TOOTH TIP DIAMETER,MIN.	(INCH)	3.5393	8.0315
EFFECTIVE TOOTH TIP DIA	(INCH)	3.5193	8.0555
ROOT DIAMETER,MAX.	(INCH)	3.0099	8.5466
ROOT DIAMETER,MIN.	(INCH)	2.9999	8.5366
TRUE INV.FORM DIA.	(INCH)	3.1106	8.4541
TOPLAND WIDTH,MIN.	(INCH)	0.0676	0.0856
ROOT FILLET RADIUS,MIN.	(INCH)	0.0570	0.0503
MACHINE BACKLASH,MAX.	(INCH)	0.0080	0.0080
MACHINE BACKLASH,MIN.	(INCH)	0.0005	0.0005
CIRCULAR TOOTH THICKNESS	(INCH)	0.1855	0.1855
MACH.CIRC.TOOTH THKNS.MAX.	(INCH)	0.1855	0.1855
MACH.CIRC.TOOTH THKNS.MIN.	(INCH)	0.1780	0.1780
TIP/ROOT CLEAR.MIN AT CD MIN.	(INCH)	0.0305	0.0163
ROLL ANGLE AT TOOTH TIP DIA.	(DEG)	33.6497	18.6170
ROLL ANGLE	(DEG)	31.1703	27.3134
AT ADD.INV.MODIFICATION DIA.	(INCH)	3.4782	8.4619
ROLL ANGLE AT PITCH DIA.	(DEG)	23.7327	23.7306
ROLL ANGLE	(DEG)	14.7804	20.7575
AT DED.INV.MODIFICATION DIA.	(INCH)	3.1554	8.1242
ROLL ANGLE AT TIFD	(DEG)	10.9436	27.6994
INSPECTION WIRE/BALL DIA.	(INCH)	0.2150	0.2050
MAX.MEASUREMENT OVER 2 WIRE/BALL	(INCH)	3.6271	7.9719
MIN.MEASUREMENT OVER 2 WIRE/BALL	(INCH)	3.6114	7.9912
EFFECTIVE WIDTH AT TOOTH TIP		1.1811	1.4184
EFFECTIVE WIDTH AT START OF FILLET		1.1811	1.4184
RADIUS TO BASE OF FILLET INPUT (INCH)		0.0	0.0
OUTSIDE RADIUS INPUT (INCH)		0.0	0.0
FILLET RADIUS INPUT (INCH)		0.0	0.0
DAMPING RATIO INPUT		0.1000	0.1000

NUMBER OF PLANETS 3
NUMBER OF BOUNDARY CONDITION ITERATIONS 20
TOLERANCE FOR BOUNDARY CONDITION CONVERGENCE 0.10000E-01

EQUIVALENT MASS OF SUN GEAR	0.28083E-01
EQUIVALENT MASS OF PLANET CARRIER	0.14459E+02
EQUIVALENT MASS OF RING GEAR	0.0
EQUIVALENT MASS OF PLANET # 1	0.77535E-01

C O M P L I A N C E C O N S T A N T S

SUN-PLANET

0.4379E-06 * (-0.1433E+00 * (S/SO) + 0.3673E+00 * (S/SO)**2 + -0.1802E-01 * (S/SO)**3 + 0.2068E+00 * (S/SO)**4)

RING-PLANET

0.3711E-06 * (0.1084E+00 * (S/SO) + 0.3392E+00 * (S/SO)**2 + 0.6926E-01 * (S/SO)**3 + 0.3216E-01 * (S/SO)**4)

********** PLANETARY GEAR SYSTEM **********

BOUNDARY CONDITION ITERATION RESULTS

SUN-PLANET; MESHES 1 THRU N, LEFT TO RIGHT

ITERATION, END DISPLACEMENT	2	0.91205E-05	0.26109E-05	0.44434E-05
STARTING DISPLACEMENT		0.79937E-05	0.22942E-05	0.55193E-05
ITERATION, ENDING VELOCITY	2	0.21083E-01	0.41541E-01	-0.12383E-02
STARTING VELOCITY		0.33018E-01	0.25863E-01	0.35519E-02

RING-PLANET; MESHES 1 THRU N, LEFT TO RIGHT

ITERATION, END DISPLACEMENT	2	-0.11569E-05	0.53522E-05	0.35215E-05
STARTING DISPLACEMENT		-0.19393E-05	0.37647E-05	0.54096E-06
ITERATION, ENDING VELOCITY	2	-0.11474E-01	-0.31932E-01	0.10848E-01
STARTING VELOCITY		-0.19306E-01	-0.11352E-01	0.10960E-01

SUN-PLANET; MESHES 1 THRU N, LEFT TO RIGHT

ITERATION, END DISPLACEMENT	3	0.86411E-05	0.30259E-05	0.45337E-05
STARTING DISPLACEMENT		0.91205E-05	0.26109E-05	0.44434E-05
ITERATION, ENDING VELOCITY	3	0.15989E-01	0.37991E-01	0.15189E-02
STARTING VELOCITY		0.21083E-01	0.41541E-01	-0.12383E-02

RING-PLANET; MESHES 1 THRU N, LEFT TO RIGHT

ITERATION, END DISPLACEMENT	3	-0.45353E-06	0.51613E-05	0.36553E-05
STARTING DISPLACEMENT		-0.11569E-05	0.53522E-05	0.35215E-05
ITERATION, ENDING VELOCITY	3	-0.66773E-02	-0.28579E-01	0.77936E-02
STARTING VELOCITY		-0.11474E-01	-0.31932E-01	0.10848E-01

SUN-PLANET; MESHES 1 THRU N, LEFT TO RIGHT

ITERATION, END DISPLACEMENT	4	0.81232E-05	0.34340E-05	0.47576E-05
STARTING DISPLACEMENT		0.86411E-05	0.30259E-05	0.45337E-05
ITERATION, ENDING VELOCITY	4	0.12158E-01	0.34464E-01	0.58185E-03
STARTING VELOCITY		0.15989E-01	0.37991E-01	0.15189E-02

RING-PLANET; MESHES 1 THRU N, LEFT TO RIGHT

ITERATION, END DISPLACEMENT	4	0.40614E-06	0.50956E-05	0.37741E-05
STARTING DISPLACEMENT		-0.45353E-06	0.51613E-05	0.36553E-05
ITERATION, ENDING VELOCITY	4	-0.43267E-02	-0.26632E-01	0.72503E-02
STARTING VELOCITY		-0.66773E-02	-0.28579E-01	0.77936E-02

SUN-PLANET; MESHES 1 THRU N, LEFT TO RIGHT

ITERATION, END DISPLACEMENT	5	0.78116E-05	0.33674E-05	0.48339E-05
STARTING DISPLACEMENT		0.81232E-05	0.34340E-05	0.47576E-05
ITERATION, ENDING VELOCITY	5	0.15193E-01	0.31219E-01	-0.26823E-03
STARTING VELOCITY		0.12158E-01	0.34464E-01	0.58185E-03

RING-PLANET; MESHES 1 THRU N, LEFT TO RIGHT

ITERATION, END DISPLACEMENT	5	0.67486E-06	0.51198E-05	0.36552E-05
STARTING DISPLACEMENT		0.40614E-06	0.50956E-05	0.37741E-05
ITERATION, ENDING VELOCITY	5	-0.61055E-02	-0.22134E-01	0.93524E-02
STARTING VELOCITY		-0.43267E-02	-0.26632E-01	0.72503E-02

```
SUN-PLANET;  MESHES 1 THRU N, LEFT TO RIGHT
ITERATION, END DISPLACEMENT      6  0.78384E-05  0.33533E-05  0.47158E-05
STARTING DISPLACEMENT               0.78116E-05  0.33674E-05  0.48339E-05
ITERATION, ENDING VELOCITY       6  0.17302E-01  0.31308E-01 -0.55812E-03
STARTING VELOCITY                   0.15193E-01  0.31219E-01 -0.26823E-03


RING-PLANET;  MESHES 1 THRU N, LEFT TO RIGHT
ITERATION, END DISPLACEMENT      6  0.76845E-06  0.52549E-05  0.38943E-05
STARTING DISPLACEMENT               0.67496E-06  0.51198E-05  0.36552E-05
ITERATION, ENDING VELOCITY       6 -0.63157E-02 -0.20321E-01  0.11544E-01
STARTING VELOCITY                  -0.61085E-02 -0.22134E-01  0.93504E-02


SUN-PLANET;  MESHES 1 THRU N, LEFT TO RIGHT
ITERATION, END DISPLACEMENT      7  0.79569E-05  0.33324E-05  0.46152E-05
STARTING DISPLACEMENT               0.78384E-05  0.33533E-05  0.47158E-05
ITERATION, ENDING VELOCITY       7  0.17850E-01  0.32039E-01 -0.28571E-03
STARTING VELOCITY                   0.17302E-01  0.31308E-01 -0.55812E-03


RING-PLANET;  MESHES 1 THRU N, LEFT TO RIGHT
ITERATION, END DISPLACEMENT      7  0.65312E-06  0.52792E-05  0.39983E-05
STARTING DISPLACEMENT               0.76845E-06  0.52549E-05  0.38943E-05
ITERATION, ENDING VELOCITY       7 -0.53275E-02 -0.19516E-01  0.12808E-01
STARTING VELOCITY                  -0.63157E-02 -0.20321E-01  0.11544E-01


SUN-PLANET;  MESHES 1 THRU N, LEFT TO RIGHT
ITERATION, END DISPLACEMENT      8  0.80073E-05  0.33923E-05  0.45310E-05
STARTING DISPLACEMENT               0.79569E-05  0.33324E-05  0.46152E-05
ITERATION, ENDING VELOCITY       8  0.17158E-01  0.32468E-01  0.37273E-03
STARTING VELOCITY                   0.17850E-01  0.32039E-01 -0.28571E-03


RING-PLANET;  MESHES 1 THRU N, LEFT TO RIGHT
ITERATION, END DISPLACEMENT      8  0.65548E-06  0.52731E-05  0.41355E-05
STARTING DISPLACEMENT               0.65312E-06  0.52792E-05  0.39983E-05
ITERATION, ENDING VELOCITY       8 -0.37275E-02 -0.19036E-01  0.13058E-01
STARTING VELOCITY                  -0.53275E-02 -0.19516E-01  0.12808E-01


SUN-PLANET;  MESHES 1 THRU N, LEFT TO RIGHT
ITERATION, END DISPLACEMENT      9  0.79706E-05  0.34209E-05  0.45103E-05
STARTING DISPLACEMENT               0.80073E-05  0.33923E-05  0.45310E-05
ITERATION, ENDING VELOCITY       9  0.17009E-01  0.32384E-01  0.72134E-03
STARTING VELOCITY                   0.17158E-01  0.32468E-01  0.37273E-03


RING-PLANET;  MESHES 1 THRU N, LEFT TO RIGHT
ITERATION, END DISPLACEMENT      9  0.65700E-06  0.52178E-05  0.41293E-05
STARTING DISPLACEMENT               0.65548E-06  0.52731E-05  0.41355E-05
ITERATION, ENDING VELOCITY       9 -0.39108E-02 -0.18305E-01  0.13357E-01
STARTING VELOCITY                  -0.37275E-02 -0.19036E-01  0.13058E-01


SUN-PLANET;  MESHES 1 THRU N, LEFT TO RIGHT
ITERATION, END DISPLACEMENT     10  0.79457E-05  0.34300E-05  0.45091E-05
```

```
STARTING DISPLACEMENT                0.79786E-05  0.34209E-05  0.45103E-05
ITERATION, ENDING VELOCITY      10   0.17135E-01  0.32266E-01  0.99112E-03
STARTING VELOCITY                    0.17090E-01  0.32384E-01  0.72134E-03


RING-PLANET;  MESHES 1 THRU N, LEFT TO RIGHT
ITERATION, END DISPLACEMENT     10   0.65155E-06  0.51741E-05  0.40953E-05
STARTING DISPLACEMENT                0.65700E-06  0.52178E-05  0.41293E-05
ITERATION, ENDING VELOCITY      10  -0.25814E-02 -0.17709E-01  0.13564E-01
STARTING VELOCITY                   -0.30120E-02 -0.18305E-01  0.13357E-01


SUN-PLANET;  MESHES 1 THRU N, LEFT TO RIGHT
ITERATION, END DISPLACEMENT     11   0.79282E-05  0.34213E-05  0.44986E-05
STARTING DISPLACEMENT                0.79487E-05  0.34300E-05  0.45091E-05
ITERATION, ENDING VELOCITY      11   0.17536E-01  0.32160E-01  0.10405E-02
STARTING VELOCITY                    0.17135E-01  0.32266E-01  0.99112E-03


RING-PLANET;  MESHES 1 THRU N, LEFT TO RIGHT
ITERATION, END DISPLACEMENT     11   0.64182E-06  0.51532E-05  0.40761E-05
STARTING DISPLACEMENT                0.65155E-06  0.51741E-05  0.40953E-05
ITERATION, ENDING VELOCITY      11  -0.25777E-02 -0.17201E-01  0.13918E-01
STARTING VELOCITY                   -0.25814E-02 -0.17709E-01  0.13564E-01


SUN-PLANET;  MESHES 1 THRU N, LEFT TO RIGHT
ITERATION, END DISPLACEMENT     12   0.79331E-05  0.34116E-05  0.44880E-05
STARTING DISPLACEMENT                0.79282E-05  0.34213E-05  0.44986E-05
ITERATION, ENDING VELOCITY      12   0.17620E-01  0.32242E-01  0.11105E-02
STARTING VELOCITY                    0.17536E-01  0.32160E-01  0.10405E-02


RING-PLANET;  MESHES 1 THRU N, LEFT TO RIGHT
ITERATION, END DISPLACEMENT     12   0.60404E-06  0.51316E-05  0.40552E-05
STARTING DISPLACEMENT                0.64182E-06  0.51532E-05  0.40761E-05
ITERATION, ENDING VELOCITY      12  -0.24176E-02 -0.17039E-01  0.14092E-01
STARTING VELOCITY                   -0.25777E-02 -0.17201E-01  0.13918E-01


SUN-PLANET;  MESHES 1 THRU N, LEFT TO RIGHT
ITERATION, END DISPLACEMENT     13   0.79407E-05  0.34062E-05  0.44781E-05
STARTING DISPLACEMENT                0.79331E-05  0.34116E-05  0.44880E-05
ITERATION, ENDING VELOCITY      13   0.17609E-01  0.32327E-01  0.11688E-02
STARTING VELOCITY                    0.17620E-01  0.32242E-01  0.11105E-02


RING-PLANET;  MESHES 1 THRU N, LEFT TO RIGHT
ITERATION, END DISPLACEMENT     13   0.57243E-06  0.51126E-05  0.40405E-05
STARTING DISPLACEMENT                0.60404E-06  0.51316E-05  0.40552E-05
ITERATION, ENDING VELOCITY      13  -0.22686E-02 -0.16957E-01  0.14171E-01
STARTING VELOCITY                   -0.24176E-02 -0.17039E-01  0.14092E-01

PLANET NUMBER   1
RPM =      6000.00

MAXIMUM LOAD FOR SUN-PLANET =        19.06

MAXIMUM LOAD FOR RING-PLANET =       16.81
```

```
PLANET NUMBER   2
RPM =      6000.00

MAXIMUM LOAD FOR SUN-PLANET =      19.13

MAXIMUM LOAD FOR RING-PLANET =     15.89

PLANET NUMBER   3
RPM =      6000.00

MAXIMUM LOAD FOR SUN-PLANET =      19.39

MAXIMUM LOAD FOR RING-PLANET =     16.14
```

NO TOOTH ERRORS SOLUTION

MAXIMUM VALUES FOR SUN-PLANET MESH 1

	SUN		PLANET
FILLET STRESS CONCENTRATION (KSUBT)	1.43617		1.39553
MAXIMUM HERTZ STRESS	19791.8		19791.8
HERTZ STRESS AT PD	19483.5		19483.5
MAXIMUM BENDING STRESS	278.1		302.8
BENDING STRESS AT PD	259.2		295.7
DEPTH TO MAXIMUM SHEAR	0.00041		0.00041
MAXIMUM DYNAMIC PV(MILLIONS OF PSI*FT/MIN)	18.67369		18.67369
MAXIMUM NORMAL LOAD		19.1	
AVERAGE COEFFICIENT OF FRICTION		0.07450	
RPM FOR STRESSES		6000.00	

* *
THE EFFECTIVE CONTACT RATIO = 1.4500
* *

MAXIMUM VALUES FOR SUN-PLANET MESH 2

	SUN		PLANET
FILLET STRESS CONCENTRATION (KSUBT)	1.45022		1.38394
MAXIMUM HERTZ STRESS	19835.1		19835.1
HERTZ STRESS AT PD	10676.7		10676.7
MAXIMUM BENDING STRESS	278.8		304.1
BENDING STRESS AT PD	138.8		69.5
DEPTH TO MAXIMUM SHEAR	0.00041		0.00041
MAXIMUM DYNAMIC PV(MILLIONS OF PSI*FT/MIN)	18.40285		18.40285
MAXIMUM NORMAL LOAD		19.1	
AVERAGE COEFFICIENT OF FRICTION		0.01433	
RPM FOR STRESSES		6000.00	

* *
THE EFFECTIVE CONTACT RATIO = 1.4400
* *

MAXIMUM VALUES FOR SUN-PLANET MESH 3

	SUN		PLANET
FILLET STRESS CONCENTRATION (KSUBT)	1.41938		1.41342
MAXIMUM HERTZ STRESS	19951.9		19951.9
HERTZ STRESS AT PD	13781.5		13781.5
MAXIMUM BENDING STRESS	282.5		307.8
BENDING STRESS AT PD	174.7		133.0
DEPTH TO MAXIMUM SHEAR	0.00041		0.00041
MAXIMUM DYNAMIC PV(MILLIONS OF PSI*FT/MIN)	18.22069		18.22069
MAXIMUM NORMAL LOAD		19.4	
AVERAGE COEFFICIENT OF FRICTION		0.01506	
RPM FOR STRESSES		6000.00	

* *

THE EFFECTIVE CONTACT RATIO = 1.4500

* * * * * * * * * * * * * * * * * * * *

MAXIMUM VALUES FOR RING-PLANET MESH 1

	PLANET		RING
FILLET STRESS CONCENTRATION (KSUBT)	1.42396		1.54019
MAXIMUM HERTZ STRESS	12713.6		12713.6
HERTZ STRESS AT PD	3373.3		3373.3
MAXIMUM BENDING STRESS	294.8		140.2
BENDING STRESS AT PD	34.8		5.8
DEPTH TO MAXIMUM SHEAR	0.00056		0.00056
MAXIMUM DYNAMIC PV(MILLIONS OF PSI*FT/MIN)	5.80265		5.80265
MAXIMUM NORMAL LOAD		16.8	
AVERAGE COEFFICIENT OF FRICTION		0.00287	
RPM FOR STRESSES		6000.00	

* * * * * * * * * * * * * * * * * * * *

THE EFFECTIVE CONTACT RATIO = 1.6400

* * * * * * * * * * * * * * * * * * * *

MAXIMUM VALUES FOR RING-PLANET MESH 2

	PLANET		RING
FILLET STRESS CONCENTRATION (KSUBT)	1.44438		1.53765
MAXIMUM HERTZ STRESS	12391.7		12391.7
HERTZ STRESS AT PD	11059.1		11059.1
MAXIMUM BENDING STRESS	275.2		128.5
BENDING STRESS AT PD	252.4		86.2
DEPTH TO MAXIMUM SHEAR	0.00054		0.00054
MAXIMUM DYNAMIC PV(MILLIONS OF PSI*FT/MIN)	5.50748		5.50748
MAXIMUM NORMAL LOAD		15.9	
AVERAGE COEFFICIENT OF FRICTION		0.00396	
RPM FOR STRESSES		6000.00	

* * * * * * * * * * * * * * * * * * * *

THE EFFECTIVE CONTACT RATIO = 1.6400

* * * * * * * * * * * * * * * * * * * *

MAXIMUM VALUES FOR RING-PLANET MESH 3

	PLANET		RING
FILLET STRESS CONCENTRATION (KSUBT)	1.40377		1.55480
MAXIMUM HERTZ STRESS	12458.3		12458.3
HERTZ STRESS AT PD	0.0		0.0
MAXIMUM BENDING STRESS	283.1		146.4
BENDING STRESS AT PD	0.0		0.0
DEPTH TO MAXIMUM SHEAR	0.00055		0.00055
MAXIMUM DYNAMIC PV(MILLIONS OF PSI*FT/MIN)	5.73373		5.73373
MAXIMUM NORMAL LOAD		16.1	
AVERAGE COEFFICIENT OF FRICTION		0.01038	
RPM FOR STRESSES		6000.00	

* * * * * * * * * * * * * * * * * * * *

BEGIN ERROR EVALUATION

SUN-PLANET ERROR MATRIX					RING-PLANET ERROR MATRIX				
TOOTH 1	TOOTH 2	TOOTH 3	TOOTH 4	TOOTH 5	TOOTH 1	TOOTH 2	TOOTH 3	TOOTH 4	TOOTH 5
0.133E-04	0.0	0.0	0.0	0.0	0.0	0.115E-04	0.0	0.0	0.0
0.0	0.0	0.0	0.0	0.0	0.0	0.0	0.0	0.0	0.0
0.0	0.0	0.0	0.0	0.0	0.0	0.0	0.0	0.0	0.0
0.0	0.0	0.0	0.0	0.0	0.0	0.0	0.0	0.0	0.0
0.0	0.0	0.0	0.0	0.0	0.0	0.0	0.0	0.0	0.0
0.0	0.0	0.0	0.0	0.0	0.0	0.0	0.0	0.0	0.0
0.0	0.0	0.0	0.0	0.0	0.0	0.0	0.0	0.0	0.0
0.0	0.0	0.0	0.0	0.0	0.0	0.0	0.0	0.0	0.0
0.0	0.0	0.0	0.0	0.0	0.0	0.0	0.0	0.0	0.0
0.0	0.0	0.0	0.0	0.0	0.0	0.0	0.0	0.0	0.0
0.0	0.0	0.0	0.0	0.0	0.0	0.0	0.0	0.0	0.0
0.0	0.0	0.0	0.0	0.0	0.0	0.0	0.0	0.0	0.0
0.0	0.0	0.0	0.0	0.0	0.0	0.0	0.0	0.0	0.0
0.0	0.0	0.0	0.0	0.0	0.0	0.0	0.0	0.0	0.0
0.0	0.0	0.0	0.0	0.0	0.0	0.0	0.0	0.0	0.0
0.0	0.0	0.0	0.0	0.0	0.0	0.0	0.0	0.0	0.0
0.0	0.0	0.0	0.0	0.0	0.0	0.0	0.0	0.0	0.0
0.0	0.0	0.0	0.0	0.0	0.0	0.0	0.0	0.0	0.0
0.0	0.0	0.0	0.0	0.0	0.0	0.0	0.0	0.0	0.0
0.0	0.0	0.0	0.0	0.0	0.0	0.0	0.0	0.0	0.0

ERROR TOOTH PASS NUMBER 1

MAXIMUM VALUES FOR SUN-PLANET MESH 1

	SUN		PLANET
FILLET STRESS CONCENTRATION (KSUBT)	1.43617		1.39553
MAXIMUM HERTZ STRESS	19792.7		19792.7
HERTZ STRESS AT PD	19495.9		19495.9
MAXIMUM BENDING STRESS	277.9		303.0
BENDING STRESS AT PD	259.5		296.0
DEPTH TO MAXIMUM SHEAR	0.00041		0.00041
MAXIMUM DYNAMIC PV(MILLIONS OF PSI*FT/MIN)	17.59886		17.59886
MAXIMUM NORMAL LOAD		19.1	
AVERAGE COEFFICIENT OF FRICTION		0.07448	
RPM FOR STRESSES		6000.00	

* * * * * * * * * * * * * * * * * * * *
THE EFFECTIVE CONTACT RATIO = 1.4500
* * * * * * * * * * * * * * * * * * * *

MAXIMUM VALUES FOR SUN-PLANET MESH 2

	SUN		PLANET
FILLET STRESS CONCENTRATION (KSUBT)	1.45022		1.38394
MAXIMUM HERTZ STRESS	20148.0		20148.0
HERTZ STRESS AT PD	10660.7		10660.7
MAXIMUM BENDING STRESS	288.2		313.6
BENDING STRESS AT PD	138.4		69.3
DEPTH TO MAXIMUM SHEAR	0.00041		0.00041
MAXIMUM DYNAMIC PV(MILLIONS OF PSI*FT/MIN)	18.17621		18.17621
MAXIMUM NORMAL LOAD		19.8	
AVERAGE COEFFICIENT OF FRICTION		0.01431	
RPM FOR STRESSES		6000.00	

* * * * * * * * * * * * * * * * * * * *
THE EFFECTIVE CONTACT RATIO = 1.4400
* * * * * * * * * * * * * * * * * * * *

MAXIMUM VALUES FOR SUN-PLANET MESH 3

	SUN		PLANET
FILLET STRESS CONCENTRATION (KSUBT)	1.41938		1.41342
MAXIMUM HERTZ STRESS	19755.9		19755.9
HERTZ STRESS AT PD	13758.2		13758.2
MAXIMUM BENDING STRESS	275.9		301.9
BENDING STRESS AT PD	174.1		132.6
DEPTH TO MAXIMUM SHEAR	0.00041		0.00041
MAXIMUM DYNAMIC PV(MILLIONS OF PSI*FT/MIN)	18.19556		18.19556
MAXIMUM NORMAL LOAD		19.0	
AVERAGE COEFFICIENT OF FRICTION		0.01511	
RPM FOR STRESSES		6000.00	

* * * * * * * * * * * * * * * * * * * *
THE EFFECTIVE CONTACT RATIO = 1.4500
* * * * * * * * * * * * * * * * * * * *

MAXIMUM VALUES FOR RING-PLANET MESH 1

	PLANET		RING
FILLET STRESS CONCENTRATION (KSUBT)	1.42396		1.54019
MAXIMUM HERTZ STRESS	13291.3		13291.3
HERTZ STRESS AT PD	0.0		0.0
MAXIMUM BENDING STRESS	309.5		147.8
BENDING STRESS AT PD	0.0		0.0
DEPTH TO MAXIMUM SHEAR	0.00058		0.00058
MAXIMUM DYNAMIC PV(MILLIONS OF PSI*FT/MIN)	5.68849		5.68849
MAXIMUM NORMAL LOAD		18.1	
AVERAGE COEFFICIENT OF FRICTION		0.00023	
RPM FOR STRESSES		6000.00	

* * * * * * * * * * * * * * * * * * * *
THE EFFECTIVE CONTACT RATIO = 1.4100
* * * * * * * * * * * * * * * * * * * *

MAXIMUM VALUES FOR RING-PLANET MESH 2

	PLANET		RING
FILLET STRESS CONCENTRATION (KSUBT)	1.44438		1.53765
MAXIMUM HERTZ STRESS	12331.7		12331.7
HERTZ STRESS AT PD	11027.0		11027.0
MAXIMUM BENDING STRESS	266.8		127.8
BENDING STRESS AT PD	250.9		85.7
DEPTH TO MAXIMUM SHEAR	0.00054		0.00054
MAXIMUM DYNAMIC PV(MILLIONS OF PSI*FT/MIN)	5.48663		5.48663
MAXIMUM NORMAL LOAD		15.6	
AVERAGE COEFFICIENT OF FRICTION		0.00836	
RPM FOR STRESSES		6000.00	

* * * * * * * * * * * * * * * * * * * *
THE EFFECTIVE CONTACT RATIO = 1.6400
* * * * * * * * * * * * * * * * * * * *

MAXIMUM VALUES FOR RING-PLANET MESH 3

	PLANET		RING
FILLET STRESS CONCENTRATION (KSUBT)	1.40377		1.55480
MAXIMUM HERTZ STRESS	12469.0		12469.0
HERTZ STRESS AT PD	0.0		0.0
MAXIMUM BENDING STRESS	284.8		152.0
BENDING STRESS AT PD	0.0		0.0
DEPTH TO MAXIMUM SHEAR	0.00055		0.00055
MAXIMUM DYNAMIC PV(MILLIONS OF PSI*FT/MIN)	5.82475		5.82475
MAXIMUM NORMAL LOAD		16.2	
AVERAGE COEFFICIENT OF FRICTION		0.01795	
RPM FOR STRESSES		6000.00	

ERROR TOOTH PASS NUMBER 2

MAXIMUM VALUES FOR SUN-PLANET MESH 1

	SUN		PLANET
FILLET STRESS CONCENTRATION (KSUBT)	1.43617		1.39553
MAXIMUM HERTZ STRESS	19664.1		19664.1
HERTZ STRESS AT PD	19441.2		19441.2
MAXIMUM BENDING STRESS	273.5		299.2
BENDING STRESS AT PD	258.1		294.4
DEPTH TO MAXIMUM SHEAR	0.00040		0.00040
MAXIMUM DYNAMIC PV(MILLIONS OF PSI*FT/MIN)	18.69389		18.69389
MAXIMUM NORMAL LOAD		18.8	
AVERAGE COEFFICIENT OF FRICTION		0.07441	
RPM FOR STRESSES		6000.00	

* *
THE EFFECTIVE CONTACT RATIO = 1.4500
* *

MAXIMUM VALUES FOR SUN-PLANET MESH 2

	SUN		PLANET
FILLET STRESS CONCENTRATION (KSUBT)	1.45022		1.38394
MAXIMUM HERTZ STRESS	19859.3		19859.3
HERTZ STRESS AT PD	10641.9		10641.9
MAXIMUM BENDING STRESS	279.5		304.7
BENDING STRESS AT PD	137.9		69.1
DEPTH TO MAXIMUM SHEAR	0.00041		0.00041
MAXIMUM DYNAMIC PV(MILLIONS OF PSI*FT/MIN)	18.50247		18.50247
MAXIMUM NORMAL LOAD		19.2	
AVERAGE COEFFICIENT OF FRICTION		0.01417	
RPM FOR STRESSES		6000.00	

* *
THE EFFECTIVE CONTACT RATIO = 1.4400
* *

MAXIMUM VALUES FOR SUN-PLANET MESH 3

	SUN		PLANET
FILLET STRESS CONCENTRATION (KSUBT)	1.41938		1.41342
MAXIMUM HERTZ STRESS	19874.7		19874.7
HERTZ STRESS AT PD	13832.9		13832.9
MAXIMUM BENDING STRESS	200.9		305.4
BENDING STRESS AT PD	176.0		134.0
DEPTH TO MAXIMUM SHEAR	0.00041		0.00041
MAXIMUM DYNAMIC PV(MILLIONS OF PSI*FT/MIN)	18.34039		18.34039
MAXIMUM NORMAL LOAD		19.3	
AVERAGE COEFFICIENT OF FRICTION		0.01508	
RPM FOR STRESSES		6000.00	

* * * * * * * * * * * * * * * * * * * *
THE EFFECTIVE CONTACT RATIO = 1.4500
* * * * * * * * * * * * * * * * * * * *

MAXIMUM VALUES FOR RING-PLANET MESH 1

	PLANET		RING
FILLET STRESS CONCENTRATION (KSUBT)	1.42396		1.54019
MAXIMUM HERTZ STRESS	12770.5		12770.5
HERTZ STRESS AT PD	2605.2		2605.2
MAXIMUM BENDING STRESS	296.5		140.4
BENDING STRESS AT PD	20.8		3.4
DEPTH TO MAXIMUM SHEAR	0.00056		0.00056
MAXIMUM DYNAMIC PV(MILLIONS OF PSI*FT/MIN)	5.81303		5.81303
MAXIMUM NORMAL LOAD		16.9	
AVERAGE COEFFICIENT OF FRICTION		0.00185	
RPM FOR STRESSES		6000.00	

* * * * * * * * * * * * * * * * * * * *
THE EFFECTIVE CONTACT RATIO = 1.6500
* * * * * * * * * * * * * * * * * * * *

MAXIMUM VALUES FOR RING-PLANET MESH 2

	PLANET		RING
FILLET STRESS CONCENTRATION (KSUBT)	1.44438		1.53765
MAXIMUM HERTZ STRESS	12191.7		12191.7
HERTZ STRESS AT PD	10773.5		10773.5
MAXIMUM BENDING STRESS	265.6		123.0
BENDING STRESS AT PD	239.5		81.8
DEPTH TO MAXIMUM SHEAR	0.00053		0.00053
MAXIMUM DYNAMIC PV(MILLIONS OF PSI*FT/MIN)	5.30084		5.30084
MAXIMUM NORMAL LOAD		15.3	
AVERAGE COEFFICIENT OF FRICTION		0.00864	
RPM FOR STRESSES		6000.00	

* * * * * * * * * * * * * * * * * * * *
THE EFFECTIVE CONTACT RATIO = 1.6400
* * * * * * * * * * * * * * * * * * * *

MAXIMUM VALUES FOR RING-PLANET MESH 3

	PLANET		RING
FILLET STRESS CONCENTRATION (KSUBT)	1.40377		1.55480
MAXIMUM HERTZ STRESS	12257.2		12257.2
HERTZ STRESS AT PD	0.0		0.0
MAXIMUM BENDING STRESS	281.1		155.0
BENDING STRESS AT PD	0.0		0.0
DEPTH TO MAXIMUM SHEAR	0.00054		0.00054
MAXIMUM DYNAMIC PV(MILLIONS OF PSI*FT/MIN)	5.87036		5.87036
MAXIMUM NORMAL LOAD		15.7	
AVERAGE COEFFICIENT OF FRICTION		0.01803	
RPM FOR STRESSES		6000.00	

ERROR TOOTH PASS NUMBER 3

MAXIMUM VALUES FOR SUN-PLANET MESH 1

	SUN		PLANET
FILLET STRESS CONCENTRATION (KSUBT)	1.43617		1.39553
MAXIMUM HERTZ STRESS	19717.8		19717.8
HERTZ STRESS AT PD	19358.0		19358.0
MAXIMUM BENDING STRESS	276.4		300.2
BENDING STRESS AT PD	255.9		291.9
DEPTH TO MAXIMUM SHEAR	0.00041		0.00041
MAXIMUM DYNAMIC PV(MILLIONS OF PSI*FT/MIN)	18.72658		18.72658
MAXIMUM NORMAL LOAD		18.9	
AVERAGE COEFFICIENT OF FRICTION		0.07454	
RPM FOR STRESSES		6000.00	

* *
THE EFFECTIVE CONTACT RATIO = 1.4500
* *

MAXIMUM VALUES FOR SUN-PLANET MESH 2

	SUN		PLANET
FILLET STRESS CONCENTRATION (KSUBT)	1.45022		1.38394
MAXIMUM HERTZ STRESS	19870.6		19870.6
HERTZ STRESS AT PD	10509.3		10509.3
MAXIMUM BENDING STRESS	280.2		305.1
BENDING STRESS AT PD	134.5		67.4
DEPTH TO MAXIMUM SHEAR	0.00041		0.00041
MAXIMUM DYNAMIC PV(MILLIONS OF PSI*FT/MIN)	18.51649		18.51649
MAXIMUM NORMAL LOAD		19.2	
AVERAGE COEFFICIENT OF FRICTION		0.01423	
RPM FOR STRESSES		6000.00	

* *
THE EFFECTIVE CONTACT RATIO = 1.4400
* *

MAXIMUM VALUES FOR SUN-PLANET MESH 3

	SUN		PLANET
FILLET STRESS CONCENTRATION (KSUBT)	1.41938		1.41342
MAXIMUM HERTZ STRESS	20022.6		20022.6
HERTZ STRESS AT PD	13785.0		13785.0
MAXIMUM BENDING STRESS	284.5		310.0
BENDING STRESS AT PD	174.8		133.1
DEPTH TO MAXIMUM SHEAR	0.00041		0.00041
MAXIMUM DYNAMIC PV(MILLIONS OF PSI*FT/MIN)	18.25066		18.25066
MAXIMUM NORMAL LOAD		19.5	
AVERAGE COEFFICIENT OF FRICTION		0.01501	
RPM FOR STRESSES		6000.00	

* * * * * * * * * * * * * * * * * * * *
THE EFFECTIVE CONTACT RATIO = 1.4500
* * * * * * * * * * * * * * * * * * * *

MAXIMUM VALUES FOR RING-PLANET MESH 1

	PLANET		RING
FILLET STRESS CONCENTRATION (KSUBT)	1.42396		1.54019
MAXIMUM HERTZ STRESS	12920.6		12920.6
HERTZ STRESS AT PD	2930.5		2930.5
MAXIMUM BENDING STRESS	304.0		142.3
BENDING STRESS AT PD	26.3		4.4
DEPTH TO MAXIMUM SHEAR	0.00057		0.00057
MAXIMUM DYNAMIC PV(MILLIONS OF PSI*FT/MIN)	5.88229		5.88229
MAXIMUM NORMAL LOAD		17.4	
AVERAGE COEFFICIENT OF FRICTION		0.00075	
RPM FOR STRESSES		6000.00	

* * * * * * * * * * * * * * * * * * * *
THE EFFECTIVE CONTACT RATIO = 1.6400
* * * * * * * * * * * * * * * * * * * *

MAXIMUM VALUES FOR RING-PLANET MESH 2

	PLANET		RING
FILLET STRESS CONCENTRATION (KSUBT)	1.44438		1.53765
MAXIMUM HERTZ STRESS	12360.6		12360.6
HERTZ STRESS AT PD	10901.5		10901.5
MAXIMUM BENDING STRESS	273.1		127.2
BENDING STRESS AT PD	245.2		83.8
DEPTH TO MAXIMUM SHEAR	0.00054		0.00054
MAXIMUM DYNAMIC PV(MILLIONS OF PSI*FT/MIN)	5.43674		5.43674
MAXIMUM NORMAL LOAD		15.8	
AVERAGE COEFFICIENT OF FRICTION		0.00880	
RPM FOR STRESSES		6000.00	

* * * * * * * * * * * * * * * * * * * *
THE EFFECTIVE CONTACT RATIO = 1.6400
* * * * * * * * * * * * * * * * * * * *

MAXIMUM VALUES FOR RING-PLANET MESH 3

	PLANET		RING
FILLET STRESS CONCENTRATION (KSUBT)	1.40377		1.55480
MAXIMUM HERTZ STRESS	12420.3		12420.3
HERTZ STRESS AT PD	0.0		0.0
MAXIMUM BENDING STRESS	287.1		154.4
BENDING STRESS AT PD	0.0		0.0
DEPTH TO MAXIMUM SHEAR	0.00055		0.00055
MAXIMUM DYNAMIC PV(MILLIONS OF PSI*FT/MIN)	5.89784		5.89784
MAXIMUM NORMAL LOAD		16.1	
AVERAGE COEFFICIENT OF FRICTION		0.01826	
RPM FOR STRESSES		6000.00	

ERROR TOOTH PASS NUMBER 4

MAXIMUM VALUES FOR SUN-PLANET MESH 1

	SUN		PLANET
FILLET STRESS CONCENTRATION (KSUBT)	1.43617		1.39553
MAXIMUM HERTZ STRESS	19876.7		19876.7
HERTZ STRESS AT PD	19572.1		19572.1
MAXIMUM BENDING STRESS	280.4		305.4
BENDING STRESS AT PD	261.5		298.3
DEPTH TO MAXIMUM SHEAR	0.00041		0.00041
MAXIMUM DYNAMIC PV(MILLIONS OF PSI*FT/MIN)	18.52185		18.52185
MAXIMUM NORMAL LOAD		19.2	
AVERAGE COEFFICIENT OF FRICTION		0.07451	
RPM FOR STRESSES		6000.00	

* *
THE EFFECTIVE CONTACT RATIO = 1.4500
* *

MAXIMUM VALUES FOR SUN-PLANET MESH 2

	SUN		PLANET
FILLET STRESS CONCENTRATION (KSUBT)	1.45022		1.38394
MAXIMUM HERTZ STRESS	19898.8		19898.8
HERTZ STRESS AT PD	10579.8		10579.8
MAXIMUM BENDING STRESS	280.5		306.1
BENDING STRESS AT PD	136.3		68.3
DEPTH TO MAXIMUM SHEAR	0.00041		0.00041
MAXIMUM DYNAMIC PV(MILLIONS OF PSI*FT/MIN)	18.38475		18.38475
MAXIMUM NORMAL LOAD		19.3	
AVERAGE COEFFICIENT OF FRICTION		0.01422	
RPM FOR STRESSES		6000.00	

* *
THE EFFECTIVE CONTACT RATIO = 1.4400
* *

MAXIMUM VALUES FOR SUN-PLANET MESH 3

	SUN		PLANET
FILLET STRESS CONCENTRATION (KSUBT)	1.41938		1.41342
MAXIMUM HERTZ STRESS	19973.0		19973.0
HERTZ STRESS AT PD	13691.6		13691.6
MAXIMUM BENDING STRESS	232.7		333.5
BENDING STRESS AT PD	172.4		131.3
DEPTH TO MAXIMUM SHEAR	0.00041		0.00041
MAXIMUM DYNAMIC PV(MILLIONS OF PSI*FT/MIN)	18.09837		18.09837
MAXIMUM NORMAL LOAD		19.4	
AVERAGE COEFFICIENT OF FRICTION		0.01504	
RPM FOR STRESSES		6000.00	

THE EFFECTIVE CONTACT RATIO = 1.4500

MAXIMUM VALUES FOR RING-PLANET MESH 1

	PLANET		RING
FILLET STRESS CONCENTRATION (KSUBT)	1.42396		1.54019
MAXIMUM HERTZ STRESS	12905.1		12905.1
HERTZ STRESS AT PD	2657.1		2657.1
MAXIMUM BENDING STRESS	301.6		140.2
BENDING STRESS AT PD	21.6		3.6
DEPTH TO MAXIMUM SHEAR	0.00057		0.00057
MAXIMUM DYNAMIC PV(MILLIONS OF PSI*FT/MIN)	5.82910		5.82910
MAXIMUM NORMAL LOAD		17.3	
AVERAGE COEFFICIENT OF FRICTION		0.00166	
RPM FOR STRESSES		6000.00	

THE EFFECTIVE CONTACT RATIO = 1.6400

MAXIMUM VALUES FOR RING-PLANET MESH 2

	PLANET		RING
FILLET STRESS CONCENTRATION (KSUBT)	1.44438		1.53765
MAXIMUM HERTZ STRESS	12371.9		12371.9
HERTZ STRESS AT PD	10952.5		10952.5
MAXIMUM BENDING STRESS	272.2		126.9
BENDING STRESS AT PD	247.5		84.5
DEPTH TO MAXIMUM SHEAR	0.00054		0.00054
MAXIMUM DYNAMIC PV(MILLIONS OF PSI*FT/MIN)	5.42049		5.42049
MAXIMUM NORMAL LOAD		15.8	
AVERAGE COEFFICIENT OF FRICTION		0.00885	
RPM FOR STRESSES		6000.00	

THE EFFECTIVE CONTACT RATIO = 1.6300

MAXIMUM VALUES FOR RING-PLANET MESH 3

	PLANET		RING
FILLET STRESS CONCENTRATION (KSUBT)	1.40377		1.55480
MAXIMUM HERTZ STRESS	12472.2		12472.2
HERTZ STRESS AT PD	0.0		0.0
MAXIMUM BENDING STRESS	285.2		149.7
BENDING STRESS AT PD	0.0		0.0
DEPTH TO MAXIMUM SHEAR	0.00055		0.00055
MAXIMUM DYNAMIC PV(MILLIONS OF PSI*FT/MIN)	5.79617		5.79617
MAXIMUM NORMAL LOAD		16.2	
AVERAGE COEFFICIENT OF FRICTION		0.01826	
RPM FOR STRESSES		6000.00	

ERROR TOOTH PASS NUMBER 5

MAXIMUM VALUES FOR SUN-PLANET MESH 1

	SUN		PLANET
FILLET STRESS CONCENTRATION (KSUBT)	1.43617		1.39553
MAXIMUM HERTZ STRESS	19804.5		19804.5
HERTZ STRESS AT PD	19504.9		19504.9
MAXIMUM BENDING STRESS	278.4		303.2
BENDING STRESS AT PD	259.8		296.3
DEPTH TO MAXIMUM SHEAR	0.00041		0.00041
MAXIMUM DYNAMIC PV(MILLIONS OF PSI*FT/MIN)	18.54405		18.54405
MAXIMUM NORMAL LOAD		19.1	
AVERAGE COEFFICIENT OF FRICTION		0.07451	
RPM FOR STRESSES		6000.00	

THE EFFECTIVE CONTACT RATIO = 1.4500

MAXIMUM VALUES FOR SUN-PLANET MESH 2

	SUN		PLANET
FILLET STRESS CONCENTRATION (KSUBT)	1.45022		1.38394
MAXIMUM HERTZ STRESS	19873.8		19873.8
HERTZ STRESS AT PD	10561.4		10561.4
MAXIMUM BENDING STRESS	280.0		305.2
BENDING STRESS AT PD	135.9		68.1
DEPTH TO MAXIMUM SHEAR	0.00041		0.00041
MAXIMUM DYNAMIC PV(MILLIONS OF PSI*FT/MIN)	18.40927		18.40927
MAXIMUM NORMAL LOAD		19.2	
AVERAGE COEFFICIENT OF FRICTION		0.01431	
RPM FOR STRESSES		6000.00	

THE EFFECTIVE CONTACT RATIO = 1.4400

MAXIMUM VALUES FOR SUN-PLANET MESH 3

	SUN		PLANET
FILLET STRESS CONCENTRATION (KSUBT)	1.41938		1.41342
MAXIMUM HERTZ STRESS	19936.9		19936.9
HERTZ STRESS AT PD	13737.9		13737.9
MAXIMUM BENDING STRESS	282.1		307.3
BENDING STRESS AT PD	173.6		132.2
DEPTH TO MAXIMUM SHEAR	0.00041		0.00041
MAXIMUM DYNAMIC PV(MILLIONS OF PSI*FT/MIN)	18.19667		18.19667
MAXIMUM NORMAL LOAD		19.4	
AVERAGE COEFFICIENT OF FRICTION		0.01506	
RPM FOR STRESSES		6000.00	

THE EFFECTIVE CONTACT RATIO = 1.4500

MAXIMUM VALUES FOR RING-PLANET MESH 1

	PLANET		RING
FILLET STRESS CONCENTRATION (KSUBT)	1.42396		1.54019
MAXIMUM HERTZ STRESS	12833.2		12833.2
HERTZ STRESS AT PD	2898.5		2898.5
MAXIMUM BENDING STRESS	298.9		139.9
BENDING STRESS AT PD	25.7		4.3
DEPTH TO MAXIMUM SHEAR	0.00056		0.00056
MAXIMUM DYNAMIC PV(MILLIONS OF PSI*FT/MIN)	5.81374		5.81374
MAXIMUM NORMAL LOAD		17.1	
AVERAGE COEFFICIENT OF FRICTION		0.00205	
RPM FOR STRESSES		6000.00	

THE EFFECTIVE CONTACT RATIO = 1.6400

MAXIMUM VALUES FOR RING-PLANET MESH 2

	PLANET		RING
FILLET STRESS CONCENTRATION (KSUBT)	1.44438		1.53765
MAXIMUM HERTZ STRESS	12385.2		12385.2
HERTZ STRESS AT PD	10986.5		10986.5
MAXIMUM BENDING STRESS	273.9		127.8
BENDING STRESS AT PD	249.1		85.1
DEPTH TO MAXIMUM SHEAR	0.00054		0.00054
MAXIMUM DYNAMIC PV(MILLIONS OF PSI*FT/MIN)	5.47461		5.47461
MAXIMUM NORMAL LOAD		15.8	
AVERAGE COEFFICIENT OF FRICTION		0.00384	
RPM FOR STRESSES		6000.00	

THE EFFECTIVE CONTACT RATIO = 1.6400

MAXIMUM VALUES FOR RING-PLANET MESH 3

	PLANET		RING
FILLET STRESS CONCENTRATION (KSUBT)	1.40377		1.55480
MAXIMUM HERTZ STRESS	12394.9		12394.9
HERTZ STRESS AT PD	0.0		0.0
MAXIMUM BENDING STRESS	283.0		150.3
BENDING STRESS AT PD	0.0		0.0
DEPTH TO MAXIMUM SHEAR	0.00055		0.00055
MAXIMUM DYNAMIC PV(MILLIONS OF PSI*FT/MIN)	5.80084		5.80084
MAXIMUM NORMAL LOAD		16.0	
AVERAGE COEFFICIENT OF FRICTION		0.01829	
RPM FOR STRESSES		6000.00	

ERROR TOOTH PASS NUMBER 6

MAXIMUM VALUES FOR SUN-PLANET MESH 1

	SUN		PLANET
FILLET STRESS CONCENTRATION (KSUBT)	1.43617		1.39553
MAXIMUM HERTZ STRESS	19804.1		19804.1
HERTZ STRESS AT PD	19508.4		19508.4
MAXIMUM BENDING STRESS	278.3		303.3
BENDING STRESS AT PD	259.8		296.4
DEPTH TO MAXIMUM SHEAR	0.00041		0.00041
MAXIMUM DYNAMIC PV(MILLIONS OF PSI*FT/MIN)	18.62094		18.62094
MAXIMUM NORMAL LOAD		19.1	
AVERAGE COEFFICIENT OF FRICTION		0.07449	
RPM FOR STRESSES		6000.00	

* * * * * * * * * * * * * * * * * * * *
THE EFFECTIVE CONTACT RATIO = 1.4500
* * * * * * * * * * * * * * * * * * * *

MAXIMUM VALUES FOR SUN-PLANET MESH 2

	SUN		PLANET
FILLET STRESS CONCENTRATION (KSUBT)	1.45022		1.38394
MAXIMUM HERTZ STRESS	19871.5		19871.5
HERTZ STRESS AT PD	10644.5		10644.5
MAXIMUM BENDING STRESS	279.8		305.2
BENDING STRESS AT PD	138.0		69.1
DEPTH TO MAXIMUM SHEAR	0.00041		0.00041
MAXIMUM DYNAMIC PV(MILLIONS OF PSI*FT/MIN)	18.39766		18.39766
MAXIMUM NORMAL LOAD		19.2	
AVERAGE COEFFICIENT OF FRICTION		0.01422	
RPM FOR STRESSES		6000.00	

* * * * * * * * * * * * * * * * * * * *
THE EFFECTIVE CONTACT RATIO = 1.4400
* * * * * * * * * * * * * * * * * * * *

MAXIMUM VALUES FOR SUN-PLANET MESH 3

	SUN		PLANET
FILLET STRESS CONCENTRATION (KSUBT)	1.41938		1.41342
MAXIMUM HERTZ STRESS	19965.6		19965.6
HERTZ STRESS AT PD	13752.5		13752.5
MAXIMUM BENDING STRESS	282.8		308.2
BENDING STRESS AT PD	174.0		132.5
DEPTH TO MAXIMUM SHEAR	0.00041		0.00041
MAXIMUM DYNAMIC PV(MILLIONS OF PSI*FT/MIN)	18.17844		18.17844
MAXIMUM NORMAL LOAD		19.4	
AVERAGE COEFFICIENT OF FRICTION		0.01505	
RPM FOR STRESSES		6000.00	

* *
THE EFFECTIVE CONTACT RATIO = 1.4500
* *

MAXIMUM VALUES FOR RING-PLANET MESH 1

	PLANET		RING
FILLET STRESS CONCENTRATION (KSUBT)	1.42396		1.54019
MAXIMUM HERTZ STRESS	12813.5		12813.5
HERTZ STRESS AT PD	3003.1		3003.1
MAXIMUM BENDING STRESS	298.4		140.2
BENDING STRESS AT PD	27.6		4.6
DEPTH TO MAXIMUM SHEAR	0.00056		0.00056
MAXIMUM DYNAMIC PV(MILLIONS OF PSI*FT/MIN)	5.81742		5.81742
MAXIMUM NORMAL LOAD		17.1	
AVERAGE COEFFICIENT OF FRICTION		0.00218	
RPM FOR STRESSES		6000.00	

* *
THE EFFECTIVE CONTACT RATIO = 1.6400
* *

MAXIMUM VALUES FOR RING-PLANET MESH 2

	PLANET		RING
FILLET STRESS CONCENTRATION (KSUBT)	1.44438		1.53765
MAXIMUM HERTZ STRESS	12360.0		12360.0
HERTZ STRESS AT PD	10970.2		10970.2
MAXIMUM BENDING STRESS	272.6		126.4
BENDING STRESS AT PD	248.3		84.8
DEPTH TO MAXIMUM SHEAR	0.00054		0.00054
MAXIMUM DYNAMIC PV(MILLIONS OF PSI*FT/MIN)	5.43570		5.43570
MAXIMUM NORMAL LOAD		15.8	
AVERAGE COEFFICIENT OF FRICTION		0.00893	
RPM FOR STRESSES		6000.00	

* *
THE EFFECTIVE CONTACT RATIO = 1.6300
* *

MAXIMUM VALUES FOR RING-PLANET MESH 3

	PLANET		RING
FILLET STRESS CONCENTRATION (KSUBT)	1.40377		1.55480
MAXIMUM HERTZ STRESS	12458.8		12458.8
HERTZ STRESS AT PD	0.0		0.0
MAXIMUM BENDING STRESS	284.4		149.0
BENDING STRESS AT PD	0.0		0.0
DEPTH TO MAXIMUM SHEAR	0.00055		0.00055
MAXIMUM DYNAMIC PV(MILLIONS OF PSI*FT/MIN)	5.78340		5.78340
MAXIMUM NORMAL LOAD		16.2	
AVERAGE COEFFICIENT OF FRICTION		0.01829	
RPM FOR STRESSES		6000.00	

ERROR TOOTH PASS NUMBER 7

MAXIMUM VALUES FOR SUN-PLANET MESH 1

	SUN		PLANET
FILLET STRESS CONCENTRATION (KSUBT)	1.43617		1.39553
MAXIMUM HERTZ STRESS	19802.0		19802.0
HERTZ STRESS AT PD	19485.9		19485.9
MAXIMUM BENDING STRESS	273.4		303.0
BENDING STRESS AT PD	259.2		295.7
DEPTH TO MAXIMUM SHEAR	0.00041		0.00041
MAXIMUM DYNAMIC PV(MILLIONS OF PSI*FT/MIN)	18.58339		18.58339
MAXIMUM NORMAL LOAD		19.1	
AVERAGE COEFFICIENT OF FRICTION		0.07452	
RPM FOR STRESSES		6000.00	

* * * * * * * * * * * * * * * * * * * *
THE EFFECTIVE CONTACT RATIO = 1.4500
* * * * * * * * * * * * * * * * * * * *

MAXIMUM VALUES FOR SUN-PLANET MESH 2

	SUN		PLANET
FILLET STRESS CONCENTRATION (KSUBT)	1.45022		1.38394
MAXIMUM HERTZ STRESS	19876.3		19876.3
HERTZ STRESS AT PD	10558.6		10558.6
MAXIMUM BENDING STRESS	280.1		305.2
BENDING STRESS AT PD	135.8		68.0
DEPTH TO MAXIMUM SHEAR	0.00041		0.00041
MAXIMUM DYNAMIC PV(MILLIONS OF PSI*FT/MIN)	18.41461		18.41461
MAXIMUM NORMAL LOAD		19.2	
AVERAGE COEFFICIENT OF FRICTION		0.01431	
RPM FOR STRESSES		6000.00	

* * * * * * * * * * * * * * * * * * * *
THE EFFECTIVE CONTACT RATIO = 1.4400
* * * * * * * * * * * * * * * * * * * *

MAXIMUM VALUES FOR SUN-PLANET MESH 3

	SUN		PLANET
FILLET STRESS CONCENTRATION (KSUBT)	1.41938		1.41342
MAXIMUM HERTZ STRESS	19953.6		19953.6
HERTZ STRESS AT PD	13748.0		13748.0
MAXIMUM BENDING STRESS	282.5		307.9
BENDING STRESS AT PD	173.9		132.4
DEPTH TO MAXIMUM SHEAR	0.00041		0.00041
MAXIMUM DYNAMIC PV(MILLIONS OF PSI*FT/MIN)	18.20615		18.20615
MAXIMUM NORMAL LOAD		19.4	
AVERAGE COEFFICIENT OF FRICTION		0.01504	
RPM FOR STRESSES		6000.00	

* * * * * * * * * * * * * * * * * * * *
THE EFFECTIVE CONTACT RATIO = 1.4500
* * * * * * * * * * * * * * * * * * * *

MAXIMUM VALUES FOR RING-PLANET MESH 1

	PLANET		RING
FILLET STRESS CONCENTRATION (KSUBT)	1.42396		1.54019
MAXIMUM HERTZ STRESS	12817.6		12817.6
HERTZ STRESS AT PD	3034.8		3034.8
MAXIMUM BENDING STRESS	298.3		139.6
BENDING STRESS AT PD	28.2		4.7
DEPTH TO MAXIMUM SHEAR	0.00056		0.00056
MAXIMUM DYNAMIC PV(MILLIONS OF PSI*FT/MIN)	5.80746		5.80746
MAXIMUM NORMAL LOAD		17.1	
AVERAGE COEFFICIENT OF FRICTION		0.00208	
RPM FOR STRESSES		6000.00	

* * * * * * * * * * * * * * * * * * * *
THE EFFECTIVE CONTACT RATIO = 1.6400
* * * * * * * * * * * * * * * * * * * *

MAXIMUM VALUES FOR RING-PLANET MESH 2

	PLANET		RING
FILLET STRESS CONCENTRATION (KSUBT)	1.44438		1.53765
MAXIMUM HERTZ STRESS	12384.6		12384.6
HERTZ STRESS AT PD	11021.8		11021.8
MAXIMUM BENDING STRESS	274.3		129.4
BENDING STRESS AT PD	250.7		85.6
DEPTH TO MAXIMUM SHEAR	0.00054		0.00054
MAXIMUM DYNAMIC PV(MILLIONS OF PSI*FT/MIN)	5.50812		5.50812
MAXIMUM NORMAL LOAD		15.8	
AVERAGE COEFFICIENT OF FRICTION		0.00388	
RPM FOR STRESSES		6000.00	

* * * * * * * * * * * * * * * * * * * *
THE EFFECTIVE CONTACT RATIO = 1.6400
* * * * * * * * * * * * * * * * * * * *

MAXIMUM VALUES FOR RING-PLANET MESH 3

	PLANET		RING
FILLET STRESS CONCENTRATION (KSUBT)	1.40377		1.55480
MAXIMUM HERTZ STRESS	12434.5		12434.5
HERTZ STRESS AT PD	0.0		0.0
MAXIMUM BENDING STRESS	284.5		150.2
BENDING STRESS AT PD	0.0		0.0
DEPTH TO MAXIMUM SHEAR	0.00055		0.00055
MAXIMUM DYNAMIC PV(MILLIONS OF PSI*FT/MIN)	5.80601		5.80601
MAXIMUM NORMAL LOAD		16.1	
AVERAGE COEFFICIENT OF FRICTION		0.01833	
RPM FOR STRESSES		6000.00	

ERROR TOOTH PASS NUMBER 8

MAXIMUM VALUES FOR SUN-PLANET MESH 1

	SUN		PLANET
FILLET STRESS CONCENTRATION (KSUBT)	1.43617		1.39553
MAXIMUM HERTZ STRESS	19823.6		19823.6
HERTZ STRESS AT PD	19525.7		19525.7
MAXIMUM BENDING STRESS	278.9		303.8
BENDING STRESS AT PD	260.3		296.9
DEPTH TO MAXIMUM SHEAR	0.00041		0.00041
MAXIMUM DYNAMIC PV(MILLIONS OF PSI*FT/MIN)	18.60809		18.60809
MAXIMUM NORMAL LOAD		19.1	
AVERAGE COEFFICIENT OF FRICTION		0.07449	
RPM FOR STRESSES		6000.00	

* * * * * * * * * * * * * * * * * * * *
THE EFFECTIVE CONTACT RATIO = 1.4500
* * * * * * * * * * * * * * * * * * * *

MAXIMUM VALUES FOR SUN-PLANET MESH 2

	SUN		PLANET
FILLET STRESS CONCENTRATION (KSUBT)	1.45022		1.38394
MAXIMUM HERTZ STRESS	19879.1		19879.1
HERTZ STRESS AT PD	10647.8		10647.8
MAXIMUM BENDING STRESS	280.0		305.5
BENDING STRESS AT PD	138.1		69.2
DEPTH TO MAXIMUM SHEAR	0.00041		0.00041
MAXIMUM DYNAMIC PV(MILLIONS OF PSI*FT/MIN)	18.38838		18.38838
MAXIMUM NORMAL LOAD		19.2	
AVERAGE COEFFICIENT OF FRICTION		0.01424	
RPM FOR STRESSES		6000.00	

* * * * * * * * * * * * * * * * * * * *
THE EFFECTIVE CONTACT RATIO = 1.4400
* * * * * * * * * * * * * * * * * * * *

MAXIMUM VALUES FOR SUN-PLANET MESH 3

	SUN		PLANET
FILLET STRESS CONCENTRATION (KSUBT)	1.41938		1.41342
MAXIMUM HERTZ STRESS	19963.9		19963.9
HERTZ STRESS AT PD	13735.5		13735.5
MAXIMUM BENDING STRESS	282.6		309.2
BENDING STRESS AT PD	173.5		132.1
DEPTH TO MAXIMUM SHEAR	0.00041		0.00041
MAXIMUM DYNAMIC PV(MILLIONS OF PSI*FT/MIN)	18.15649		18.15649
MAXIMUM NORMAL LOAD		19.4	
AVERAGE COEFFICIENT OF FRICTION		0.01504	
RPM FOR STRESSES		6000.00	

* * * * * * * * * * * * * * * * * * * *
THE EFFECTIVE CONTACT RATIO = 1.4500
* * * * * * * * * * * * * * * * * * * *

MAXIMUM VALUES FOR RING-PLANET MESH 1

	PLANET		RING
FILLET STRESS CONCENTRATION (KSUBT)	1.42396		1.54019
MAXIMUM HERTZ STRESS	12812.0		12812.0
HERTZ STRESS AT PD	3014.4		3014.4
MAXIMUM BENDING STRESS	298.0		139.5
BENDING STRESS AT PD	27.8		4.6
DEPTH TO MAXIMUM SHEAR	0.00056		0.00056
MAXIMUM DYNAMIC PV(MILLIONS OF PSI*FT/MIN)	5.80195		5.80195
MAXIMUM NORMAL LOAD		17.0	
AVERAGE COEFFICIENT OF FRICTION		0.00220	
RPM FOR STRESSES		6000.00	

* * * * * * * * * * * * * * * * * * * *
THE EFFECTIVE CONTACT RATIO = 1.6400
* * * * * * * * * * * * * * * * * * * *

MAXIMUM VALUES FOR RING-PLANET MESH 2

	PLANET		RING
FILLET STRESS CONCENTRATION (KSUBT)	1.44438		1.53765
MAXIMUM HERTZ STRESS	12350.9		12350.9
HERTZ STRESS AT PD	10989.6		10989.6
MAXIMUM BENDING STRESS	272.3		126.3
BENDING STRESS AT PD	249.2		85.1
DEPTH TO MAXIMUM SHEAR	0.00054		0.00054
MAXIMUM DYNAMIC PV(MILLIONS OF PSI*FT/MIN)	5.45306		5.45306
MAXIMUM NORMAL LOAD		15.8	
AVERAGE COEFFICIENT OF FRICTION		0.00893	
RPM FOR STRESSES		6000.00	

* * * * * * * * * * * * * * * * * * * *
THE EFFECTIVE CONTACT RATIO = 1.6300
* * * * * * * * * * * * * * * * * * * *

MAXIMUM VALUES FOR RING-PLANET MESH 3

	PLANET		RING
FILLET STRESS CONCENTRATION (KSUBT)	1.40377		1.55480
MAXIMUM HERTZ STRESS	12491.6		12491.6
HERTZ STRESS AT PD	0.0		0.0
MAXIMUM BENDING STRESS	285.5		148.9
BENDING STRESS AT PD	0.0		0.0
DEPTH TO MAXIMUM SHEAR	0.00055		0.00055
MAXIMUM DYNAMIC PV(MILLIONS OF PSI*FT/MIN)	5.78464		5.78464
MAXIMUM NORMAL LOAD		16.2	
AVERAGE COEFFICIENT OF FRICTION		0.01830	
RPM FOR STRESSES		6000.00	

ERROR TOOTH PASS NUMBER 9

MAXIMUM VALUES FOR SUN-PLANET MESH 1

	SUN		PLANET
FILLET STRESS CONCENTRATION (KSUBT)	1.43617		1.39553
MAXIMUM HERTZ STRESS	19800.7		19800.7
HERTZ STRESS AT PD	19486.6		19486.6
MAXIMUM BENDING STRESS	278.4		303.0
BENDING STRESS AT PD	259.3		295.7
DEPTH TO MAXIMUM SHEAR	0.00041		0.00041
MAXIMUM DYNAMIC PV(MILLIONS OF PSI*FT/MIN)	18.58292		18.58292
MAXIMUM NORMAL LOAD		19.1	
AVERAGE COEFFICIENT OF FRICTION		0.07452	
RPM FOR STRESSES		6000.00	

* *
THE EFFECTIVE CONTACT RATIO = 1.4500
* *

MAXIMUM VALUES FOR SUN-PLANET MESH 2

	SUN		PLANET
FILLET STRESS CONCENTRATION (KSUBT)	1.45022		1.38394
MAXIMUM HERTZ STRESS	19876.4		19876.4
HERTZ STRESS AT PD	10569.5		10569.5
MAXIMUM BENDING STRESS	280.1		305.2
BENDING STRESS AT PD	136.1		68.2
DEPTH TO MAXIMUM SHEAR	0.00041		0.00041
MAXIMUM DYNAMIC PV(MILLIONS OF PSI*FT/MIN)	18.41505		18.41505
MAXIMUM NORMAL LOAD		19.2	
AVERAGE COEFFICIENT OF FRICTION		0.01431	
RPM FOR STRESSES		6000.00	

* *
THE EFFECTIVE CONTACT RATIO = 1.4400
* *

MAXIMUM VALUES FOR SUN-PLANET MESH 3

	SUN		PLANET
FILLET STRESS CONCENTRATION (KSUBT)	1.41938		1.41342
MAXIMUM HERTZ STRESS	19949.3		19949.3
HERTZ STRESS AT PD	13740.6		13740.6
MAXIMUM BENDING STRESS	282.4		307.7
BENDING STRESS AT PD	173.7		132.2
DEPTH TO MAXIMUM SHEAR	0.00041		0.00041
MAXIMUM DYNAMIC PV(MILLIONS OF PSI*FT/MIN)	18.19902		18.19902
MAXIMUM NORMAL LOAD		19.4	
AVERAGE COEFFICIENT OF FRICTION		0.01504	
RPM FOR STRESSES		6000.00	

* *
THE EFFECTIVE CONTACT RATIO = 1.4500
* *

MAXIMUM VALUES FOR RING-PLANET MESH 1

	PLANET		RING
FILLET STRESS CONCENTRATION (KSUBT)	1.42396		1.54019
MAXIMUM HERTZ STRESS	12813.7		12813.7
HERTZ STRESS AT PD	3044.1		3044.1
MAXIMUM BENDING STRESS	298.0		139.2
BENDING STRESS AT PD	28.4		4.7
DEPTH TO MAXIMUM SHEAR	0.00056		0.00056
MAXIMUM DYNAMIC PV(MILLIONS OF PSI*FT/MIN)	5.79806		5.79806
MAXIMUM NORMAL LOAD		17.1	
AVERAGE COEFFICIENT OF FRICTION		0.00208	
RPM FOR STRESSES		6000.00	

* *
THE EFFECTIVE CONTACT RATIO = 1.6400
* *

MAXIMUM VALUES FOR RING-PLANET MESH 2

	PLANET		RING
FILLET STRESS CONCENTRATION (KSUBT)	1.44438		1.53765
MAXIMUM HERTZ STRESS	12372.3		12372.3
HERTZ STRESS AT PD	11020.7		11020.7
MAXIMUM BENDING STRESS	273.9		129.6
BENDING STRESS AT PD	250.6		85.6
DEPTH TO MAXIMUM SHEAR	0.00054		0.00054
MAXIMUM DYNAMIC PV(MILLIONS OF PSI*FT/MIN)	5.50976		5.50976
MAXIMUM NORMAL LOAD		15.8	
AVERAGE COEFFICIENT OF FRICTION		0.00387	
RPM FOR STRESSES		6000.00	

* *
THE EFFECTIVE CONTACT RATIO = 1.6400
* *

MAXIMUM VALUES FOR RING-PLANET MESH 3

	PLANET		RING
FILLET STRESS CONCENTRATION (KSUBT)	1.40377		1.55490
MAXIMUM HERTZ STRESS	12446.4		12446.4
HERTZ STRESS AT PD	0.0		0.0
MAXIMUM BENDING STRESS	284.9		150.4
BENDING STRESS AT PD	0.0		0.0
DEPTH TO MAXIMUM SHEAR	0.00055		0.00055
MAXIMUM DYNAMIC PV(MILLIONS OF PSI*FT/MIN)	5.81020		5.81020
MAXIMUM NORMAL LOAD		16.1	
AVERAGE COEFFICIENT OF FRICTION		0.01833	
RPM FOR STRESSES		6000.00	

ERROR TOOTH PASS NUMBER 10

MAXIMUM VALUES FOR SUN-PLANET MESH 1

	SUN		PLANET
FILLET STRESS CONCENTRATION (KSUBT)	1.43617		1.39553
MAXIMUM HERTZ STRESS	19818.4		19818.4
HERTZ STRESS AT PD	19519.7		19519.7
MAXIMUM BENDING STRESS	278.7		303.7
BENDING STRESS AT PD	260.1		296.8
DEPTH TO MAXIMUM SHEAR	0.00041		0.00041
MAXIMUM DYNAMIC PV(MILLIONS OF PSI*FT/MIN)	18.61253		18.61253
MAXIMUM NORMAL LOAD		19.1	
AVERAGE COEFFICIENT OF FRICTION		0.07449	
RPM FOR STRESSES		6000.00	

* * * * * * * * * * * * * * * * * * * *
THE EFFECTIVE CONTACT RATIO = 1.4500
* * * * * * * * * * * * * * * * * * * *

MAXIMUM VALUES FOR SUN-PLANET MESH 2

	SUN		PLANET
FILLET STRESS CONCENTRATION (KSUBT)	1.45022		1.38394
MAXIMUM HERTZ STRESS	19879.8		19379.8
HERTZ STRESS AT PD	10650.5		10650.5
MAXIMUM BENDING STRESS	280.0		305.5
BENDING STRESS AT PD	138.2		69.2
DEPTH TO MAXIMUM SHEAR	0.00041		0.00041
MAXIMUM DYNAMIC PV(MILLIONS OF PSI*FT/MIN)	18.39218		18.39218
MAXIMUM NORMAL LOAD		19.2	
AVERAGE COEFFICIENT OF FRICTION		0.01423	
RPM FOR STRESSES		6000.00	

* * * * * * * * * * * * * * * * * * * *
THE EFFECTIVE CONTACT RATIO = 1.4400
* * * * * * * * * * * * * * * * * * * *

MAXIMUM VALUES FOR SUN-PLANET MESH 3

	SUN		PLANET
FILLET STRESS CONCENTRATION (KSUBT)	1.41938		1.41342
MAXIMUM HERTZ STRESS	19965.2		19965.2
HERTZ STRESS AT PD	13735.4		13735.4
MAXIMUM BENDING STRESS	282.7		308.2
BENDING STRESS AT PD	173.5		132.1
DEPTH TO MAXIMUM SHEAR	0.00041		0.00041
MAXIMUM DYNAMIC PV(MILLIONS OF PSI*FT/MIN)	18.15807		18.15807
MAXIMUM NORMAL LOAD		19.4	
AVERAGE COEFFICIENT OF FRICTION		0.01504	
RPM FOR STRESSES		6000.00	

* * * * * * * * * * * * * * * * * * * *
THE EFFECTIVE CONTACT RATIO = 1.4500
* * * * * * * * * * * * * * * * * * * *

MAXIMUM VALUES FOR RING-PLANET MESH 1

	PLANET		RING
FILLET STRESS CONCENTRATION (KSUBT)	1.42396		1.54019
MAXIMUM HERTZ STRESS	12813.0		12813.0
HERTZ STRESS AT PD	3015.4		3015.4
MAXIMUM BENDING STRESS	297.9		139.3
BENDING STRESS AT PD	27.8		4.6
DEPTH TO MAXIMUM SHEAR	0.00056		0.00056
MAXIMUM DYNAMIC PV(MILLIONS OF PSI*FT/MIN)	5.79929		5.79929
MAXIMUM NORMAL LOAD		17.0	
AVERAGE COEFFICIENT OF FRICTION		0.00215	
RPM FOR STRESSES		6000.00	

* * * * * * * * * * * * * * * * * * * *
THE EFFECTIVE CONTACT RATIO = 1.6400
* * * * * * * * * * * * * * * * * * * *

MAXIMUM VALUES FOR RING-PLANET MESH 2

	PLANET		RING
FILLET STRESS CONCENTRATION (KSUBT)	1.44438		1.53765
MAXIMUM HERTZ STRESS	12344.0		12344.0
HERTZ STRESS AT PD	10985.1		10985.1
MAXIMUM BENDING STRESS	272.0		126.3
BENDING STRESS AT PD	249.0		85.0
DEPTH TO MAXIMUM SHEAR	0.00054		0.00054
MAXIMUM DYNAMIC PV(MILLIONS OF PSI*FT/MIN)	5.45210		5.45210
MAXIMUM NORMAL LOAD		15.7	
AVERAGE COEFFICIENT OF FRICTION		0.00892	
RPM FOR STRESSES		6000.00	

* * * * * * * * * * * * * * * * * * * *
THE EFFECTIVE CONTACT RATIO = 1.6300
* * * * * * * * * * * * * * * * * * * *

MAXIMUM VALUES FOR RING-PLANET MESH 3

	PLANET		RING
FILLET STRESS CONCENTRATION (KSUBT)	1.40377		1.55480
MAXIMUM HERTZ STRESS	12496.9		12496.9
HERTZ STRESS AT PD	0.0		0.0
MAXIMUM BENDING STRESS	285.9		149.2
BENDING STRESS AT PD	0.0		0.0
DEPTH TO MAXIMUM SHEAR	0.00055		0.00055
MAXIMUM DYNAMIC PV(MILLIONS OF PSI*FT/MIN)	5.79119		5.79119
MAXIMUM NORMAL LOAD		16.3	
AVERAGE COEFFICIENT OF FRICTION		0.01830	
RPM FOR STRESSES		6000.00	

PLANET 1

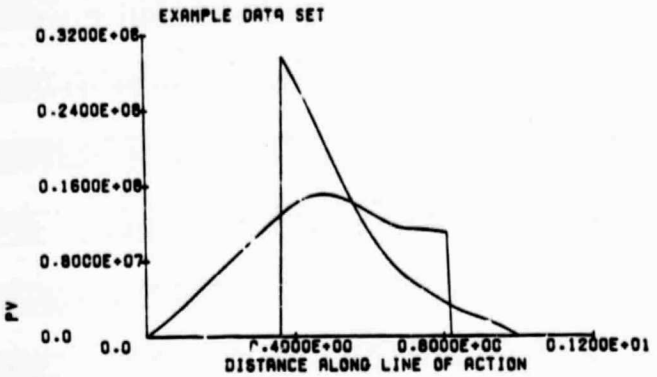
EXAMPLE DATA SET
PV
0.3200E+08
0.2400E+08
0.1600E+08
0.8000E+07
0.0
0.0
0.4000E+00
0.8000E+00
0.1200E+01
DISTANCE ALONG LINE OF ACTION

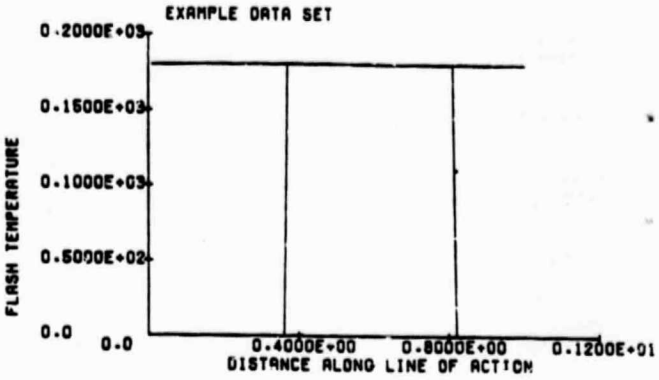
EXAMPLE DATA SET
FLASH TEMPERATURE
0.2000E+03
0.1500E+03
0.1000E+03
0.5000E+02
0.0
0.0
0.4000E+00
0.8000E+00
0.1200E+01
DISTANCE ALONG LINE OF ACTION

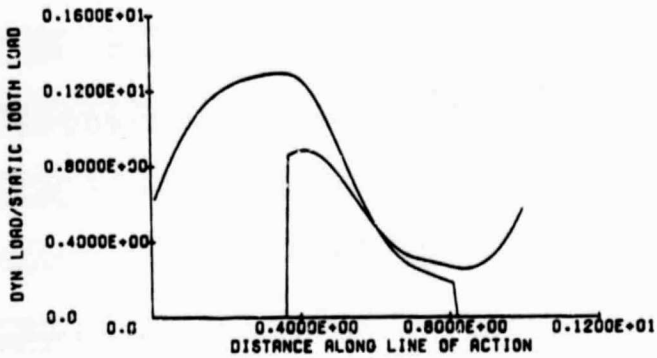
DYN LOAD/STATIC TOOTH LOAD
0.1600E+01
0.1200E+01
0.8000E+00
0.4000E+00
0.0
0.0
0.4000E+00
0.8000E+00
0.1200E+01
DISTANCE ALONG LINE OF ACTION

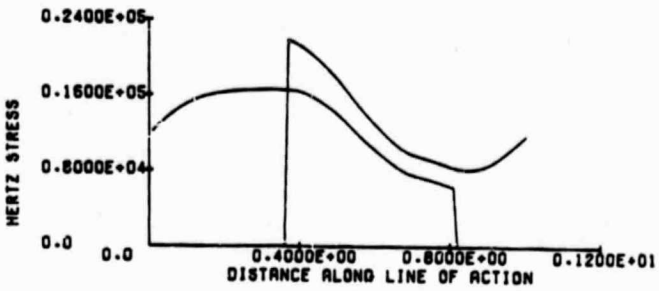
HERTZ STRESS
0.2400E+05
0.1600E+05
0.8000E+04
0.0
0.0
0.4000E+00
0.8000E+00
0.1200E+01
DISTANCE ALONG LINE OF ACTION

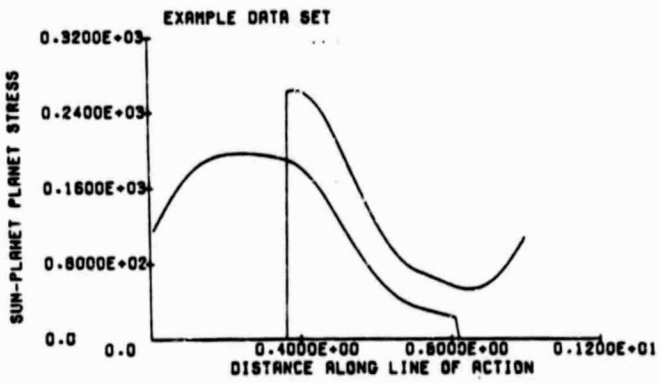
EXAMPLE DATA SET
SUN-PLANET PLANET STRESS
0.3200E+03
0.2400E+03
0.1600E+03
0.8000E+02
0.0
0.0
0.4000E+00
0.8000E+00
0.1200E+01
DISTANCE ALONG LINE OF ACTION

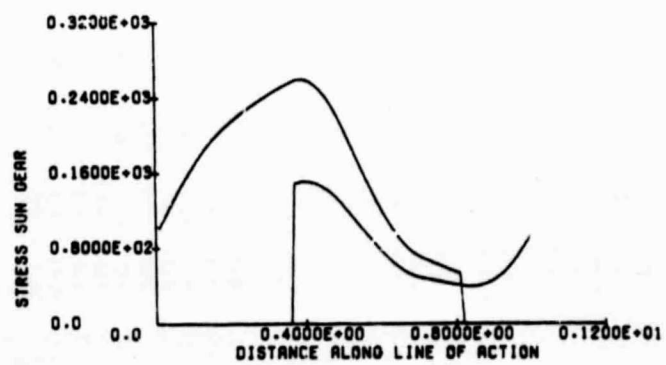
STRESS SUN GEAR
0.3200E+03
0.2400E+03
0.1600E+03
0.8000E+02
0.0
0.0
0.4000E+00
0.8000E+00
0.1200E+01
DISTANCE ALONG LINE OF ACTION

PLANET 2

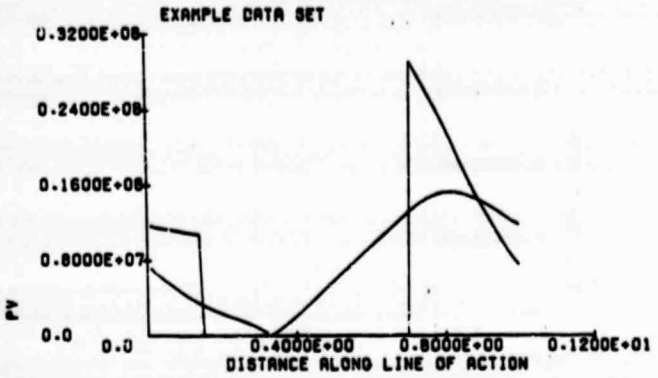
EXAMPLE DATA SET
0.3200E+08
0.2400E+08
0.1600E+08
0.8000E+07
0.0
PV
0.0
0.4000E+00
0.8000E+00
0.1200E+01
DISTANCE ALONG LINE OF ACTION

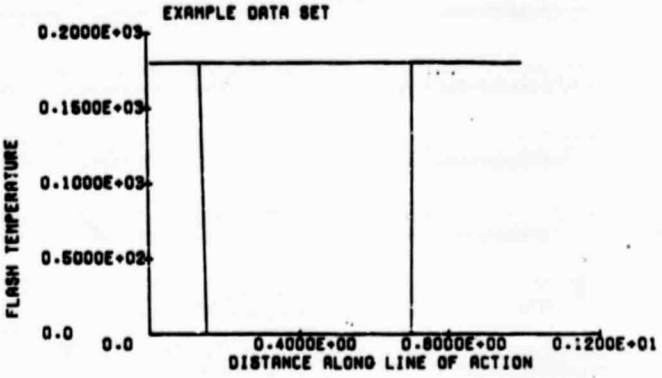
EXAMPLE DATA SET
0.2000E+03
0.1500E+03
0.1000E+03
0.5000E+02
0.0
FLASH TEMPERATURE
0.0
0.4000E+00
0.8000E+00
0.1200E+01
DISTANCE ALONG LINE OF ACTION

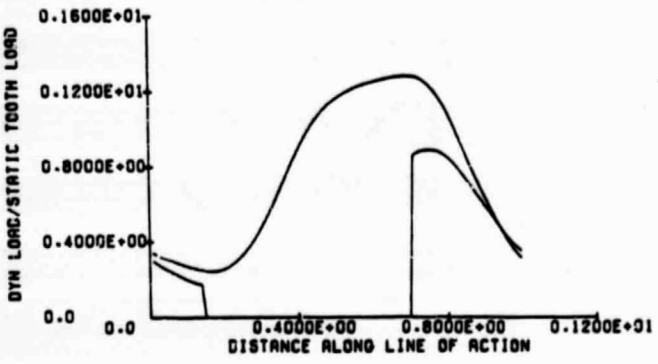
0.1600E+01
0.1200E+01
0.8000E+00
0.4000E+00
0.0
DYN LOAD/STATIC TOOTH LOAD
0.0
0.4000E+00
0.8000E+00
0.1200E+01
DISTANCE ALONG LINE OF ACTION

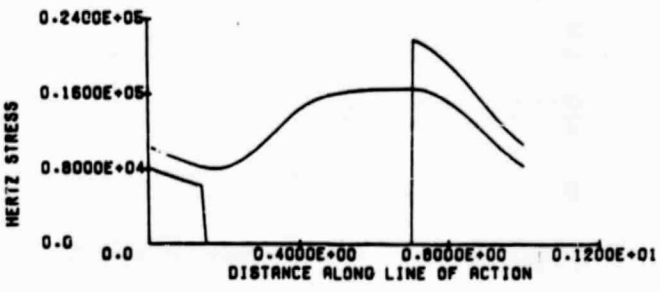
0.2400E+05
0.1600E+05
0.8000E+04
0.0
HERTZ STRESS
0.0
0.4000E+00
0.8000E+00
0.1200E+01
DISTANCE ALONG LINE OF ACTION

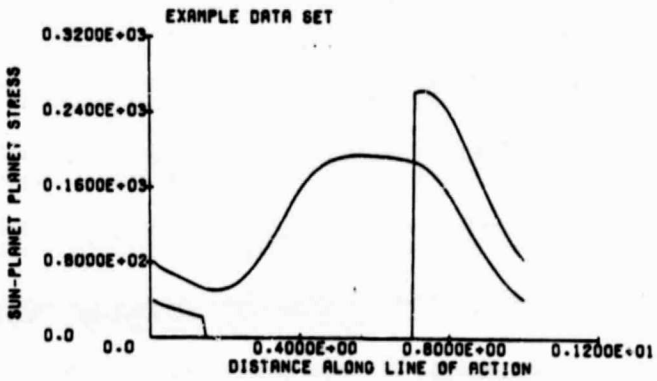
EXAMPLE DATA SET
0.3200E+03
0.2400E+03
0.1600E+03
0.8000E+02
0.0
SUN-PLANET PLANET STRESS
0.0
0.4000E+00
0.8000E+00
0.1200E+01
DISTANCE ALONG LINE OF ACTION

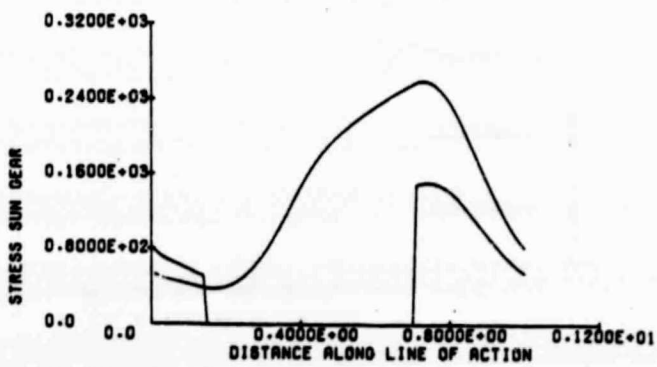
0.3200E+03
0.2400E+03
0.1600E+03
0.8000E+02
0.0
STRESS SUN GEAR
0.0
0.4000E+00
0.8000E+00
0.1200E+01
DISTANCE ALONG LINE OF ACTION

PLANET 3

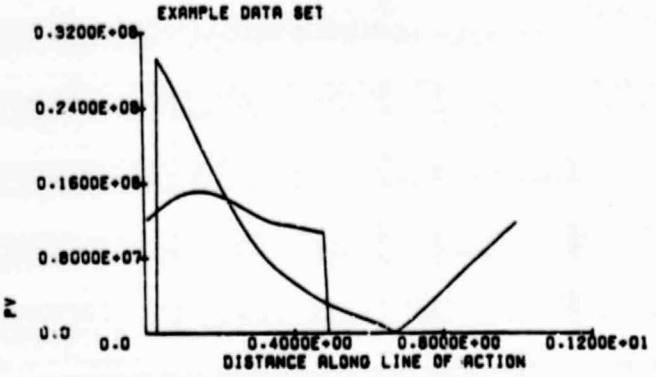
EXAMPLE DATA SET
0.3200E+08
0.2400E+08
0.1600E+08
0.8000E+07
0.0
PV
0.0
0.4000E+00
0.8000E+00
0.1200E+01
DISTANCE ALONG LINE OF ACTION

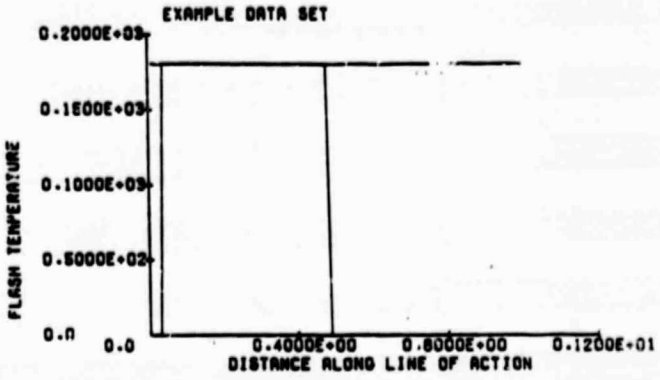
EXAMPLE DATA SET
0.2000E+03
0.1500E+03
0.1000E+03
0.5000E+02
0.0
FLASH TEMPERATURE
0.0
0.4000E+00
0.8000E+00
0.1200E+01
DISTANCE ALONG LINE OF ACTION

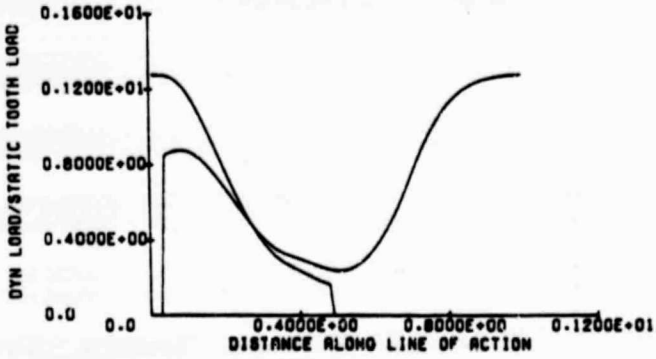
0.1600E+01
0.1200E+01
0.8000E+00
0.4000E+00
0.0
DYN LOAD/STATIC TOOTH LOAD
0.0
0.4000E+00
0.8000E+00
0.1200E+01
DISTANCE ALONG LINE OF ACTION

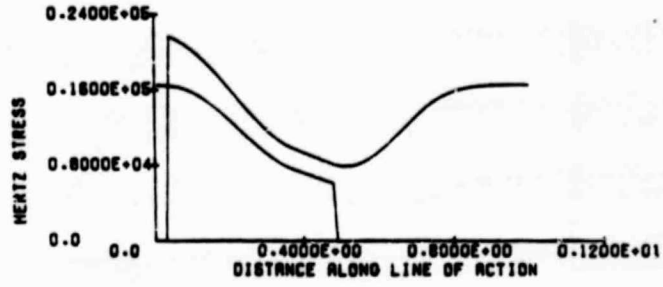
0.2400E+05
0.1600E+05
0.8000E+04
0.0
HERTZ STRESS
0.0
0.4000E+00
0.8000E+00
0.1200E+01
DISTANCE ALONG LINE OF ACTION

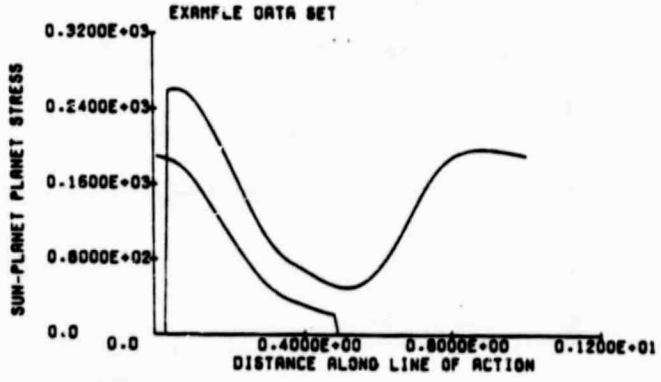
EXAMPLE DATA SET
0.3200E+03
0.2400E+03
0.1600E+03
0.8000E+02
0.0
SUN-PLANET PLANET STRESS
0.0
0.4000E+00
0.8000E+00
0.1200E+01
DISTANCE ALONG LINE OF ACTION

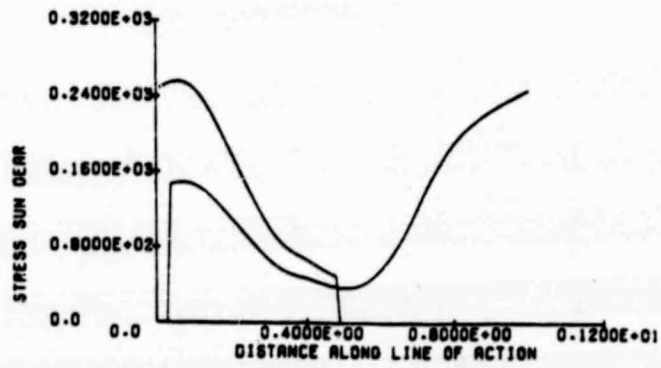
0.3200E+03
0.2400E+03
0.1600E+03
0.8000E+02
0.0
STRESS SUN GEAR
0.0
0.4000E+00
0.8000E+00
0.1200E+01
DISTANCE ALONG LINE OF ACTION

PLANET 1

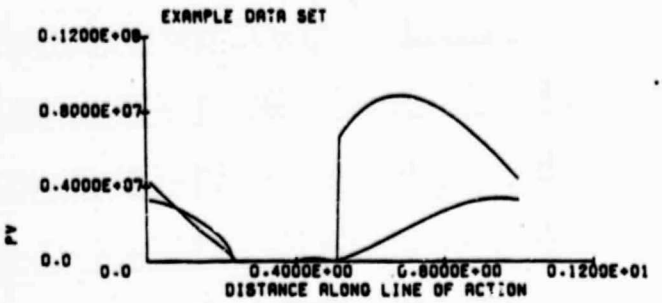
EXAMPLE DATA SET
0.1200E+08
0.8000E+07
0.4000E+07
0.0
PV
0.0
0.4000E+00
0.8000E+00
0.1200E+01
DISTANCE ALONG LINE OF ACTION

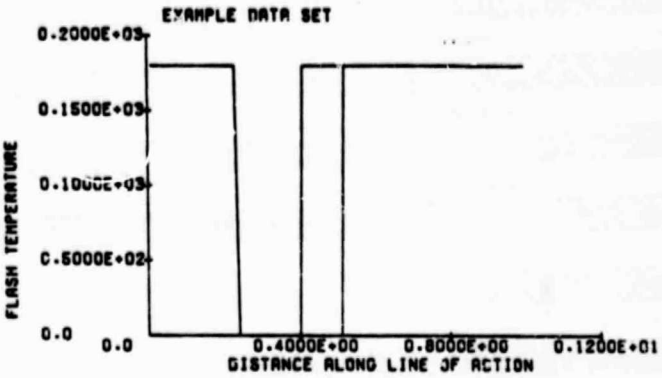
EXAMPLE DATA SET
0.2000E+03
0.1500E+03
0.1000E+03
0.5000E+02
0.0
FLASH TEMPERATURE
0.0
0.4000E+00
0.8000E+00
0.1200E+01
DISTANCE ALONG LINE OF ACTION

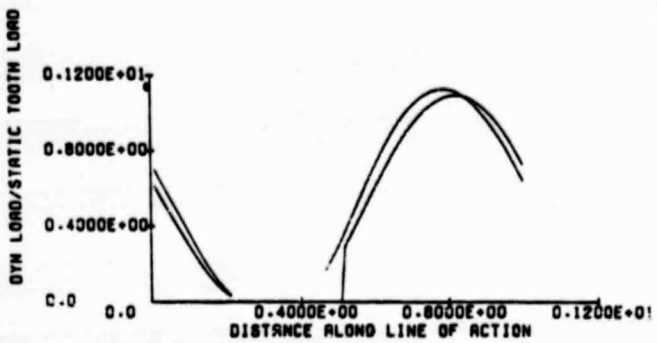
0.1200E+01
0.8000E+00
0.4000E+00
0.0
DYN LOAD/STATIC TOOTH LOAD
0.0
0.4000E+00
0.8000E+00
0.1200E+01
DISTANCE ALONG LINE OF ACTION

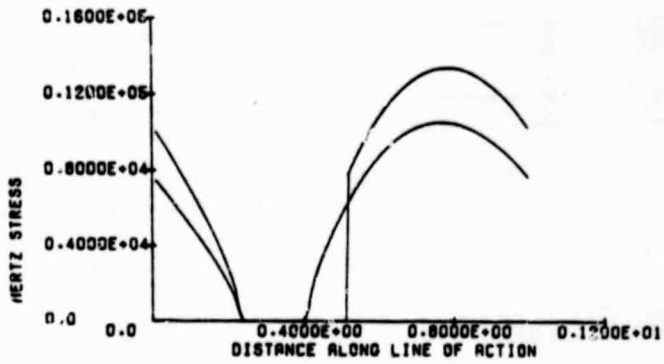
0.1600E+05
0.1200E+05
0.8000E+04
0.4000E+04
0.0
HERTZ STRESS
0.0
0.4000E+00
0.8000E+00
0.1200E+01
DISTANCE ALONG LINE OF ACTION

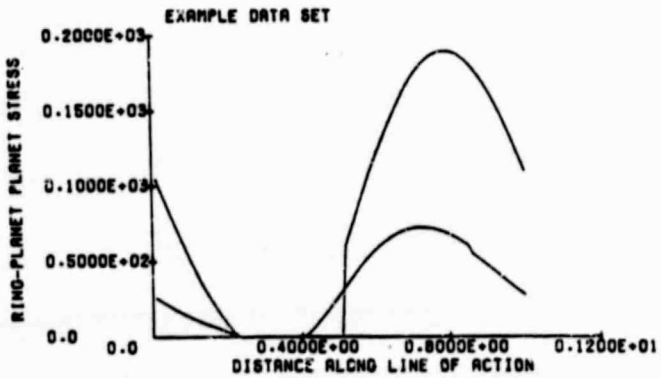
EXAMPLE DATA SET
0.2000E+03
0.1500E+03
0.1000E+03
0.5000E+02
0.0
RING-PLANET PLANET STRESS
0.0
0.4000E+00
0.8000E+00
0.1200E+01
DISTANCE ALONG LINE OF ACTION

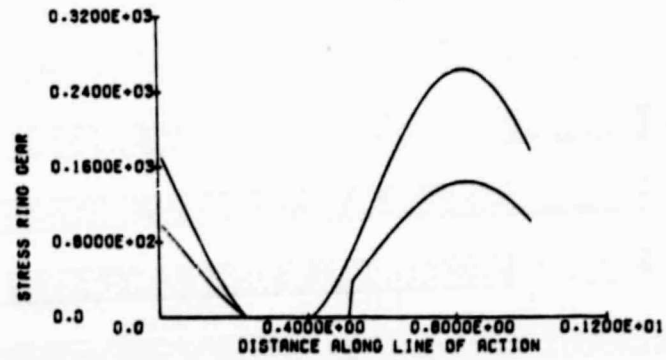
0.3200E+03
0.2400E+03
0.1600E+03
0.8000E+02
0.0
STRESS RING GEAR
0.0
0.4000E+00
0.8000E+00
0.1200E+01
DISTANCE ALONG LINE OF ACTION

PLANET 2

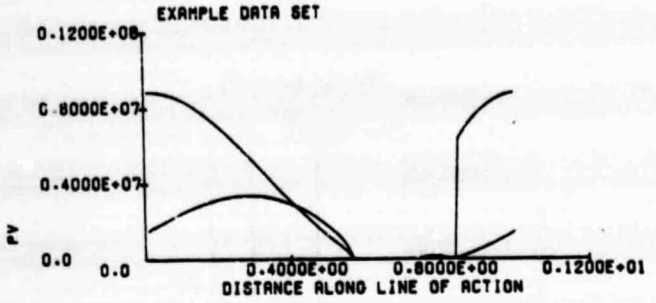
EXAMPLE DATA SET
0.1200E+08
0.8000E+07
0.4000E+07
0.0
PV
0.0
0.4000E+00
0.8000E+00
0.1200E+01
DISTANCE ALONG LINE OF ACTION

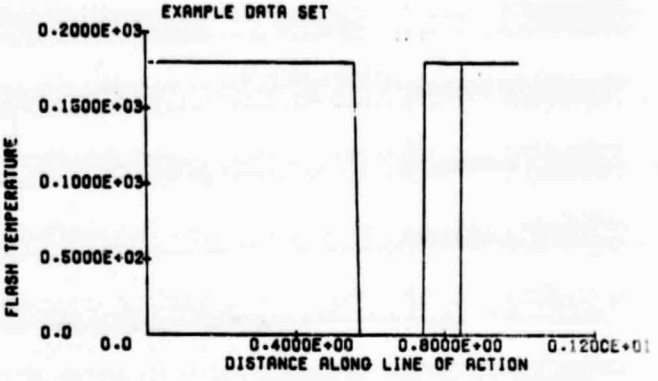
EXAMPLE DATA SET
0.2000E+03
0.1500E+03
0.1000E+03
0.5000E+02
0.0
FLASH TEMPERATURE
0.0
0.4000E+00
0.8000E+00
0.1200E+01
DISTANCE ALONG LINE OF ACTION

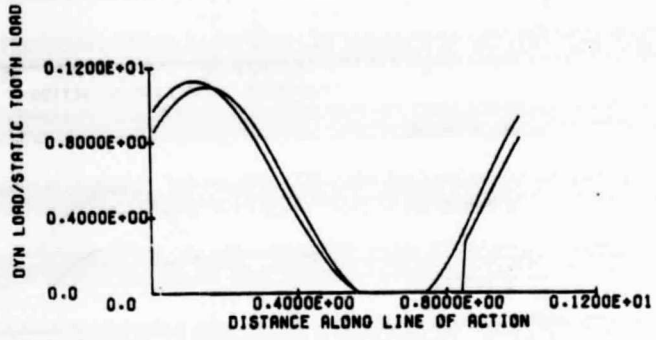
0.1200E+01
0.8000E+00
0.4000E+00
0.0
DYN LOAD/STATIC TOOTH LOAD
0.0
0.4000E+00
0.8000E+00
0.1200E+01
DISTANCE ALONG LINE OF ACTION

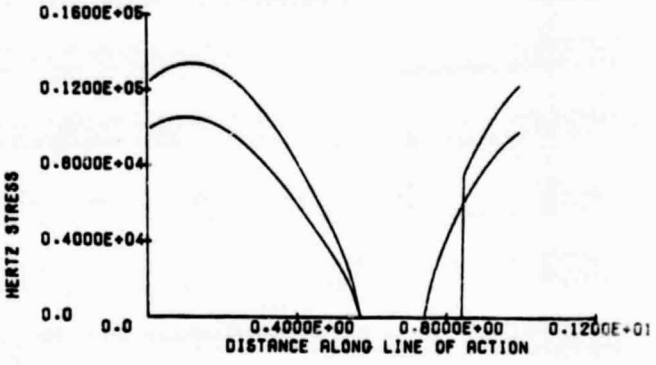
0.1600E+05
0.1200E+05
0.8000E+04
0.4000E+04
0.0
HERTZ STRESS
0.0
0.4000E+00
0.8000E+00
0.1200E+01
DISTANCE ALONG LINE OF ACTION

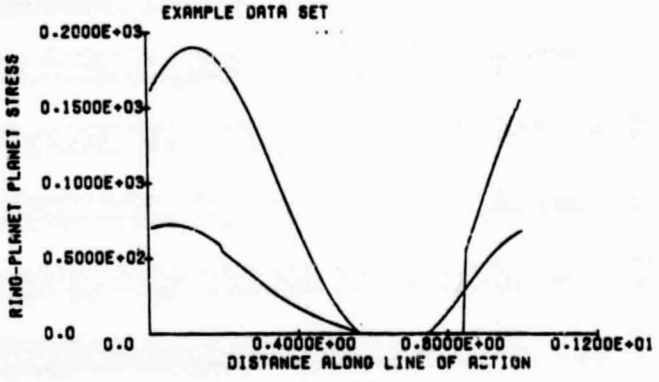
EXAMPLE DATA SET
0.2000E+03
0.1500E+03
0.1000E+03
0.5000E+02
0.0
RING-PLANET PLANET STRESS
0.0
0.4000E+00
0.8000E+00
0.1200E+01
DISTANCE ALONG LINE OF ACTION

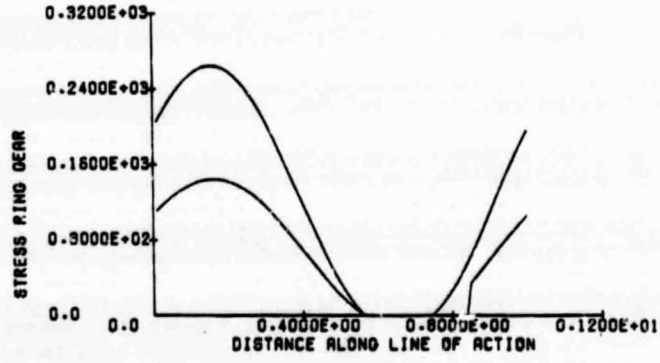
0.3200E+03
0.2400E+03
0.1600E+03
0.9000E+02
0.0
STRESS RING GEAR
0.0
0.4000E+00
0.8000E+00
0.1200E+01
DISTANCE ALONG LINE OF ACTION

PLANET 3

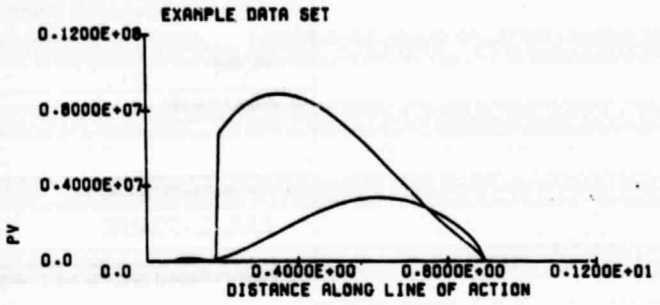
EXAMPLE DATA SET
0.1200E+08
0.8000E+07
0.4000E+07
0.0
PV
0.0
0.4000E+00
0.8000E+00
0.1200E+01
DISTANCE ALONG LINE OF ACTION

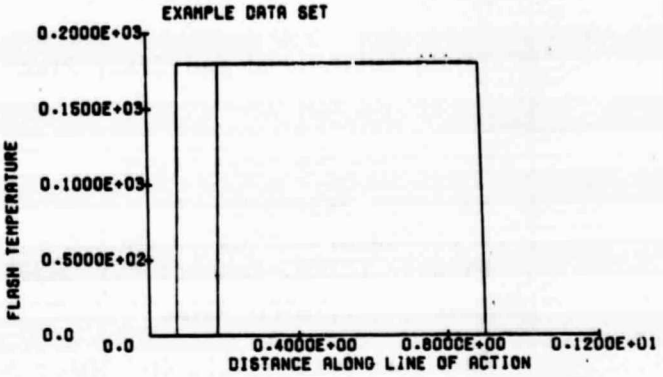
EXAMPLE DATA SET
0.2000E+03
0.1500E+03
0.1000E+03
0.5000E+02
0.0
FLASH TEMPERATURE
0.0
0.4000E+00
0.8000E+00
0.1200E+01
DISTANCE ALONG LINE OF ACTION

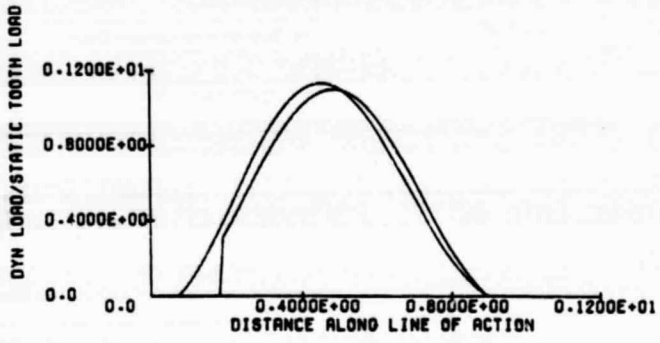
0.1200E+01
0.8000E+00
0.4000E+00
0.0
DYN LOAD/STATIC TOOTH LOAD
0.0
0.4000E+00
0.8000E+00
0.1200E+01
DISTANCE ALONG LINE OF ACTION

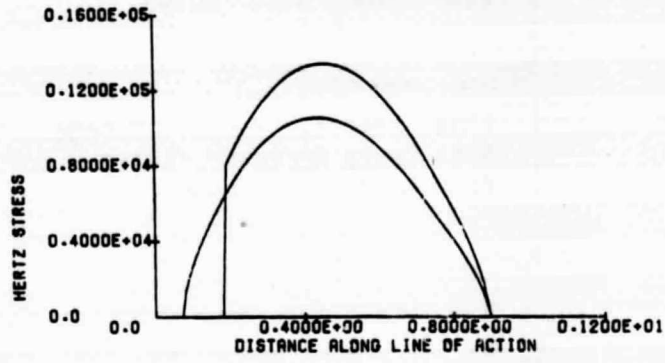
0.1600E+05
0.1200E+05
0.8000E+04
0.4000E+04
0.0
HERTZ STRESS
0.0
0.4000E+00
0.8000E+00
0.1200E+01
DISTANCE ALONG LINE OF ACTION

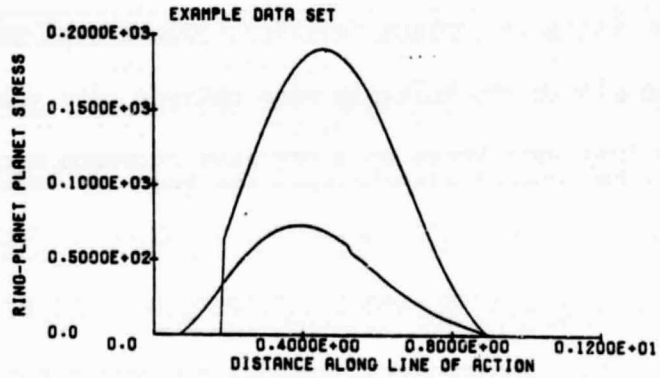
EXAMPLE DATA SET
0.2000E+03
0.1500E+03
0.1000E+03
0.5000E+02
0.0
RING-PLANET PLANET STRESS
0.0
0.4000E+00
0.8000E+00
0.1200E+01
DISTANCE ALONG LINE OF ACTION

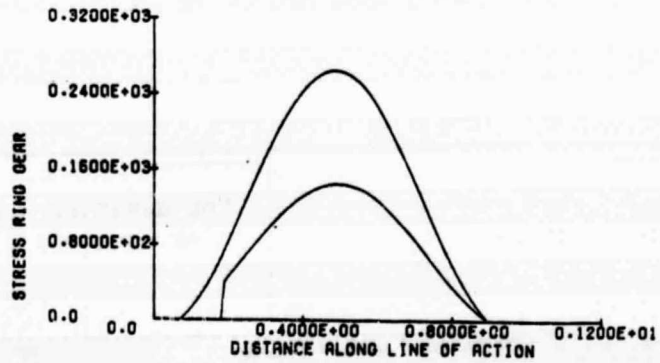
0.3200E+03
0.2400E+03
0.1600E+03
0.8000E+02
0.0
STRESS RING GEAR
0.0
0.4000E+00
0.8000E+00
0.1200E+01
DISTANCE ALONG LINE OF ACTION

1. Report No.	2. Government Accession No.	3. Recipient's Catalog No.
NASA CR-174747		

4. Title and Subtitle	5. Report Date
Multi-Mesh Gear Dynamics Program Evaluation and Enhancements	May 1985
	6. Performing Organization Code

7. Author(s)	8. Performing Organization Report No.
Linda Smith Boyd and James Pike	None
	10. Work Unit No.

9. Performing Organization Name and Address	11. Contract or Grant No.
Hamilton Standard Division of United Technologies Corporation Windsor Locks, Connecticut 06096	NAS 3-23928
	13. Type of Report and Period Covered
12. Sponsoring Agency Name and Address	Contractor Report
National Aeronautics and Space Administration Washington, D.C. 20546	14. Sponsoring Agency Code
	505-42-94

15. Supplementary Notes

Final report. Project Manager, Dennis P. Townsend, Propulsion Systems Division, NASA Lewis Research Center, Cleveland, Ohio 44135. FORTRAN listing available from NASA project manager or COSMIC.

16. Abstract

A multiple mesh gear dynamics computer program has been continually developed and modified during the last four years under NASA funding. The program can handle epicyclic gear systems as well as single mesh systems with internal, buttress, or helical tooth forms. The following modifications have been added under the current funding: variable contact friction, planet cage and ring gear rim flexibility options, user friendly options, dynamic side bands, a speed survey option and combining the single and multiple mesh options into one general program. The modified program has been evaluated by comparing calculated values to published test data and to test data taken on a Hamilton Standard turboprop reduction gearbox. In general, the correlation between the test data and the analytical data is good.

17. Key Words (Suggested by Author(s))	18. Distribution Statement
Epicyclic gears Gear tooth dynamic stresses	Unclassified - unlimited STAR Category 37

19. Security Classif. (of this report)	20. Security Classif. (of this page)	21. No. of pages	22. Price*
Unclassified	Unclassified	127	A07

*For sale by the National Technical Information Service, Springfield, Virginia 22161